THE INFLUENCE OF CONCRETE PRINTED LOST FORMWORK ON THE LOAD BEARING CAPACITY OF A COLUMN

J. van der Linde

bam TU Delft

The influence of concrete printed lost formwork on the load bearing capacity of a column

Master thesis

by

J. van der Linde

to obtain the degree of Master of Science
at the Delft University of Technology,
to be defended publicly on Friday March 27, 2020.

Student number:	4222156	
Date:	March 20, 2020	
Thesis committee:	Prof. dr. ir. E. Schlangen,	TU Delft
	Dr. Ir. H. R. Schipper,	TU Delft
	Ir. W. J. van den Bos,	TU Delft / BAM Infraconsult
	Ir. J. Bolhuis,	BAM Infraconsult / Hochtief AG

Preface

Before you lies my master thesis to finalise the study Civil Engineering at the Technical University Delft. This thesis discusses the influence of a concrete printed lost formwork on the compressive strength of the column. This research is performed with guidance my graduation committee, and mental support of my family and friends. I therefore would like to express my gratitude for those who have helped me complete this research.

First of all I would like to thank my daily supervisor: Jeannette van den Bos for her enthusiasm about this topic. I always felt welcome to discuss all thesis and concrete related questions that occurred during my thesis, I really appreciate this. I also want to thank Johan Bolhuis for giving me the opportunity to perform my thesis at BAM Infraconsult and helping me to find this interesting thesis topic. I would also like to thank him for the times he linked me to people with an expertise in concrete printing, I always enjoyed these meetings. I would like to thank both Johan and Jeannette for giving me the possibility to contribute to the experiment of the concrete elements BAM had to perform.

Last but not least I would like to thank Erik Schlangen and Roel Schipper for their valuable input during the meetings, the guidance and the all the good questions of which I did not think about myself. Their critical look improved my thesis significantly.

In the end I would thank, my parents and Mark for always having faith in me, and the support I got for every step I took in my life. My friends for making the student life even better. With a special thanks to Lot for all the million times you helped me during my whole study.

And I am very grateful for Stephan, who had to deal with all my complaining at stressful moments when things did not go as I wanted it to go. You always made me feel understood and if I became too perfectionist, you always told me not to worry. This, always cheers me up. Without your help in FEM, this thesis would have been way more difficult for me.

Judith van der Linde
Delft, March 2020

Abstract

Concrete is a very popular building material since it can be cast into almost any shape. Unfortunately, one of the main limitations is that the formwork, in which the concrete is cast, is expensive. As a result, the formwork is reused as often as possible which results in a limited variation of shapes of the concrete elements. Another limitation is that the manufacturing of the formwork is quite difficult and requires significant manual labour, which can result in injury of the persons doing this work. A solution for both problems is printing of concrete. [17][13] There are a number of different ways in which concrete can be printed. The following method is used within this research: A computer directs the robot's arm to an exact location and lays a layer of concrete there. When these layers are built up, a concrete printed element is created. [23] Concrete printing could be used to create concrete columns by printing the concrete formwork. The formwork is then filled with traditional concrete. How the printed concrete affects the structural properties of the traditional concrete is yet unknown. To guarantee that the element is safe, only the traditional concrete is included in the strength calculation, resulting in a conservative load bearing resistance. This study looks at the influence of printed lost formwork on the load bearing resistance of the column. The following research question is answered: What is the influence of concrete printed lost formwork on the load bearing capacity of a circular element?

A case study is set up to answer the research question. The case study consists of a short column; A hollow concrete printed cylinder with an outer diameter of 250 mm, an inner diameter of 90 mm and a height of 470 mm. The printed formwork is filled with traditional concrete. The element is tested in Eindhoven on a pressure bench where it is loaded until failure. Subsequently, finite element models are made of this element: a linear model and a nonlinear model. The linear model is used as a basis for the nonlinear model and for a sensitivity analysis. The nonlinear model can, in contrast to the linear model, show cracks. The nonlinear model is then compared to the experiment which shows whether the results of the nonlinear model are credible. In addition, the nonlinear model is compared to a monolithic element. Based on this, the influence of the printed formwork on the strength of the element can be determined.

The nonlinear model, similar to the experiment, is discussed first. The cracks just before failure are located at the contact area between the printed and traditional concrete and run in longitudinal direction. The cracks run from the top to two-third of the element. At two-third of the element, small vertical cracks are located from the inner- to the outer circle of the printed concrete formwork. It is assumed that the concrete printed formwork will break off the small concrete column, which will have a brittle failure of the element as result. This corresponds to the results of the experiment. This conclusion is also found in the sensitivity analysis, where the influence of several parameters is defined. For all these parameters, it is observed that the difference in shrinkage between the printed and traditional concrete and prescribed vertical displacement have most influence on the stresses.

These and further conclusions have limitations due to assumptions made within this research. The conclusions are not applicable to a realistic sized printed column, as a short printed column is used within this research. The vertical load applied on top of the element is considered to be short-term. This means that the difference in shrinkage causes initial stresses are not taken into account. Moreover creep and relaxation are not taken into account. At the experiment, only one filled element is tested and the failure cannot be seen in the Ansys model, this means that the assumptions coming from the comparison cannot be proven.

The effect of the concrete printed lost formwork on the load bearing resistance of a small concrete printed column is mainly determined by the maximum occurring tensile stresses. The tensile stresses are created by the prescribed vertical deformation and the difference in shrinkage between the two types of concrete. The load bearing resistance is defined by the amount of prescribed displacement that can be applied before the element fails.

From this research, it can be concluded that the load bearing resistance of a printed cylindrical element mostly depends on the difference in shrinkage between the printed and traditional concrete.

Contents

List of Figures

List of Tables

I

Research definition

1 Introduction

1.1. Background Information

Concrete is a very popular construction material, one of the most used in the world. It is a proper material for different applications. It can be used for basic road constructions till glamours projects like the Burj Dubai Skyscraper [13] It is a natural material consisting of cement, sand, aggregates and water. 2000 years ago the Greek and Roman started using the technique of combining sand, gravel a cement-like binder and water to build walls and vaults. The Pantheon in Rome is still one of the most impressive non-reinforced Roman concrete structure in the world. Since the development of Portland cement and reinforced concrete the quality of concrete has been improved drastically [17][13]

There are a few disadvantages of traditional concrete, three of them are listed below:

- The production of concrete produces a lot of CO_2, probably 5% of the global CO_2 production is originating of the concrete industry. This CO_2 is created by the energy used to reach the reaction temperature of 1500 degrees and the chemical reaction itself: the breakdown of calcium carbonate into calcium oxide and CO_2 [13]
- Traditional concrete is cast inside a formwork. The production of the formwork is expensive, therefore the moulds reused as often as possible. This concludes in standardised elements which are less interesting than elements made especially for one project. It concludes in a mindset where simplicity became more important than material use. [9]
- The production of formwork and placing of the reinforcement is a demanding job. This can conclude in physical issues for people working on the construction site. This should be avoided as much as possible [9]

Concrete printing could be the solution to solve these problems. There are multiple ways to print concrete, but they all have the same principle. A 3D computer model of the desired element is divided into thin 2D layers. These 2D layers will be printed one by one by connecting powder, liquid or sheet materials. This creates a concrete element without intervention of a human.

The different techniques for concrete printing:

- **D-Shape** The printing is done by a powder deposition process. At the exact location a powder (sand) is combined with a chemical agent (binder) to create a 3-dimensional element.[23]
- **Contour Crafting** The 3D printer prints layers of paste on top of each other. It is based on a thick-layer extrusion method.[23]. The paste, which is a bit like cement, is extruded against the side trowel, which will create a smooth surface finish. [20] The nozzle of a contour crafting printing robot can be seen, on the next page in figure 1.1a

- **Concrete printing** Concrete printing is a bit like contour crafting. It is also an extrusion method without use of formwork. A robot with nozzle will go to the exact location, which is digitally drawn. At this location the nozzle will put a thin layer of concrete. By building up these different layers an 3D printed element is created. [23] This can be seen in figure 1.1b.
- **Smart Dynamic Casting** Smart Dynamic Casting is the digital way of the slip forming process. The slip forming process is a way to build concrete cores in high rise buildings. Elements made by smart dynamic casting are constructed the following way: a moving formwork, much shorter than the final element, is moving upwards while concrete is being poured in the formwork [12].

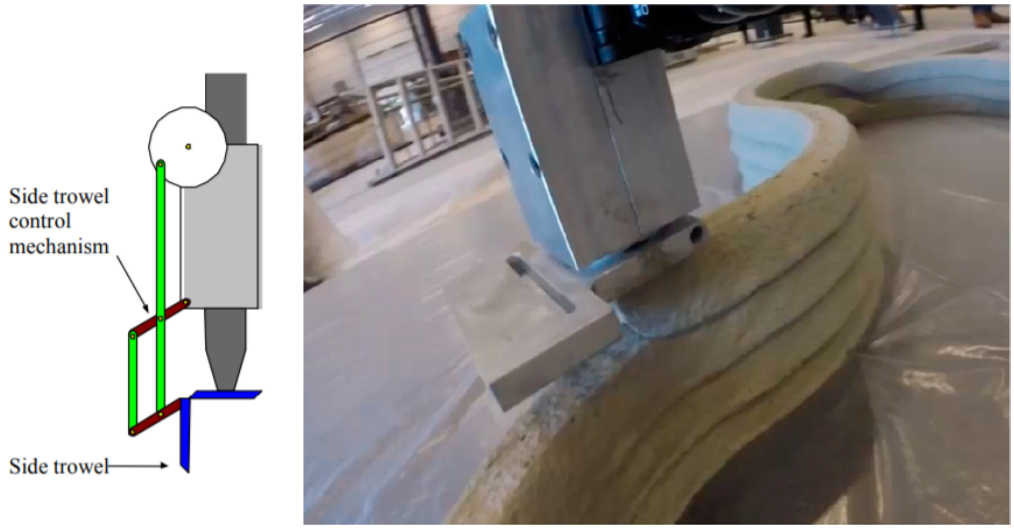

(a) Contour crafting nozzle [18]

(b) Concrete printing nozzle [9]

Figure 1.1: The different nozzles used with contour crafting and concrete printing

In this research concrete printing is the technique being used. Concrete printing is a new technique, it is not used that often and therefore little is known. One issue that usually occurs it the fact that there are no codes made for concrete printing. This concludes in a lot of research going on right now. For example: in printing of concrete columns, where the structural design is still very conservative.

1.2. Problem Definition

A 3D printed column is constructed in the following way: first the formwork is 3D printed, then the steel reinforcement is placed inside the concrete formwork, subsequently the concrete is cast inside it. It is not known yet, how to calculate the load bearing resistance of a composite (printed concrete & traditional concrete) column. This concludes in the fact that only cast concrete inside the formwork is taken into account during a calculation. This is considered as a safe method to calculate the load bearing resistance. To make a less conservative calculation, the influence of the printed concrete on the load bearing resistance of the concrete column must be known. The question is if the printed concrete and the traditional concrete will work together like a monolith structure, or if the printed concrete and the traditional concrete will not work together, which will mean that the safe method is not as conservative as thought.

This can be summarised in the following research goal:
Gain insight into the influence of a 3D printed concrete lost-formwork on the load bearing resistance of a column.

This goal will be reached by creating a calculation model which estimates the behaviour and will be verified by experiments. This will be done with a circular element, similar like a column, but shorter. The element used within this research will not contain any reinforcement.

1.3. Research questions

The main research question is stated as:

What is the influence of concrete printed lost-formwork on the load bearing capacity of a circular element?

The main research question is divided in smaller elements, which are easier to solve. These smaller elements are the sub-questions below:

- What are the mechanical and material properties of printed concrete and traditional concrete?
- How does a concrete circular element react when it is loaded by a compressive force till failure?
- How to model a circular concrete element with printed formwork in a finite element program?
- What is the influence of the following parameters?
  - The type of traditional concrete, which will fill the printed concrete
  - The volume ratio: printed concrete / traditional concrete
  - The amount of shrinkage that will take place after filling the printed formwork
  - The type of contact area
  - The boundary conditions

2

Methodology

This research will consist of five parts. The first part contains the introductions and the last part the conclusions. For the two parts in between contain the main content, please see figure 2.1 on the following page.

I Research definition

II **Theoretical framework**

III **Case study**

IV Final remarks

All the parts follow need information from the part above, to eventually end up with the answer of the research question:
What is the influence of concrete printed lost-formwork on the load bearing capacity of a cast column?

I **Research definition:** This part contains the introduction and methodology. The introduction includes the background information of this research. In this part it is explained why this research is important, what the research goal is and the questions that must be answered to reach that research goal in this report are formed. The methodology discusses the method to answer the research questions.

II **Theoretical framework:** The second part contains the theoretical framework. A theoretical background will be formed about the geometry, material properties, bonding of two types of concrete, boundary conditions and the failure mechanisms. These subjects are elements that influence the strength of the concrete printed element, provide extra knowledge to ease the decision making or make it easier to analyse the results. This chapter concludes in recommendations and boundary conditions for the choices that have to be made in the case study.

III **Case study:** The third part contains the case study. This case study contains a circular concrete element similar to a concrete column, but shorter, which is loaded by a compressive force. The concrete element will be analysed by an experiment and a theoretical finite element model. This analysis will give insight in the relation of the theoretical model and practice, the influence of the printed concrete formwork on the compressive load bearing resistance of the case study element and the influence of the different parameters on the stresses of the element.

All the parameters that influence the case study have to be discussed first. These are the geometry, material properties, contact area between the printed and cast concrete and the boundary conditions. Thereafter the experiment can be performed and the linear model can be build. The linear model will be the basis of the nonlinear model, which will be able to calculate failure. The nonlinear model will be compared to the experiment to verify the model. It will also be compared to a monolith column to find the influence of the printed formwork on the compressive load bearing capacity of the element.

The linear model will be used to find the influence of the parameters: the type of traditional concrete that will be cast inside the printed formwork, the volume ratio printed concrete/traditional concrete, the

amount of shrinkage that still has to occur after filling the concrete formwork, the type of contact area (bonded, frictionless) and the boundary conditions.

IV **Final remarks:** The final remarks contains the conclusions, recommendations and the discussion. This is the closing part of the research. The answer on the research question, the flaws in this research and ideas for further research can be found here.

An elaborate figure which explains the methodology in this research can be seen in figure 2.1. Figure 2.2 explains in short the goals of the different parts.

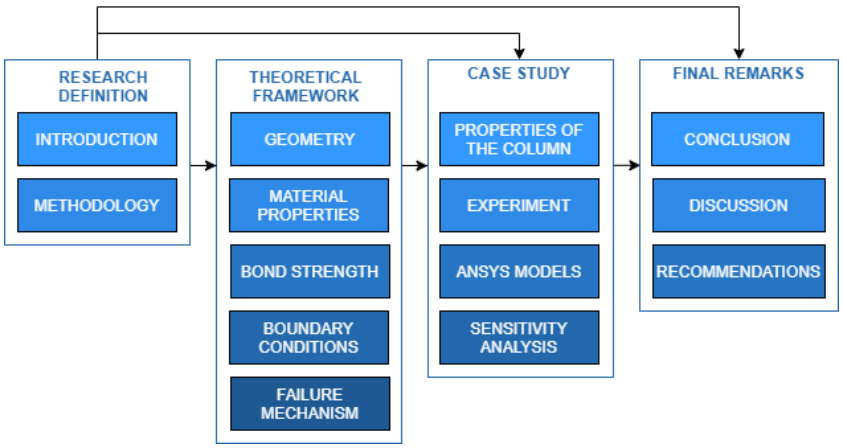

Figure 2.1: Methodology

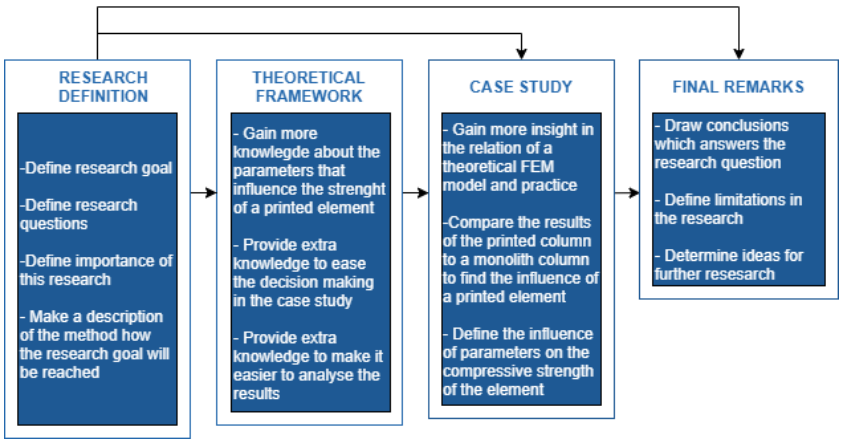

Figure 2.2: The goals of the different parts

II

Theoretical Framework

This part contains the theoretical framework for this thesis. It includes theoretical background information about the geometry, material properties, bond strength, boundary conditions and failure mechanisms. The theoretical information will give knowledge about the information about the parameters that influence the strength of the element, ease the decision making for the case study and make it easier to analyse the results of the case study. The relation of this part to the whole thesis can be seen in figure 2.3.

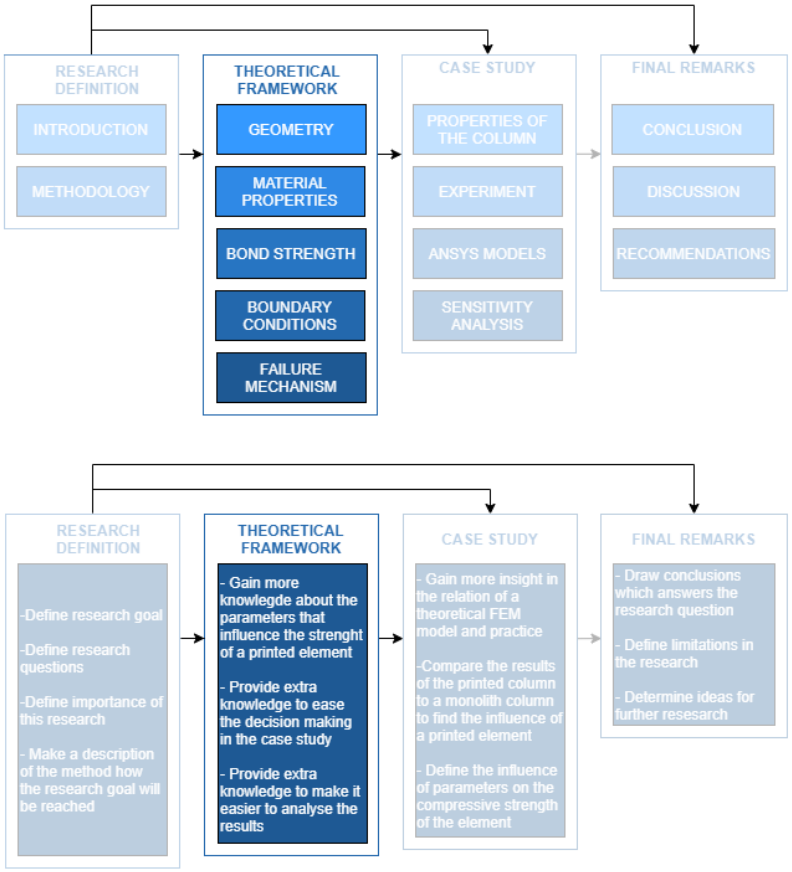

Figure 2.3: Methodology theoretical framework

3

Geometry

3.1. Introduction

The geometry of the concrete column has influence on the stress distribution, and therefore influence on the load bearing resistance. This chapter will give boundary conditions to the shapes and sizes for the case study of this research. These boundary conditions will be influenced by the ability to perform an experiment and the possibility to relate the element to the reality.

3.2. Shape of the column

The shape of the column influences the stress distribution. To reduce the variables in this research are chosen to investigate a column with a circular shape. Because this research is something completely new, it is chosen to start with a basic column shape. From the basic column shapes there can be chosen from circular or rectangular. The rectangular shape contains sharp corners, which are not possible to be printed by a concrete 3D printer, therefore is a circular shape a more obvious choice. The circular shape has the advantage that the shape is symmetric in all directions. To make the column basic, it will be straight and will have the same cross-section over the whole length.

3.3. Dimensions of the column

The dimensions are primary restricted to the experiment that will take place. At the same time the element will preferably be as realistic as possible.

- *Printing limitations*: The printed concrete element will be printed with the printer of BAM in Eindhoven. This printer can print a full size column. When it starts to become too slender stability measurements have to be taken into account. It is possible to print with the following width: 50, 70 or 100mm (figure 3.1, on the next page). From experience the width can differ with 5 mm. In height there will be limitations due to the stability of the printed formwork. If new print layers on top of the earlier printed layers are applied, the weight of the new layers will load the earlier printed layers. As the earlier printed layers area not that old, they are also not that strong. This means that the element can collapse. It is also possible for the printed part to buckle.

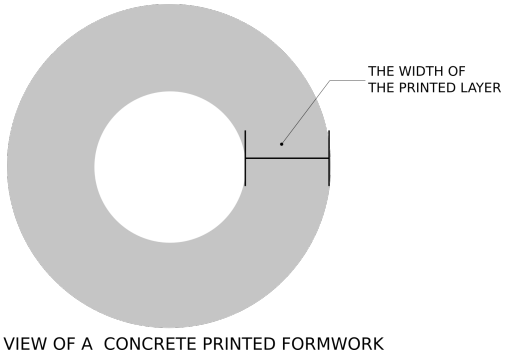

Figure 3.1: The top of a concrete printed formwork, which shows the width of the concrete printed layer

- *Transport limitations*: The printed column will be tested at the Technical University of Eindhoven or at the TU Delft. Because the column will be printed at the printer of BAM in Eindhoven transport is needed. Preferably by car, because this is the most cheap and easy way. This means that the height of the column cannot be larger than 1000mm. A limitation due to lifting of the column might be necessary. Everything more than 50kg cannot be lifted by humans. Most things can be carried by the forklift, but this is not possible everywhere. During all transport damage of the elements should be avoided.

- *Experiment limitations*: There are 2 different standard test setups to perform a compressive test in Eindhoven. One has a limit of 2500 kN: with this machine it is possible to measure deformations and the failure load. The other has a limit of 4000 kN, but this machine will only give the failure load. It is also possible to build a special test setup, which can have other dimensions and limits, this is less standard and therefore more expensive to perform. To estimate the failure load of a concrete column, it is calculated with the GTB graph in figure B.4 (Appendix B). The strength of the column will be calculated without safety factors, as they will be compared to experiments.

- *Scaling limitations*: Scaling limitations depend on the width of the print path and the diameter of the whole column. Ideally the ratio printed concrete and traditional concrete will be similar to a 1:1 column. One thing to take into account is the fact that the diameter of the traditional concrete part must not be too small in comparing to the printed concrete. The height width ratio of a traditional concrete column is mostly: $Height = Width * 10$.

3.4. Conclusion

The column will straight, with the same circular section over the whole length. To perform the experiment there are some limitations to the element. These boundary conditions can be separated in transport, experiment and scaling limitations. The limitations can be seen in table 3.1.

	Diameter	Height	Weight	Strength
Printing limitations	W_{print}= 50, 80 or 100 mm	prevent collapse	none	none
Transport limitations	none	1000mm	50kg	none
Experiment limitations	none	unknown	none	4000kN (preferably 2500kN)
Scaling limitations	$H = D * 10$	$D = H/10$	none	none

Table 3.1: Boundary conditions of the research due to the experiment, the geometry definitions are explained in figure 3.2

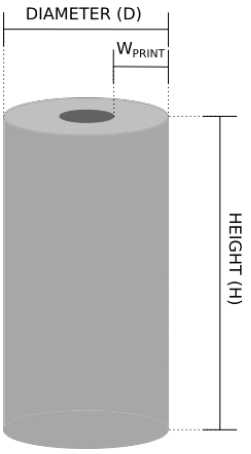

Figure 3.2: The graphic explanation of the geometry definitions of table 3.1

4

Material properties

4.1. Introduction

The material properties have influence on the stresses and the strength of the column. The printed column exists two different types of concrete, with both different properties. The interaction between these materials is depending on the properties. The material property: shrinkage, needs extra attention in this chapter. The shrinkage of printed concrete is very large in comparing to traditional concrete, therefore this subject is discussed more elaborately. [26]

4.2. Type of printed concrete

The concrete that will be used for this research is Weber 3D 160-1. This type of concrete is used at the 3D printer of BAM. The properties can be found in table 4.1.

4.3. Type of traditional concrete

The type of traditional concrete is still free of choice. There are a few factors to be taken into account when a type of material is chosen, because of the substantial difference between traditional and printed concrete. There can be chosen to pick a traditional concrete which is in strength, Youngs modulus or in shrinkage similar to the printed concrete. This has different effects on the final strength of the column.

- **Similar strength:** The column will have the same strength. It will fail at the same stress.
- **Similar Young's modulus:** If the E-modulus of the materials are similar, the two materials will contain similar stresses when the same displacement is applied.
- **Similar shrinkage:** The two types of materials in the element will restrict each other to deform. This restricted shrinkage causes stresses. The two materials shrink the same amount, no shrinkage will be restricted and no stresses will occur due to shrinkage.

4.4. Shrinkage

The difference in shrinkage is expected to have a large influence in the stress distribution in the column. Therefore a separate chapter to discuss the phenom shrinkage. Shrinkage in concrete can have two different causes: shrinkage related to water, and shrinkage related to temperature. First the shrinkage related to water will be discussed.

Shrinkage related to water

There are three types of shrinkage, which are related to water:

- Plastic shrinkage
- Autogenous shrinkage
- Drying shrinkage

Plastic shrinkage occurs before the chemical process that creates cement to concrete has taken place. When the cement, aggregates and water are mixed, it separates water from the mix (bleeding). The more heavier parts will sink, the lighter parts will go to the top. Depending on the humidity of the outer air water evaporates from the mix. The evaporation reduces the mass and volume of the mix, which is considered as shrinkage.

Evaporation of water creates a different equilibrium between: the relative humidity in the pores, the amount of absorbed water by the pore wall and the amount of capillary water (figure 4.1). If water evaporates, the relative humidity reduces and the surface tension causes a reduction in volume of the concrete.

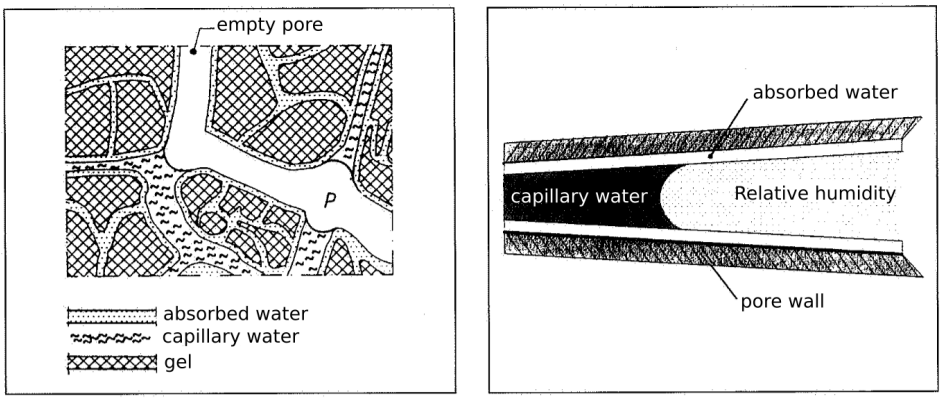

Figure 4.1: A schematic representation of the equilibrium between the relative humidity, amount of absorbed water by the pore wall and the amount of capillary water [30]

Plastic shrinkage happens in the first few hours and can be reduced by covering the mix, place it in a room with a large humidity.

[30]

Autogeneous shrinkage occurs during the chemical process that transfers the cement mix into concrete. The volume of the hydration product of water and cement is smaller than the summation of original volumes of water and cement. This is makes the concrete to shrink. It causes internal cracks (look like pores) in the concrete. The mass of both stages stays the same. This types of shrinkage happens during a few months. The amount of shrinkage differs per type of concrete, but it will take place in all cases.[30]

Drying shrinkage occurs during, or after the chemical process that transfers the cement mix into concrete. Free water evaporates, this gives a reduction in the volume and mass of the concrete element. This type of shrinkage will happen till the end of the lifetime of the structure. The amount of shrinkage depends on the humidity of the place the concrete element is located. [30]

Thermal shrinkage

During the chemical reactions in the hydration, heat will be one of the resulting products. The temperature in the hardened concrete will increase, and as a result of that, the young concrete wants to expand. The tension that might occur is really small because of the fact that young concrete is not that stiff yet. If the concrete cools down again, the strength and the stiffness have reached such an level that the concrete wants to shrink. If this shrinkage is prevented, cracks will occur. The thermal shrinkage is dependent on the expansion coefficient. The aggregates will play an important role in defining this coefficient. [30]

The strain can be calculated by [30]:

$$\epsilon = \Delta T \times \alpha \tag{4.1}$$

ϵ = Strain due to temperature differences
α = Expansion coefficient
ΔT = Temperature difference

Shrinkage in concrete printed elements
Printed concrete is more sensible for shrinkage than traditional concrete. There are multiple factors influencing this.

- When an element is printed, it is in direct contact with the outer air. This will have a negative effect on the plastic shrinkage and the drying shrinkage. The mortar and the concrete can both, very easily, lose water in the air.
- The mortar which is used when printing an element, contains a high cement ratio and little large aggregates. This concludes in relatively large shrinkage. [10]

The difference between the shrinkage in the cast concrete and the printed concrete can cause stresses if they prevent each other to deform. Plastic shrinkage can be reduce by curing the concrete. Autogenous shrinkage will happen anyway, this will be the most relevant type of shrinkage. Drying shrinkage happens over years, this will not cause significant difference in amount of shrinkage between the two materials if the cast within a relative short time.

The shrinkage of the printed concrete: Weber 3D 160-1 is equal to: <1,0 mm/m = 1000 m/m.

The shrinkage of traditional concrete will be around 0,1 to 0,8 mm/m. This can be increased by the following factors: increase the amount of cement paste, increase the W/C factor, decrease the relative humidity, increase the amount of cement, decrease the average radius ($h_0 = \frac{\text{area of the cross-section}}{\text{circumference of the cross-section of the part exposed to drying}}$) of the element, choose a cement type which hardens faster. [24]

4.5. Conclusion

The choice of the traditional concrete to fill the lost framework with, depends on the strength, shrinkage and E-modulus. The printed concrete which is used at the printer of BAM will be used in this research. This type of concrete is called: Weber 3D 160-1. The material properties can be seen in table 4.1.

The shrinkage in the printed concrete is large in comparing to the traditional concrete. This might cause stresses if the two materials restrict each other to deform. Plastic shrinkage can be prevented if by curing the concrete. Drying shrinkage will not cause a significant difference in shrinkage between the printed and traditional concrete if the traditional concrete is cast inside the printed formwork within a year. There can be concluded that the autogenous shrinkage will be most relevant to define the stresses that might occur due to restricted shrinkage.

Material properties	
Property	Weber 3D 160-1
f_{ck}	50 MPa
Density	2200 kg/m3
Shrinkage	<1,0 mm/m

Table 4.1: Material properties of printed concrete [26]

5

Bond Strength

5.1. Introduction

The contact area between the printed and traditional concrete is an unknown factor. This influences the stress distribution as it does or does not transfer forces to one another. Whether it transfers stresses depends on the bond strength between these materials.

5.2. Types of bond strength

There are two main types of bond strength: based on tension and based on shear[28]. In the figure 5.1 and figure 5.2 the two main types of bond strength are shown.

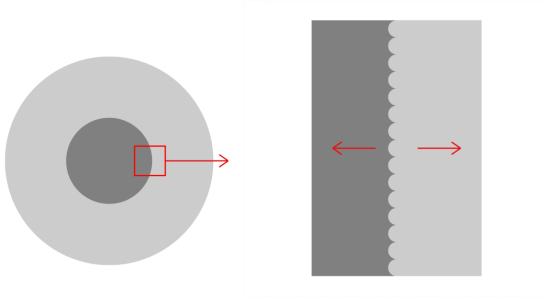

Figure 5.1: The top of the concrete element, which shows the bond strength based on tension

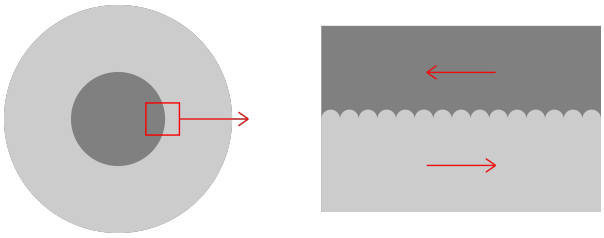

Figure 5.2: The top of the concrete element, which shows the bond strength based on shear

5.3. Influencing factors

There are different factors that influence the bonding strength of concrete structures. The most important factors which can influence the bonding in a negative way are: micro-cracking, a laitance layer, no clean surface, no compaction and no curing. In figure 5.3 a graph is showing the factors that might influence bonding of concrete.[28] These different factors can be divided in the following groups [11]:

- **Substrate characteristics:** Microcracks, laitance layer and cleanliness
- **Overlay characteristics and application technique:** Compaction and curing

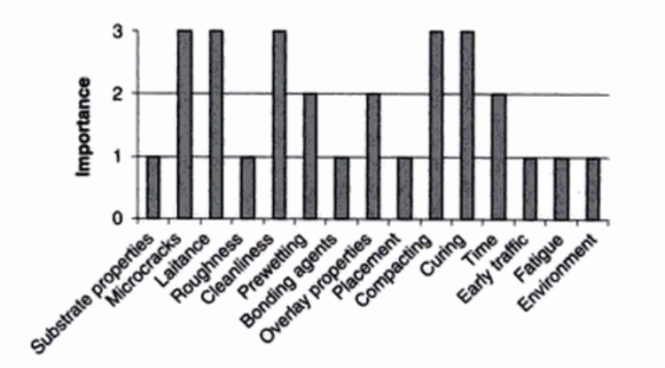

Figure 5.3: Factors that influence the bond strength of concrete structures. 3: a lot of influence, 2: medium influence, 1: little influence [28]

- **Microcracks**

  Micro-cracks in the surface of the older concrete can occur during surface treatments. These treatments are used for cleaning, removing laitance layer and roughening the surface. [11] In section 5.5 surface treatments are better explained. There are also other ways how micro cracks can occur, for example shrinkage.

- **Laitance**

  Laitance is a layer of cement and fines form the aggregates brought on top by bleeding. This is a weak and non-durable material because it contains a lower water/cement ratio and therefore reduces the bonding strength of concrete. [28]

  A laitance layer in a concrete printed structure can be seen in figure 5.4. It this picture, the laitance layer can be seen so clear due to the following phenomena: When the volume mortar per minute is everywhere the same in the whole element, the width of the layers will increase in the corner because of the difference in speed that occurs when the nozzle rotates. This causes a visible laitance layer.[19]

Figure 5.4: Visable laitance layer in printed concrete at the corner [19]

- **Cleanliness**

  A clean surface is needed to guarantee proper bonding. Loose particles and dust will reduce the bonding intensively

- **Compaction**

  Compaction is important to prevent air pockets in the surface structure. It creates an dense and homogeneous concrete which has a uniform bond with the printed concrete.[28]. Most probably will the column be too small to compact the traditional concrete.

- **Curing**

  Curing of concrete is mostly done to reduce plastic shrinkage and to ensure full drying of the concrete.

  Curing can be done in the following way [22]:

  - **Curing with water**
    - ◇ A layer of water
    - ◇ Spray with water
    - ◇ Sand or soil, in case it does not have any harmful elements
    - ◇ Straw or hay with a thickness of at least 15 cm
  - **Curing by sealing**
    - ◇ Plastic foil
    - ◇ Fibre reinforced bitumized paper
    - ◇ Curing compound: Cannot be applied on surfaces where bonding of other materials is needed, unless it is proven that there are none negative effects. [22]

  The time needed for curing the concrete (curing time) is dependent on the hardening-time and the hardening-temperature (strength development).

  At the 3D printer in Eindhoven, plastic foil is usually used to protect the concrete element in the drying process.

- **Surface roughness**

  Figure 5.3 shows that the surface roughness has less influence than the other parameters on the bond strength. The interface of a concrete printed formwork exist of a really rough surface, this might have a lot of influence on the load bearing resistance of the printed column and will be taken into account within this research. This rough surface will have a positive effect on the bonding between the printed and cast concrete. The positive effect occurs due to interlocking of the two materials.

  There are a few different things that can be meant with a surface. [29] Drawings that show these different surface areas can be seen in: figure 5.5

  - **Geometrically surface area**
    This is the area which does not take the roughness into account.
  - **True surface**
    This is the exact area of the surface, it takes all the small ribs into account.
  - **Effective surface area**
    This is the area which is equal to the amount of surface area that touches the printed and cast concrete.

  The larger the effective area, the better the bond. This means the that bonding depends on the fact if the cast concrete will touch every part of the true surface. It can also happen that the ridges of the concrete printed formwork will break off.

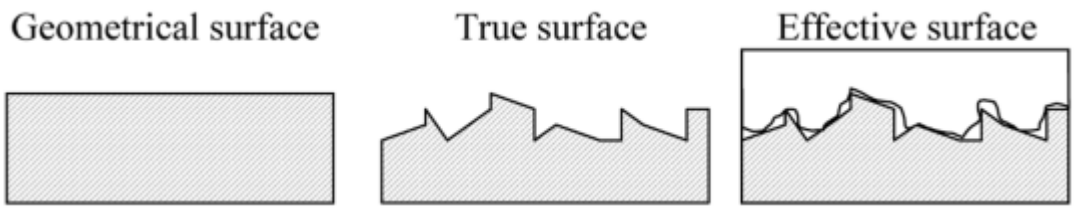

Figure 5.5: Three different things that can be meant with the word "surface": Geometrical surface, true surface and effective surface [29]

There are different ways to measure the roughness of a surface. The Eurocode [21] use a visual inspection to determine if the surface is very smooth, smooth, rough of very rough. This is subjective and can therefore easily lead to the wrong results. [27] Other methods can been seen in figure 5.6.

Roughness quantification method	Quantitative evaluation	Non-destructive	Cost	Portability	Work intensive	Contact with surface
Concrete Surface Profiles	No	Yes	Low	Yes	No	No
Sand Patch Test	Yes	Yes	Low	Yes	No	Yes
Outflow Meter	Yes	Yes	Low	Yes	No	Yes
Mechanical Stylus	Yes	No	Medium	No	Yes	Yes
Circular Track Meter	Yes	Yes	Medium	Yes	No	No
Digital Surface Roughness Meter	Yes	Yes	Medium	Yes	No	No
Microscopy	Yes	No	High	No	Yes	No
Ultrasonic Method	No	Yes	Medium	Yes	No	No
Slit-Island Method	Yes	No	Low	No	Yes	Yes
Roughness Gradient Method	Yes	No	Low	No	Yes	Yes
Photogrammetric Method	Yes	Yes	Medium	Yes	Yes	No
Shadow Profilometry	Yes	Yes	Low	Yes	Yes	Yes
Air Leakage Method	No	Yes	Low	Yes	No	Yes
PDI Method	Yes	No	Low	No	Yes	Yes
2D-LRA Method	Yes	Yes	Medium	Yes	No	No
3D Laser Scanning Method	Yes	Yes	High	Yes	No	No

Figure 5.6: Different methods to define the roughness of a concrete surface [27]

An ideal method will be quantitative and non-destructive[27] For this research it will also be important to be a method with low costs and one which is not work intensive. This means that a the Sand Patch Test and the Outflow Meter are best suitable in this case.

- **Sand Patch Test**

  This test is originally made to measure the roughness of pavement. In this test a known volume of sand is spread over a clean and dry surface. When the area which is covered is calculated, the average depth can be determined. This test is prescribed in the ASTM International Standard. This test is not applicable for grooved surfaces. [1] This means that this test cannot be used to define the roughness of the printed surface.

- **Outflow Meter**

  This test is originally made to measure the texture drainage of pavement. This method will give an average value for the surface roughness. It works as follows: A cylinder with a rubber ring where it touches the surface, is filled with water. The time needed for water to flow out of this cylinder indicates the surface roughness. A big disadvantage is that the permeability of the material can influence the result.

The results of these experiments needs to be analysed to relate them to the strength of the element.

5.4. Definition bond strength

Eurocode 2 [21] contains a formula to calculate the shear resistance at the connecting surface between concrete of different ages. This method is not ideal because it needs a visual inspection of the roughness, which makes is subjective. [27]

$$v_{\mathrm{Edi}} \leq v_{\mathrm{Rdi}} \tag{5.1}$$

$$v_{\mathrm{Edi}} = \beta V_{\mathrm{Ed}} / (z b_{\mathrm{i}}) \tag{5.2}$$

$$v_{\mathrm{Rdi}} = c f_{\mathrm{ctd}} + \mu \sigma_{\mathrm{n}} + \rho f_{\mathrm{yd}} (\mu \sin\alpha + \cos\alpha) \leq 0,5 \nu f_{\mathrm{cd}} \tag{5.3}$$

With:

β = The relation between the longitudinal force in the youngest concrete and the total longitudinal force in the compressive or tensile zone, both calculated for the considered

V_{Ed} = Shear force

z = The lever arm of the considered cross section

b_i = The width of the connected surface

c and μ = factors which depends on the roughness of the surface, these factors differ if the surface is very smooth, smooth or rough. This classification can be done visually.

σ_n = The stress per surface caused by the minimum external normal force perpendicular to the connecting surface which can occur at the same time with the shear force. It is positive for pressure, and negative for tension. In case of tension $cf_{ctd} = 0$, in case of pressure: $\sigma_n < 0.6 f_{cd}$

$\rho = A_s / A_i$

A_s = The area of the reinforcement which crosses the connecting surface, including eventual stirrups, with enough anchoring at both sides

A_i = Surface of the connection

α = In between $45^\circ \leq \alpha \leq 90^\circ$

ν = Strength reduction factor = $0,6(1 - f_{ck}/250)$

In case of the concrete printed column the following values can be assumed:

c and μ = The surface is considered as a rough surface: c=0,4 and μ = 0,7

σ_n = The stress per surface caused by the minimum external normal force perpendicular to the connecting surface which can occur at the same time with the shear force. It is positive for pressure, and negative for tension. In case of tension $cf_{ctd} = 0$, in case of pressure: $\sigma_n < 0.6 f_{cd}$

$\rho = A_s / A_i = 0$

A_s = No reinforcement is crossing the two surfaces = 0

ν = Strength reduction factor = $0,6(1 - f_{ck}/250)$

5.5. Surface treatment

The negative influence of the substrate characteristics (existence of laitance and not enough cleanliness) can be reduced by using a surface treatment. These treatments are used for cleaning, removing a laitance layer and roughening the surface [11]. There are different techniques that can be used like: wire-brushing, shot blasting, grinding, sand water blasting, water jetting chipping, use of a pneumatic hammer, milling and hydro demolition. [16] Some of these techniques are relatively aggressive (the use of a pneumatic hammer for example), they can only be used in combination with a high concrete substrate strength to prevent micro-cracking. The more aggressive the techniques used, the more it increases the surface roughness. [11]

Surface treatment is an extra manual action that can be performed during the production process of the column. The main advantage of concrete printing is the fact that little interference is needed to produce a concrete element. Using a surface treatment makes it less efficient to use concrete printing. Most likely, the printed concrete will get damaged due to the surface treatments, because it is a thin and vulnerable concrete layer. To avoid this no surface treatment will be used in this research.

5.6. Experiments used for bonding

To make sure the bonding strength is as calculated experiments can be performed. Different types of tests can be used to test the bonding of concrete: Tensile bond, slant-shear, twist-off, flexural strength and patch tests.[6] In this research only the core pull off test and the slant shear test are explained as these are considered most standard.

Core pull off test: This test is a tensile bond strength test. A core is drilled in a repaired element, through the repair material. At this location a metallic disk is glued with a suitable epoxy adhesive to the upper surface. Thereafter, it is pulled by a tension machine till failure. In figure 5.7, on the next page the test is drawn.

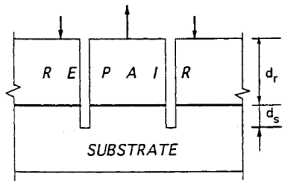

Figure 5.7: Core pull off test, which defines the tensile bond strength between two materials[5]

Slant shear test: A slant shear test measures the bond strength of two types of concrete with different casting times. This test is used by many manufactures to determine the properties of their repair material. The experiment is best explained in figure 5.8. The α will mostly be 30 degrees, which is the standard value. Extra attention have to be paid to the following shortcomings of this test: the failure is dependent on α, it is also very dependent of the surface roughness and it is sensitive to differences in E-modulus[6]

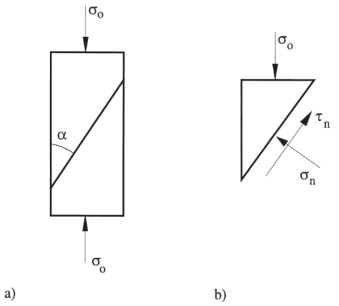

Figure 5.8: Slant Shear test, which defines the bond strength between two materials [6]

5.7. Conclusion

Bonding of two different types of concrete of different ages will influence the stress distribution in an element. The bond strength can be divided in tensile and shear bond strength. The shear bond strength can be calculated with Eurocode 2[21]. This has as disadvantage that the method used to define the surface roughness for this formula is subjective. Another method is to perform an experiment: the core pull off test for tensile bond strength or the slant shear test for shear bond strength.

6

Boundary conditions

The boundary conditions influence the stress distribution in the column. The boundary conditions in reality are mostly different than at the experiment.

In reality

The boundary condition of a column depends on the structure in which the column is implemented. Hinged and clamped conditions are possible, these are shown in figure 6.1. The hinged and clamped versions shown in the figure, are schematizations of the reality.

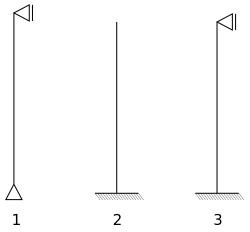

Figure 6.1: Schematizations of different boundary conditions, that are relevant for a column

At the Experiment

The concrete element will only be restricted in vertical direction at the experiment. The friction between the concrete element and the machine plate define the resistance in the horizontal directions. This resistance indicate the boundary conditions. If the friction between the machine plate and the concrete element is high, the element is not able to translate in horizontal direction. If the friction is low, translations and rotations can exist. This can be seen in figure 6.2. During the experiment the stresses will occur by translating the machine plate on top of the column in vertical direction.

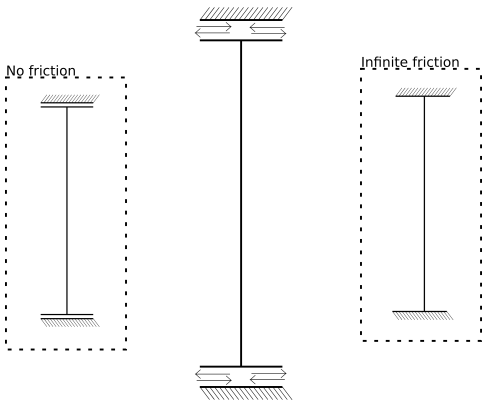

Figure 6.2: A schematization of different boundary conditions that might occur during the experiment

7

Failure mechanisms

7.1. Introduction

There are different ways for concrete columns to fail. This can happen when the stresses in the element are higher than the ultimate compressive, tensile or shear stresses. A crack in the element does not mean it failed, the column is failed when it cannot perform its main function anymore.

A circular element consisting of two materials will be tested in a compessive testing machine at the experiment. This is pretty similar to a circular compressive test which is used to define the strength of concrete. Both are a circular concrete element loaded in compression. The largest difference is the fact that the circular compressive test is performed on an monolith element, while the printed element consists of two different materials. Keeping this last fact in mind, the failure methods of the concrete compressive test can give insight in the failure mechanisms of the column of this research.

7.2. Circular compressive test

The International standard ASTM C39/C39M-18: Standard Test Method for Compressive Strength of Cylindrical Concrete Specimens, describes this method to define the concrete strength and gives several possible failure mechanisms that might occur. [4]. All these possible failure mechanisms can be seen in figure 7.1, on the next page. The friction between the machine plates and the test specimen will have a substantial influence on which failure mechanism will occur [7]. In figure 7.2 on the next page, an explanation can be seen: the friction between the machine plate and the specimen causes shear stresses at the top and bottom of the column. The shear stresses occur due to later expansion. Small horizontal displacements occur due to the prescribed vertical displacement which is applied at the top of the column .When these horizontal displacements are restricted, shear stresses occur. The shear stresses create the hourglass failure mode which can be seen in type 1 of figure 7.1, on the next page. Failure mechanism type 3 occurs if (almost) no friction between the specimen and the machine plate is present. This can be seen by the fact that cracks are vertical. Type two indicates a combination between the conic (type 1) and the column-like (type 3) failure. The hourglass failure mechanism is the most common one. If another failure mechanism than type 1 occurs during an experiment, it has mostly something to do with the geometric features instead of the material itself. There are also other factors that might influence the failure mechanism or the failure strength which is defined during an experiment: the stress rate, the height to base ratio, surface-related defects (horizontally, parallelism) and contact related defects (friction and roughness between specimen and the machine) [7]

Failure mechanism type four demonstrates pure shear failure. When failure mechanisms type 5 or 6 occur, the maximum failure load has not been reached yet and there must me continuing loading the specimen, to reach complete failure. [4].

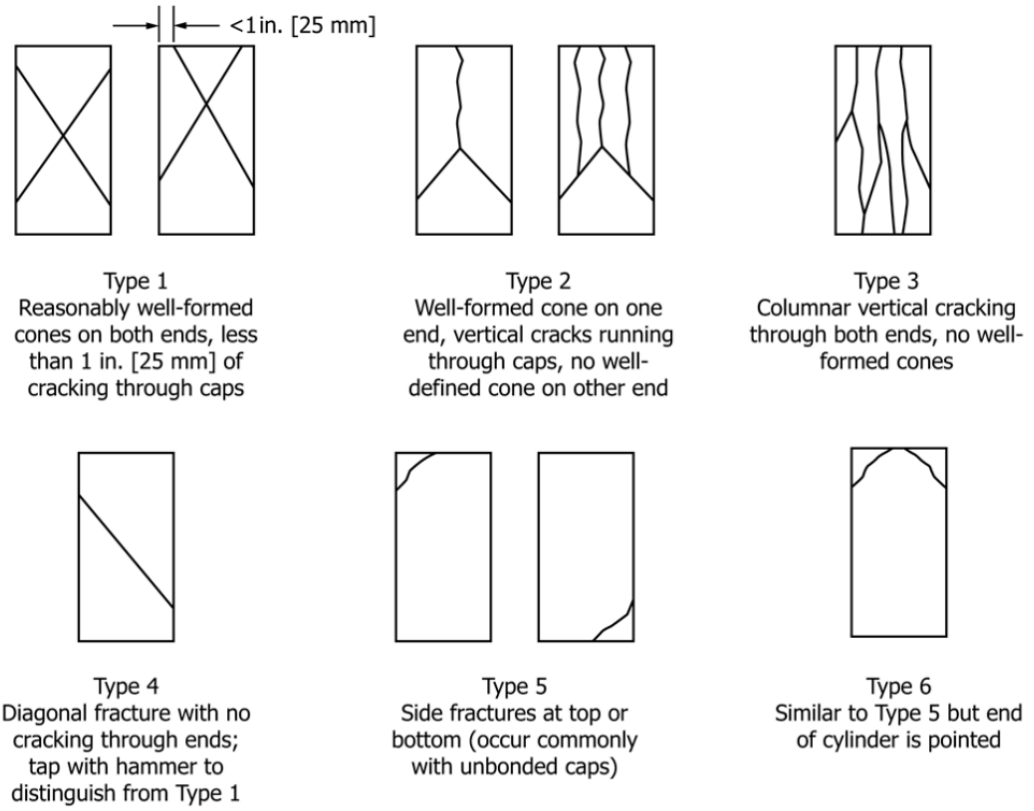

Figure 7.1: Failure mechanisms of a cylindrical compressive strength test [4]

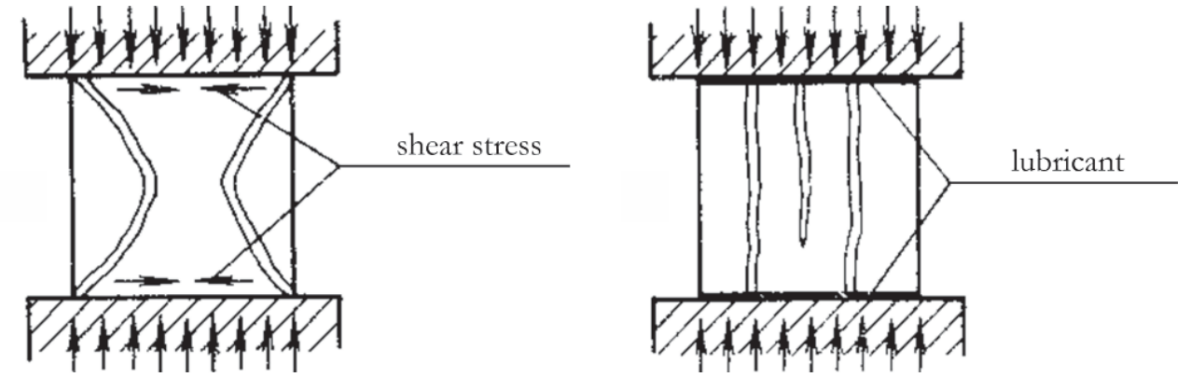

Figure 7.2: The influence of shear on the failure mode on a cylindrical compressive strength test [7]

7.3. Conclusion

There are four different types of failure with in case monolith concrete cylinder is tested for its loadbearing capacity. These mostly differ because depending on the friction between the machine plate and the concrete element. If the concrete cylinder contains vertical cracks, little to none friction between the element is present. If diagonal cracks with a corner of around 45 degrees can be seen, it means shear forces took overhand. This mostly happens when the surface between the element and the machine has a high friction. This is true of a monolith element, which is not the case with the printed concrete. This means that these failure mechanisms cannot be directly implemented in this research.

III

Case Study

This part of the thesis contains a case study. First the properties of the case study are discussed. These properties are implemented in the experiment. The experiment is a compressive test performed on the concrete printed element. In this part the experiment itself, and the results are discussed. With the same properties two Ansys models are made: a linear and a nonlinear model. The linear model forms the basis for the nonlinear model and will be used for the sensitivity analysis. The results of the nonlinear model will be compared to the results of the experiment. This will verify the finite element model. It will also be compared to a monolith element, to check the influence of the printed formwork on the compressive load bearing resistance of the element. At last a sensitivity analysis will be discussed. The influence of several parameters (discussed in the corresponding chapter) on height of the stresses in the element will be researched. The relation of this part in comparing to the whole thesis can be seen in figure 7.3

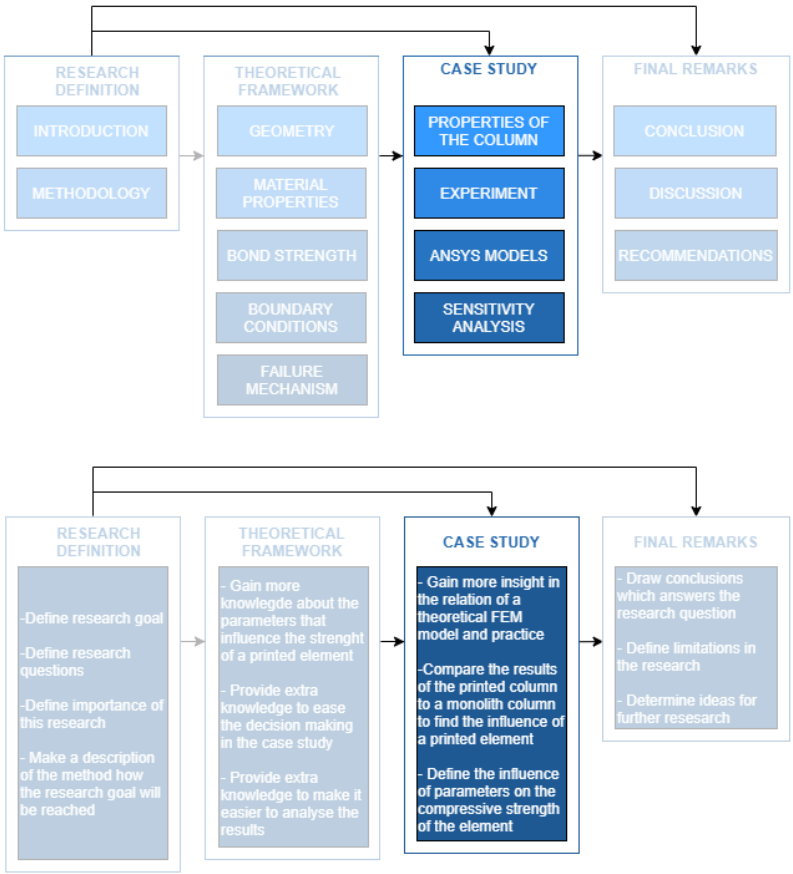

Figure 7.3: Methodology case study

8

Properties of the concrete element

8.1. Introduction

This chapter contains the dimensions and material properties of the concrete element which will be used for the case study. First the dimensions are discussed, afterwards the strength, Youngs modulus, Poisson factors and the shrinkage of both materials at the time of the experiment. The experiment will take place after 6 days, otherwise the concrete element will be too strong. The traditional concrete will be cast inside the printed formwork one day after the element is printed. This means that the traditional concrete will be 5 days old.

8.2. Dimensions

The experiment and the Ansys model are based on a printed concrete element with the properties as shown in table 8.1. The properties are chosen together with BAM Infraconsult, who needed to perform a similar experiment. The size of the column is decided with transport requirements as highest priority, this means that the scale of the column is not realistic. The column is a bit to heavy to carry by humans, the forklift is used as much as possible.

Parameters	
Geometry	
Shape of the column	Circular
Diameter column	250 mm
Length column	470 mm
Width printed concrete	80 mm
Weight column	max. 51kg

Table 8.1: The geometrical properties of the concrete element used in the case study

8.3. Compressive strength

The printed formwork is made of the concrete: Weber 3D 160-1. During the experiment the concrete compressive strength of the printed concrete has been determined. A strip has been printed, three test specimen are cut out of this strip. All the specimen have the following size: 40x40x100 mm^3. During a comperssive strength test, the average compressive strength of the specimen is determined to be equal to 45,3 MPa at the age of 6 days.

Weber Constructiebeton 100 is used to fill the concrete printed formwork. This concrete has the strength class C30/37. At the time of the experiment, the concrete was only 5days old. The strength is determined by testing the compressive strength of 3 cubes of 100x100x100 mm^2. The concrete in these cubes have the same age as the concrete used in the experiment. The average compressive strenght was equal to 36.1 MPa at the age of days.

8.4. Tensile strength

The tensile strength of the material has not been tested. Assumed is that the tensile strength of printed concrete is equal to the tensile strength of the equivalent traditional concrete C50/60. The tensile strength at the time of the experiment has been calculated with Eurocode 2 [21]

Printed concrete
f_{ctm} = 4.1 MPa [21]
t = 6 days
s = 0.2 (which is the smallest value, most safe)
α = 1 (if t < 28)

$$\begin{aligned} \beta_{cc}(t) &= exp(s(1-(\frac{28}{t})^{\frac{1}{2}})) \\ \beta_{cc}(6) &= exp(0.2(1-(\frac{28}{6})^{\frac{1}{2}})) \\ \beta_{cc}(6) &= 0.792907 \end{aligned} \tag{8.1}$$

$$\begin{aligned} f_{ctm} &= (\beta_{cc}(t))^{\alpha} * f_{ctm} \\ f_{ctm} &= (0.792907)^{1} * 4.1 \\ f_{ctm} &= 3.25Mpa \end{aligned} \tag{8.2}$$

Traditional concrete
f_{ctm} = 2.9 MPa [21]
t = 5 days
s = 0.2 (the smallest value, which is most conservative as it reduces the tensile strength)
α = 1 (if t < 28)

$$\begin{aligned} \beta_{cc}(t) &= exp(s(1-(\frac{28}{t})^{\frac{1}{2}})) \\ \beta_{cc}(5) &= exp(0.2(1-(\frac{28}{5})^{\frac{1}{2}})) \\ \beta_{cc}(5) &= 0.760875 \end{aligned} \tag{8.3}$$

$$\begin{aligned} f_{ctm} &= (\beta_{cc}(t))^{\alpha} * f_{ctm} \\ f_{ctm} &= (0.760875)^{1} * 2.9 \\ f_{ctm} &= 2.20654MPa \end{aligned} \tag{8.4}$$

8.5. Youngs modulus

The Youngs modulus is a material property which will influence the stress distribution. It defines the elasticity of the element. This parameters will be different for printed and traditional concrete.

The Youngs modulus of the printed concrete at the time of the experiment has not been tested. An estimation of the E-modulus will be made with the help of the experiment on the hollow concrete element. This experiment took place at the same time as the experiment of the filled concrete element. A description of the experiment, including results, can be seen in the appendix A. When the concrete behaves elastic, the Youngs modules can be defined by dividing stress by strain.

- **Strain**

  To define the strain, the vertical deformation of the element during the experiment is needed. The strain can be estimated by digital image correlation: This method can be used to measure changes in pictures. Ncorr is a program made by Justin Blaber from the Georgia Institute of Technology based on MATLAB software, which can perform a digital image correlation analysis [8]. A movie which was made during the experiment is used to retrieve the needed pictures. The result of the digital image correlation can be seen in figure 8.1, on the next page. It is important to measure the strain before any cracks occur, this makes sure that the material still behaves elastic at the time of the measurement. It is chosen to choose it just before

- **Stress**

  To define the stress in the column, the results from the experiment can be used. The test machine gave as a result the force applied on the element, deformation in horizontal direction at the middle of the element and the deformation of the machine in vertical direction. The graph showed in figure 8.2 on the next page, can be used to define the force just before cracking of the element. A buckle in the graph shows a crack: the force increases, but the deformation does not. This moment, just before the first crack occurs, will be used to define the Young's modulus.

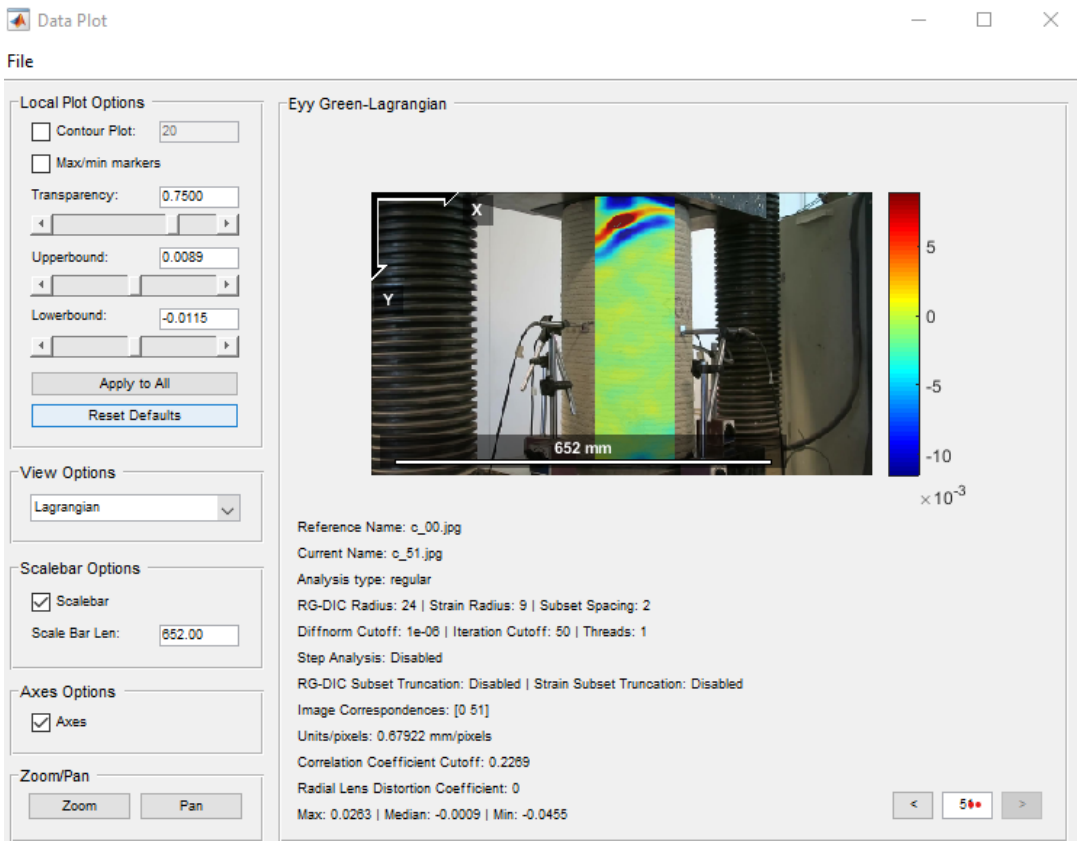

Figure 8.1: The vertical strain of the concrete printed hollow element, used to define the Young's Modulus of printed concrete. The strain is measured just before cracking, by digital image correlation

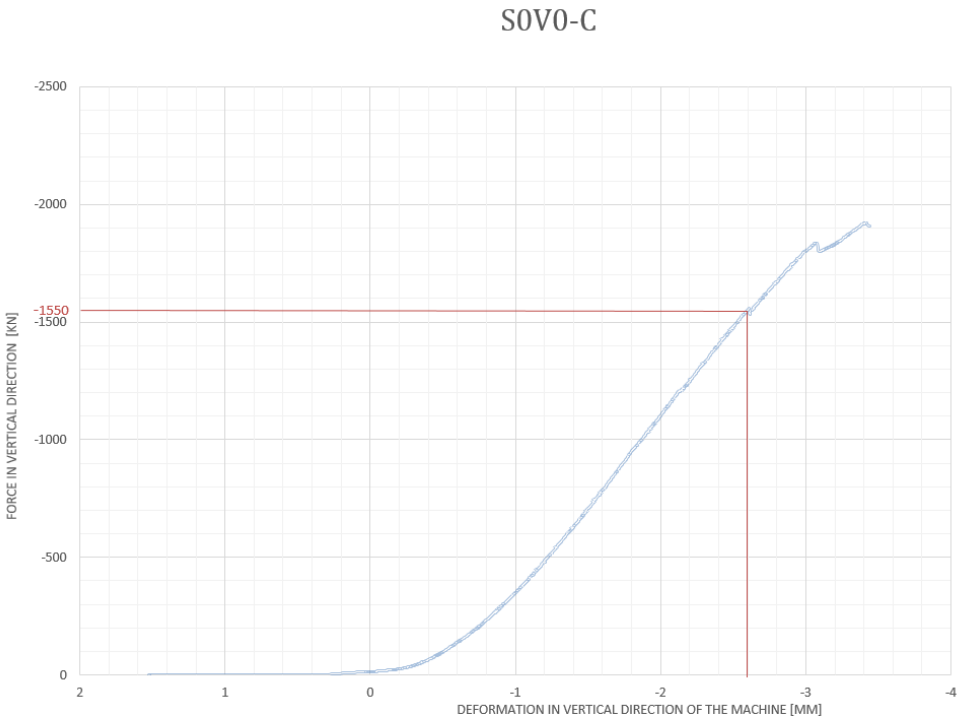

Figure 8.2: The force displacement diagram of the concrete printed hollow element, used to define the Young's Modulus of printed concrete. It shows the force applied on the hollow printed concrete element, before any crack that influences the vertical displacement occurred

The median strain measured with digital image correlation is equal to -0.0009 (figure 8.1). The amount of loading at the time of the crack is equal to 1550 kN, this can be seen in figure 8.2. The stress is calculated with formula 8.5. The Young's modulus can be estimated by dividing the strength at the first crack, by the deformation at the first crack. This can be seen in forumula 8.6.

$$\begin{aligned} \sigma_{print} &= \frac{F_{C,experiment}}{A_{C,experiment}} \\ \sigma_{print} &= \frac{-1550 * 10^3}{42116.977} = -36.80MPa \end{aligned} \tag{8.5}$$

$$\begin{aligned} E_{print} &= \frac{\sigma_{print}}{\epsilon_{print}} \\ E_{print} &= \frac{-36.80}{-0.0009} = 40891MPa \end{aligned} \tag{8.6}$$

The E-modulus of the traditional concrete (C30/37) is calculated with Eurocode 2 [21]. This can be seen in forumula 8.7.

$$\begin{aligned} E_{cm}(5) &= (f_{cm}(5)/f_{cm})^{0.3} * E_{cm} \\ E_{cm}(5) &= (36.1/38)^{0.3} * 33000 \\ E_{cm}(5) &= 32496MPa \end{aligned} \tag{8.7}$$

8.6. Poisson factor

The Poisson factor defines to what ratio the material will deform in x- and y- direction when the element deforms in z-direction. This can influence the stresses in the element, especially if it differs with both materials. Sadly, not enough information to find the Poisson factor of printed concrete is available. Traditional concrete has, in general, a Poisson factor of 0.2 [21], independent of the age of the concrete. The Poisson factor of printed concrete is assumed to be equal to the Poisson factor of traditional concrete.

8.7. Shrinkage

Printed concrete shrinks a lot in comparing to traditional concrete, this causes large differences in shrinkage between both materials. If the printed and the traditional concrete are connected, they restrict each other to deform freely. This can cause initial stresses inside the element due to the difference in shrinkage. To compare the theoretical model to the experiment, the shrinkage at the time of the experiment must be known.

The order in which the stresses occur can be seen in figure 8.3. First the formwork is printed. This printed concrete shrinks but, will cause no stresses as it can deform freely. After some time the traditional concrete is cast inside the printed formwork. There are two materials involved that both have a different amount of shrinkage. The two materials will restrict each other to deform. This will cause stresses in the element. After some time the element is loaded by a prescribed deformation. The loading is applied over a short time span, therefore the shrinkage during the loading of the element is assumed to be negligible.

This means that the difference in shrinkage will cause initial stresses in the element before the loading is applied. This difference in shrinkage is visualised in the shrinkage graphs in figure 8.4. This order of events will hold for the whole research

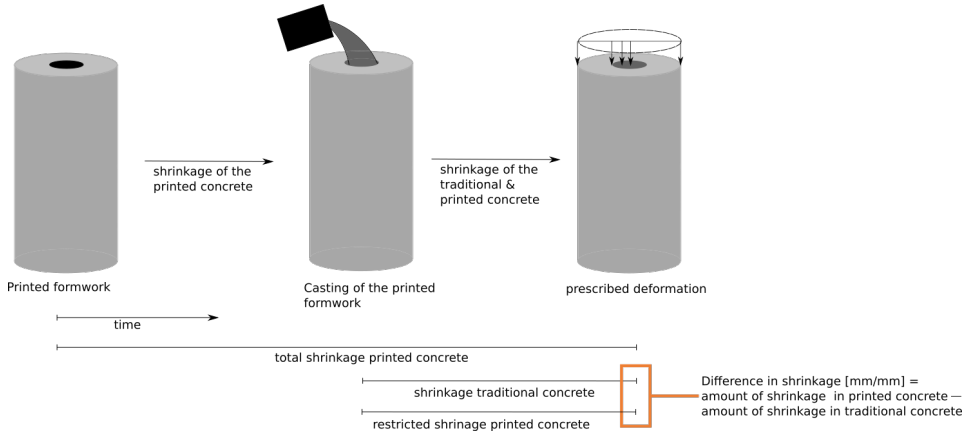

Figure 8.3: The initial stresses due to shrinkage are caused by the difference in shrinkage. The difference in shrinkage is defined as the restricted shrinkage in the printed concrete minus the shrinkage in the traditional concrete, before the element is loaded.

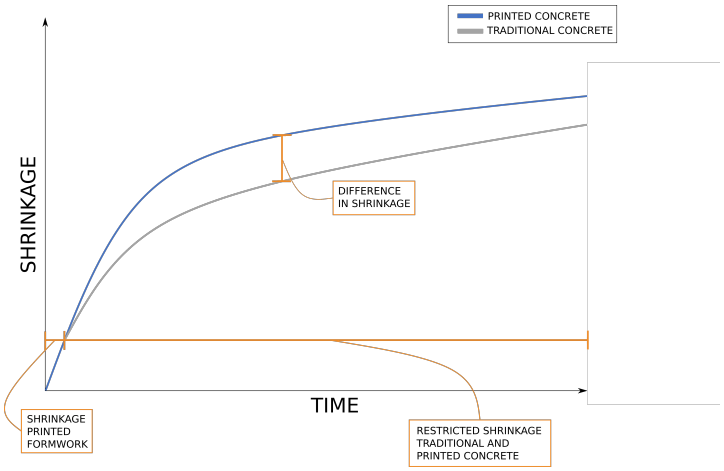

Figure 8.4: The shrinkage graph of printed and traditional concrete, that shows the difference in shrinkage between the two materials.

The total shrinkage of printed concrete is already defined in Chapter 4, table 4.1. At the experiment the printed concrete is 6 days old. Due to curing, there is assumed that little plastic shrinkage has occurred yet. This means that, if the case study is compared to the experiment, only autogenous shrinkage is of interest. The amount of autogenous shrinkage in the total shrinkage of the printed concrete is defined by the ratio autogenous shrinkage and drying shrinkage in the traditional concrete: C50/60.

$$\epsilon_{total} = \epsilon_{drying} + \epsilon_{autogenous} \tag{8.8}$$

The amount of autogenous shrinkage of the printed and traditional concrete are calculated with Eurocode 2 [21]. The whole calculation is as follows:

Amount of drying shrinkage C50/60:
The formula 8.10 contains 'A', the area. The areas of the element can be seen in figure 8.5 on the next page.

$$\epsilon_{cd}(\infty) = k_h * \epsilon_{cd,0} \tag{8.9}$$

with:

$$h_0 = \frac{A*2}{circumference_{exposed}} = \frac{42725.7*2}{Pi*(250+90)} = 80mm \tag{8.10}$$

$$k_h = 1.0\frac{day + mm^{3/2}}{day} \tag{8.11}$$

$$epsilon_{cd,0} = 0.34‰ \tag{8.12}$$

The drying shrinkage at t=6days can be calculated with formula 8.10:

$$\epsilon_{cd,print}(\infty) = 1.0 * 0.34 = 0.34‰$$

The autogenous shrinkage of the concrete C50/60

$$\begin{aligned} \epsilon_{ca}(\infty) &= 2.5(f_{ck} - 10)10^{-6} \\ \epsilon_{ca}(\infty) &= 2.5(50 - 10)10^{-6} \\ \epsilon_{ca}(\infty) &= 0.1‰ \end{aligned} \tag{8.13}$$

The percentage of autogenous shrinkage on the total amount of shrinkage for concrete C50/60

$$\begin{aligned} \epsilon_{total} &= \epsilon_{drying} + \epsilon_{autogenous} \\ \epsilon_{total} &= 0.34 + 0.1 \\ \epsilon_{total} &= 0.44‰ \end{aligned} \tag{8.14}$$

The percentage autogenous shrinkage is equal to:

$$\%_{autogenous} = \frac{\epsilon_{ca}(\infty)}{\epsilon_{total}} * 100\% \quad = 22.7\% \tag{8.15}$$

The total amount of autogenous shrinkage in the printed concrete

$$\begin{aligned} \epsilon_{ca,print}(\infty) &= \%_{autogenous} * \epsilon_{total,print} \\ \epsilon_{ca,print}(\infty) &= 0.227 * 0.001 \\ \epsilon_{ca,print}(\infty) &= 0.227‰ \end{aligned} \tag{8.16}$$

The amount of autogenous shrinkage in the printed concrete at day 1

$$\begin{aligned} \epsilon_{ca,print}(1) &= \beta_{as}(1) * \epsilon_{ca,print}(\infty) \\ \epsilon_{ca,print}(1) &= (1 - e^{-0.2*1^{0.5}} * \epsilon_{ca,print}(\infty) \\ \epsilon_{ca,print}(1) &= 0.041‰ \end{aligned} \tag{8.17}$$

The amount of autogenous shrinkage in the printed concrete at day 6

$$\begin{aligned} \epsilon_{ca,print}(6) &= \beta_{as}(6) * \epsilon_{ca,print}(\infty) \\ \epsilon_{ca,print}(1) &= (1 - e^{-0.2*6^{0.5}} * \epsilon_{ca,print}(\infty) \\ \epsilon_{ca,print}(6) &= 0.088‰ \end{aligned} \tag{8.18}$$

The amount of restricted autogenous shrinkage in the printed concrete

$$\epsilon_{ca,print}(6) - \epsilon_{ca,print}(1) = 0.088 - 0.041 = 0.047‰ \tag{8.19}$$

The amount of restricted autogenous shrinkage in the traditional concrete C30/37

$$\begin{aligned} \epsilon_{ca,print}(5) &= \beta_{as}(5) * \epsilon_{ca,trad}(\infty) \\ \epsilon_{ca,print}(5) &= (1 - e^{-0.2*5^{0.5}}) * (2.5(f_{ck} - 10) * 10^{-}6) \\ \epsilon_{ca,print}(5) &= 0.018‰ \end{aligned} \tag{8.20}$$

The values that are calculated will only be used when the model is compared to the experiment. Within the other parts of this research the following values for the shrinkage in the traditional and printed concrete are used:

- **Amount of restricted shrinkage in the printed concrete:** $0.034‰$
- **Amount of restricted shrinkage in the traditional concrete:** $0.019‰$

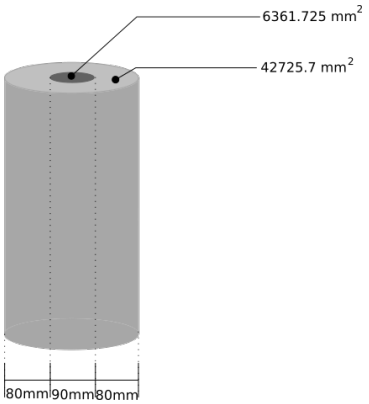

Figure 8.5: The areas 'A' of the cross-section of the concrete element

8.8. Discussion

Not all material properties of the printed concrete are known, some are estimated by comparing it to traditional concrete. Printed concrete cannot be considered as traditional concrete as it is a different material. The estimations are made carefully, but there might be (small) deviations in comparing to the real printed concrete material properties.

- The Young's Modulus of the printed concrete concrete at the age of 6 days is defined by digital image correlation. The movie which is used to define the vertical deformation of the printed concrete did not have the perfect quality to guarantee the trustworthiness of the result.
- The tensile strength of the printed concrete is assumed to be equal to the tensile strength of the traditional concrete with similar compression strength (C50/60). As this traditional concrete is a different material than the printed concrete, it can't be guaranteed that the tensile strength of the two materials are the same.
- The Poisson ratio for the printed concrete is assumed to be 0.2, similar to all the types of traditional concrete.
- Only the total shrinkage of the printed concrete is known. To calculate the amount of shrinkage that occurred before the experiment, the autogenous shrinkage is of interest. The ratio autogenous shrinkage/total shrinkage of traditional concrete (C50/60) is assumed to be equal to the ratio autogenous shrinkage/total shrinkage of printed concrete. This is again a estimation based on traditional concrete, which is not proven to be trustworthy.

Most of the material properties only influence the comparison to the experiment.

8.9. Conclusion

Table 8.2 contains all the material and dimensional properties of the case study element. These parameters will be used through this part to make a realistic and trustworthy model of the element.

Parameters	
1. Geometry	
Shape of the column	Circular
Diameter column	250 mm
Length column	470 mm
Width printed concrete	80 mm
Weight column	max. 51kg
2. Material properties printed concrete at t=6days	
Type of printed concrete	Weber 3D 160-1
Compressive strength	45.3 MPa
Tensile strength	3.25 MPa
E-modulus	40891 MPa
Poisson ratio	0.2
Shrinkage, when compared to experiment	0.047‰
Shrinkage, used in rest of the research	0.034 ‰
3. Material properties traditional concrete at t=5days	
Type of traditional concrete	C30/37, 12mm (Weber Beamix Constructiebeton 100)
Compressive strength	36.1 MPa
Tensile strength	2.21 MPa
E-modulus	32496 MPa
Poisson ratio	0.2
' Shrinkage, when compared to experiment	0.018 ‰
Shrinkage,used in rest of the research	0.019 ‰

Table 8.2: Geometry and material properties of the concrete column used in this case study

9

The experiment

9.1. Introduction

The behaviour of a concrete printed column under compressive loading was not known yet at the beginning of this research. To get more insight in the failure mechnanism and to compare the Ansys model with, a small experiment has been performed. During this experiment three hollow printed concrete elements and one filled element has been tested. The material properties are as discussed in Chapter 8. This chapter (9) discusses the experiment and the result of the filled element. The hollow element is discussed in Appendix A

9.2. Dimensions column

The dimensions are intended to be the same as discussed in Chapter 3 but, when the element is produced by the concrete printer deviations in the sizing will occur. To know the exact size of the element, it is measured before the experiment took place. The results can be seen in table A.1 and figure 9.1. The dimensions were irregular, so differences of half a centimetre might occur.

	D_{top}	$t_{print(top)}$	D_{bottom}	$t_{print(bottom)}$	h	A_{top}
S0V1	250 mm	85 mm	260 mm	90 mm	475 mm	49087 mm^2

Table 9.1: The dimensions of the concrete printed element during the experiment

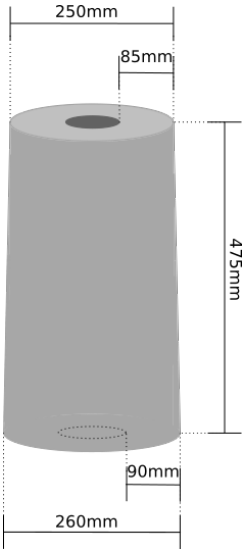

Figure 9.1: A sketch of the dimensions of the concrete printed element during the experiment

9.3. The experiment

The experiment took place in a standard force controlled test machine. With this machine it is only possible to measure the failure load. The machine will apply a compressive force at the top of the element until it fails.

The top surface of the column is not completely flat, therefore it is flatten by sawing a few millimetres from the top. This might cause small cracks in the concrete. The sawing machine was not able to saw a height of 250mm. To create a top surface of the element which is as flat as possible, the concrete cylinder is rotated during sawing. This means that the top surface is still not completely flat. To make sure the force is still equally distributed, cardboard is placed in between the top surface and the test machine. This has not been done at the bottom surface, this might cause for different boundary conditions at the top and bottom surface. This can be seen in figure 9.2

Figure 9.2: The concrete printed element in the test-setup. This picture shows the cardboard placed between the machine and the top surface of the element.

9.4. Result

Strength

The concrete element failed at 2345.2 kN, when this failure load is divided by the surface of the element it failed at a stress of -47.8 MPa. This is larger than the strength of the column: -45.3 MPa.

Observations

The first signs of failure can be seen around one fourth of the top of the element as small cracks. These vertical cracks in the printed concrete propagated. When the machine pushed further, a loud "crack" was heard and the element had suddenly failed.

When the structure is failed, vertical cracks are located in the printed concrete. These vertical cracks are as long as 3/4 of the column height. The crack is largest at the top, and not visible at the bottom. Possible cracks in the traditional concrete cannot be seen. At the top of the column the one crack is located from one end to another end, and it avoids the traditional concrete core (figure 9.4a, on the next page).

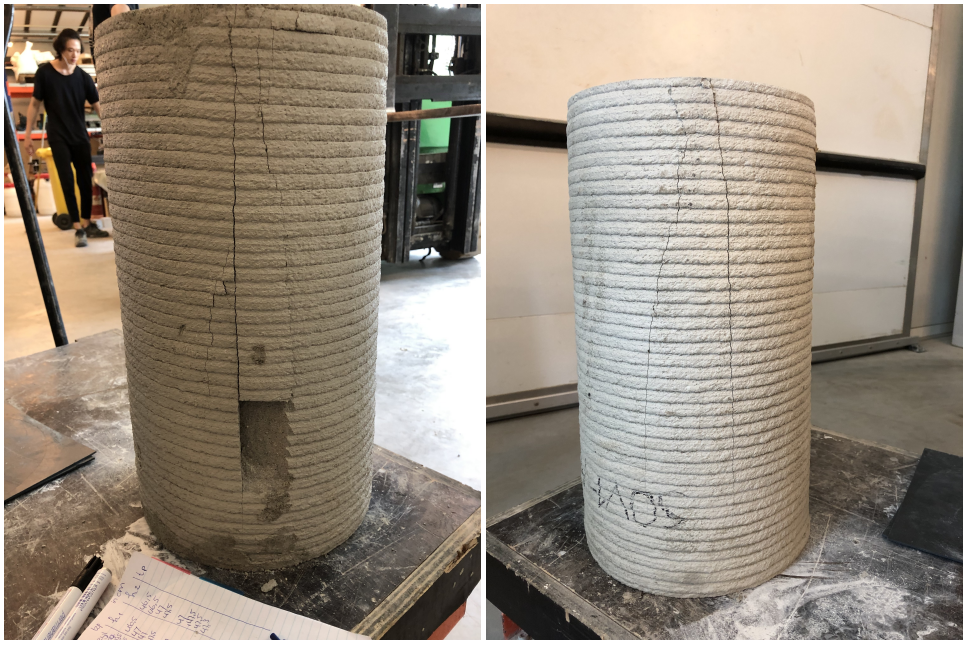

(a) Left side (b) Right side

Figure 9.3: The cracks of the concrete printed element, after it failed

(a) Top of the column (b) Back

Figure 9.4: The cracks of the concrete printed element, after it failed

9.5. Analysis

During the experiment the element failed suddenly, this is a possible indication for a brittle failure.

A piece of cardboard is placed in between the machine and the top surface at the experiment. This is not the case at the bottom surface, this might cause for different boundary conditions at the top and bottom surface. As discussed in Chapter 7 a frictionless boundary condition will conclude in a vertical crack pattern (like the top of the element) and a frictional boundary condition will conclude in a hourglass shape crack pattern (like the bottom of the element).

The column failed at 2345.2kN, which is larger than the expected strength limit from the hand calculations of the Appendix B: 2165.13 MPa. This is a difference of 7% which is not considered as significant. The hand calculations are based on average values, which can be a bit higher or lower by chance.

As can be seen at the dimensions of the element (figure 9.1), the column is not completely straight. While measuring the element, large differences in sizing of the element can be seen. This happens due to the process of concrete printing. Eccentricity in the element are most likely. The eccentricity can influence the way of failure.

9.6. Discussion

This experiment is only performed on one element. This means that this experiment can give an indication of the failure principle, but it cannot be concluded that this failure principle and cracking pattern will hold for every printed element of this size.

9.7. Conclusion

The experiment took place in a force controlled testing machine. The failure load and the failure pattern are the only things that can be retrieved from this experiment. The carton which is applied between the machine plate and the top of the element, might give a different failure pattern at the top and the bottom part of the element. The vertical cracks at the top of the element indicate little friction between the top of the element and the machine. The hourglass failure pattern at the bottom of the element indicate that significant friction exist between the bottom of the element and the machine.

The failure pattern looks like the printed concrete is split in half. A crack can be seen at the contact area between the printed and traditional concrete. The traditional concrete looks uncracked. The sudden failure during the experiment imply brittle failure.

10

The Ansys models

10.1. Introduction

This chapter consists of finite element models made in Ansys. There are two different models made:

1. A Linear model
2. A nonlinear model

The linear model is based on a linear stress-strain distribution. This means that the Hooke's Law holds (equation B.5) in the whole model. Cracks and failure cannot be calculated in the linear model.

$$\sigma = E * \epsilon \tag{10.1}$$

To model cracks and failure in a finite element model, a nonlinear material distribution is needed. This is more realistic, as concrete has not a linear behaviour in reality.

The linear and nonlinear model will be used for the following reasons:

1. Linear model
    - The linear model will be the basis to the nonlinear model
    - The linear model will be used to determine the influence of several parameters (for example: the diameter of the traditional concrete) on the stresses of the element
2. Nonlinear model
    - The nonlinear model will be used to calculate the strength of the concrete element
    - The results of the nonlinear model will be compared to the experiment. This will verify the theoretical model.
    - The results will be compared to a monolith model, this will explain the influence of the printed formwork on the strength of the element.

First the set up of the linear model is discussed, afterwards the set up of the nonlinear model.

10.2. Linear model

10.2.1. Introduction

The linear model will be used as a valid basis for the nonlinear model. The set-up of the model is described in this section. The validation can be found in Appendix. C. Chapter 11 will contain a sensitivity analysis based on this linear model.

10.2.2. Set-up

The column is modelled in Ansys Workbench. The user interface of Workbench makes the program more user friendly. In workbench the model is set up in multiple steps:

1. Engineering data
2. Geometry
3. Model
4. Result

The rest of this section will also be divided in that order. The input values that will be used to model the concrete element are shown underneath the step in which the values have to be filled in. All the input values are chosen to match the experiments as close as possible.

1. **Engineering Data**

   In this part the material properties are defined. The material is considered as linear with the properties similar to table 8.2.The input can be see in figure 10.1 and figure 10.2.

	A	B	C	D	E
1	Property	Value	Unit		
2	Material Field Variables	Table			
3	Density	2400	kg m^-3		
4	Isotropic Secant Coefficient of Thermal Expansion				
5	Coefficient of Thermal Expansion	1,4E-05	C^-1		
6	Isotropic Elasticity				
7	Derive from	Young's Modulus and Poisson...			
8	Young's Modulus	40891	MPa		
9	Poisson's Ratio	0,2			
10	Bulk Modulus	2,2717E+10	Pa		
11	Shear Modulus	1,7038E+10	Pa		
12	Tensile Ultimate Strength	2,7	MPa		
13	Compressive Ultimate Strength	45,3	MPa		

Figure 10.1: The material properties used for the printed concrete as input for the Ansys model

	A	B	C	D	E
1	Property	Value	Unit		
2	Material Field Variables	Table			
3	Density	2400	kg m^-3		
4	Isotropic Secant Coefficient of Thermal Expansion				
5	Coefficient of Thermal Expansion	1,4E-05	C^-1		
6	Isotropic Elasticity				
7	Derive from	Young's Modulus a...			
8	Young's Modulus	32496	MPa		
9	Poisson's Ratio	0,2			
10	Bulk Modulus	1,8053E+10	Pa		
11	Shear Modulus	1,354E+10	Pa		
12	Tensile Ultimate Strength	2,21	MPa		
13	Compressive Ultimate Strength	36,1	MPa		

Figure 10.2: The material properties used for the traditional concrete as input for the Ansys model

2. **Geometry**

   The element is symmetric, therefore only one quarter of the element is modelled. This quarter has rotational symmetric boundary conditions at the cut surfaces. This reduces the calculation-time of one run. The dimensions of the whole element are given in table 8.2. The geometry of the model can be found in figure 10.3.

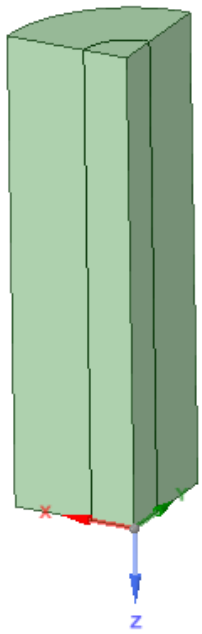

Figure 10.3: The geometry used as input for the linear model. A quarter of the circular element is modelled, it has symmetric boundary conditions at the cut surface.

3. **Model**

   Boundary conditions:

   There are three possible ways to define the boundary conditions in this model:

   (a) The first one is to restrict the x, y and z-direction of the bottom area, and the x and y direction at the top area. The represents infinite friction between the concrete column and the compression machine.

   (b) The second option is to restrict the z-direction of the bottom surface and restrict one nodes, in x- and in y- direction to prevent solid body movement. This represent no friction between the concrete element and the compression machine.

   (c) The third option is to restrict the x, y and z-direction of the bottom area.

   Figure 10.4 on the next page, shows the different boundary conditions in a drawing.

   Depending to what the model is compared to, the boundary condition differ. When the model is compared to the hand calculation, which will be done in the verification (Appendix C), boundary condition B will be used. If the model is compared to the experiment, boundary condition C will be used.

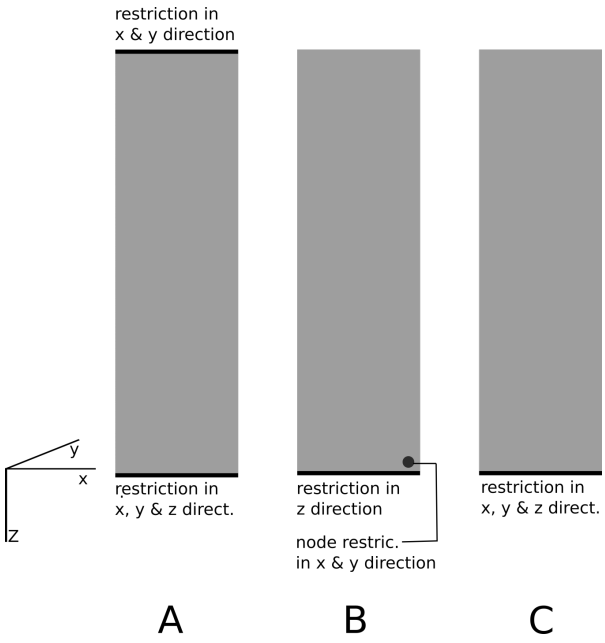

Figure 10.4: The possible boundary conditions that can be used as input for the Ansys model

Mesh

The mesh is used to divide the element in finite parts to calculate the stresses. The meshes of the geometry is shown in the figure 10.5. The element will have completely symmetric mesh in case the mesh method: "MultiZone" is used, with "Hexa" as mapped mesh type.

The sizing of the mesh is defined by dividing edges. The division of the edges can be seen in figure 10.6 on the next page. For example: the vertical edges (shown in red) are divided in 60 parts.

The edges in yellow and green depend on the ratio printed and traditional concrete. It is prefered to choose the size in such a way, the mesh in the traditional concrete has the same size as the mesh in the printed concrete. When the traditional concrete will have a diameter of 90mm (as discussed in Section 8.2) and the printed concrete width of 80 mm, the following values will be used: $n_{trad} = 9$ and $n_{print} = 16$.

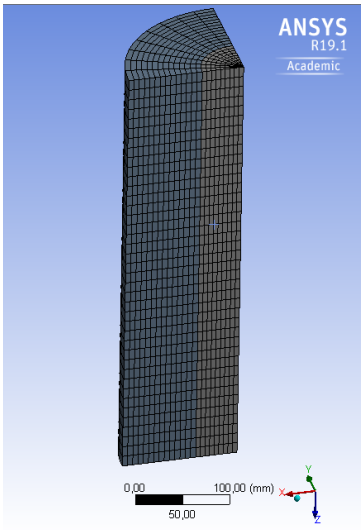

Figure 10.5: The mesh that will be used in the linear model

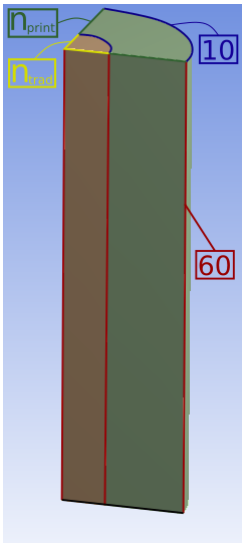

Figure 10.6: The mesh sizes of the element, which will be used in the Ansys model

Loading:

The element can be subjected to a prescribed deformation in z-direction or a force in z-direction. A displacement-controlled model has a higher chance to converge. A displacement is added at the top surface of the element.

Contact area:

The contact area between the printed and traditional concrete must be defined. In Ansys there are a few standard options to do so, they are shown in table 10.1.

Type of contact area	Shear bond strength	Tensile bond strength
Frictionless	no	no
Frictional	user defined	no
Rough	infinity	no
Bonded	infinity	infinity
No separation	no	infinity

Table 10.1: The different types of contact area which can be used within Ansys

It is expected that the contact area: 'bonded', will be most realistic due to the friction of the rough surface and interlocking. This input will be used in the validation.

Shrinkage:

Shrinkage of a concrete element can be modelled with a thermal condition. The shrinkage caused by a temperature decrease will be set equal to the shrinkage in the material. This concludes in a temperature change, which can be used to determine the input value. The surrounding temperature, used in Ansys is equal to 22 degrees. The temperature change equivalent to a certain shrinkage can be determined by formula 10.3.

When the model is compared to the experiment the following input values are used:

The input values for the shrinkage, to compare the output of the model to the experiment:

$$\begin{aligned} \Delta T_{change} &= \frac{shrinkage}{\alpha} \\ \Delta T_{change,print} &= \frac{-0.000047}{1.4E-5} = -3.36°C \\ T_{input,print} &= T_{surrounding} - \Delta T = 22 - 3.36 = 18.64°C \\ \Delta T_{change,trad} &= \frac{-0.000018}{1.4E-5} = -1.29°C \\ T_{input,trad} &= T_{surrounding} - \Delta T = 22 - 1.29 = 20.71°C \end{aligned} \tag{10.2}$$

In all the other cases, for example when the printed element is compared to a monolith element, the following input values are used.

The input values for the shrinkage:

$$\begin{aligned} \Delta T_{change} &= \frac{shrinkage}{\alpha} \\ \Delta T_{change,print} &= \frac{-0.00003376}{1.4E-5} = -2.4114°C \\ T_{input,print} &= T_{surrounding} - \Delta T = 22 - 2.4114 = 19.59°C \\ \Delta T_{change,trad} &= \frac{-0.000019}{1.4E-5} = -1.3571°C \\ T_{input,trad} &= T_{surrounding} - \Delta T = 22 - 1.3571 = 20.64°C \end{aligned} \tag{10.3}$$

4. **Solution**

   The output of the linear model will be used for the validation (Appendix C). The stresses and deformations in x- y- and z-direction are of interest. These will be given in a coloured plot.

10.3. Nonlinear model

10.3.1. Introduction

The nonlinear model will be used to model the cracks and the failure mechanism. This model will be compared to the experiment to see if the theoretical model has similarities with the practice. When it does, this model can be used to calculate a realistic concrete element.

The results of the printed concrete element will be compared to the results of a similar monolith concrete element. This will point out the influence the printed concrete has on the compressive strength of a cast concrete element.

10.3.2. Set-up model

The linear model described in section 10.2.2 forms the basis for this element. The linear model is verified by hand-calculations in Appendix C. The input for the nonlinear model is the same as the linear model (section 10.2.2), except from the following changes:

1. **Engineering data**

   The input values of the engineering data will be entered by APDL code, as described in bullet point 2: Geometry.

2. **Geometry**

   The nonlinear Ansys model will be used to model failure and cracks in the concrete element. To model failure and cracks the element type should change to Solid 65. Changing the element can be done by entering APDL code underneath "Geometry" and the specific element. The input can be seen in the figures 10.7a and 10.7b, on the next page.

```
/go

ET,MATID,SOLID65
R,MATID,0,0,0,0,0,0
RMORE,0,0,0,0,0

MP,EX,MATID,40891
MP,NUXY,MATID,0.2
!MPTEMP,MATID,0

TB,CONCR,MATID,1,9
TBTEMP,22
TBDATA,3,3.25,45.3
```

(a) Printed concrete

```
/go

ET,MATID,SOLID65
R,MATID,0,0,0,0,0,0
RMORE,0,0,0,0,0

MP,EX,MATID,32496
MP,NUXY,MATID,0.2
!MPTEMP,MATID,0

TB,CONCR,MATID,1,9
TBTEMP,22
TBDATA,3,2.21,36.1
```

(b) Traditional concrete

Figure 10.7: The APDL code to create a Solid 65 element with the material properties as defined in table 8.2.

Symmetry, as being used in the linear model, cannot be used to model cracks. The quarter concrete element will contain symmetry axis, which will react differently than a complete circular concrete element. This means that the whole element must be modelled in this case. The geometry is in radial direction split in 16 parts , which was needed to make a symmetric mesh. (figure 10.8, on the next page)

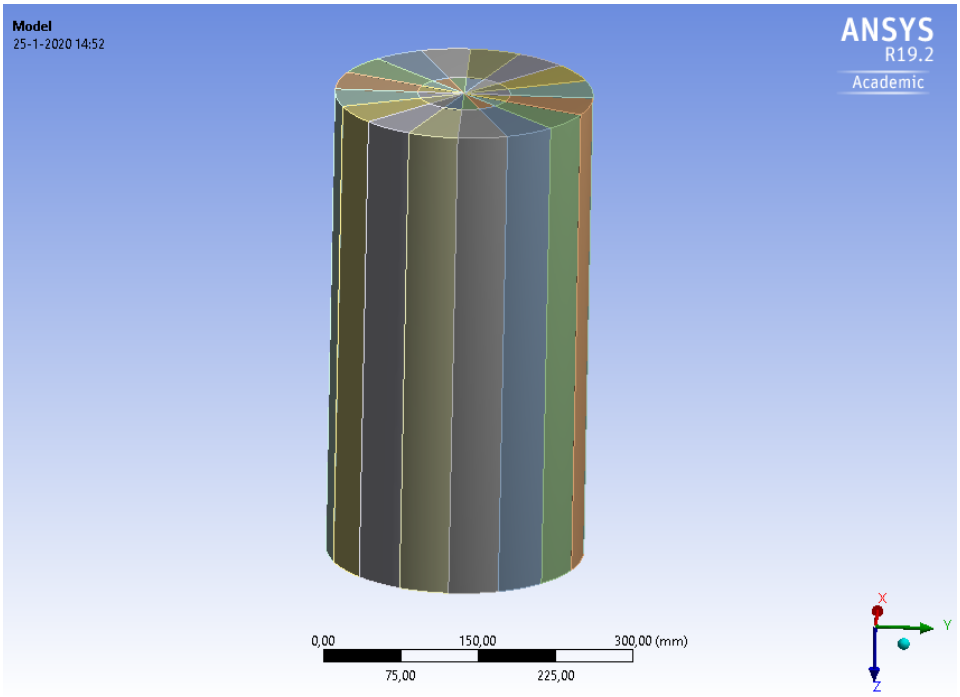

Figure 10.8: The geometry used in the nonlinear model

3. **Model**

Boundary conditions:

The model is used to be compared to the results of the experiment. As discussed before, the concrete element during the experiment has at the top and bottom of the element a different boundary condition. The boundary condition C will be used, the schematization can be seen in figure 10.4, on the next page.

Mesh:

The geometry is split in smaller parts to create a symmetric mesh. Mesh method "Multizone" with "Hexa" as mapped mesh type are used in all parts. Almost all the mesh sizes, used in the linear model (section 10.2.2), are also used in the nonlinear model.

The radial mesh size is the exception, these are the blue lines in 10.6. This edge is divided in 2 parts instead of 10.

Loading:

The element is loaded by a prescribed displacement in vertical direction applied at the top of the element. The displacement will be applied in small steps till failure. The displacement will increase with steps of 0.01mm. When the element reaches failure, the step size is reduced to 0.0005mm. The different steps are applied by making the prescribed displacement parametric in Ansys. At the parameter set that will be created, different input values for the prescribed displacement can be entered. Ansys will calculate a numerical output for all the input values.

Contact area:

The contact area is the same as the linear model: bonded.

Shrinkage:

This will stay similar to the linear model.

4. **Solution**

   The force related to the prescribed displacement can be calculated with the "force probe". This output will calculate the force needed to create similar deformation as the prescribed deformation. This force will be calculated for every input in the parameter set. With this force and the prescribed displacement a force-displacement diagram can be created

The theoretical background information of the nonlinear model can be read in Appendix D. This explains when cracks are formed

The nonlinear model is validated by comparing the results of the linear model to the results of the nonlinear model. This comparison will be performed when a small vertical loading is applied in which the both the concrete materials behave linear. The validation can be seen in Appendix E.

10.3.3. Comparison to the experiment

To decrease the time needed to calculate the results of the Ansys model, the mesh size is increased. The location of the sizes can be seen in figure 10.6. The following sizes are used:

- n_{print}: 8
- n_{trad}: 4
- n_{hoop} (blue lines): 5
- $n_{longitudinal}$ (red lines): 30

To determine the actual displacement that is applied on the element the initial vertical displacement due to the shrinkage is calculated. This deformation due to the shrinkage in vertical direction is equal to 0.019986 mm (please see, figure 10.9 on the next page).

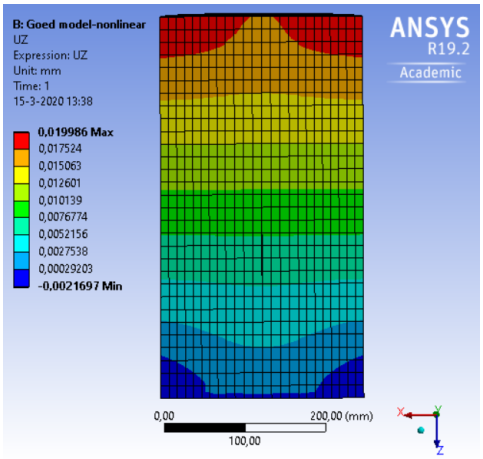

Figure 10.9: The vertical displacement in the printed element due to the difference in shrinkage. This vertical displacement occurs before the vertical loading is applied. The shrinkage applied is equivalent to the shrinkage at the experiment

The input values (the prescribed vertical displacement) will start at a vertical displacement of 0.019986 and will be raised by 0.01mm till failure.

The initial stresses cause by restricted difference in shrinkage between the two types of concrete are given in the figures 10.10. High tensile stresses occur at the bottom of the element, due to the restricted deformations in the horizontal plane. In theory this tensile stresses cause cracks in the printed concrete. In reality will the boundary condition never restrict all deformations, this has as result that the the tensile stresses are less than the theoretical value. The lateral expansion due to the vertical loading causes compressive stresses close to the boundary condition, these will reduce the tensile stresses due to shrinkage. Therefore it is important to not deformations in the horizontal plane when the element is not yet vertically loaded.

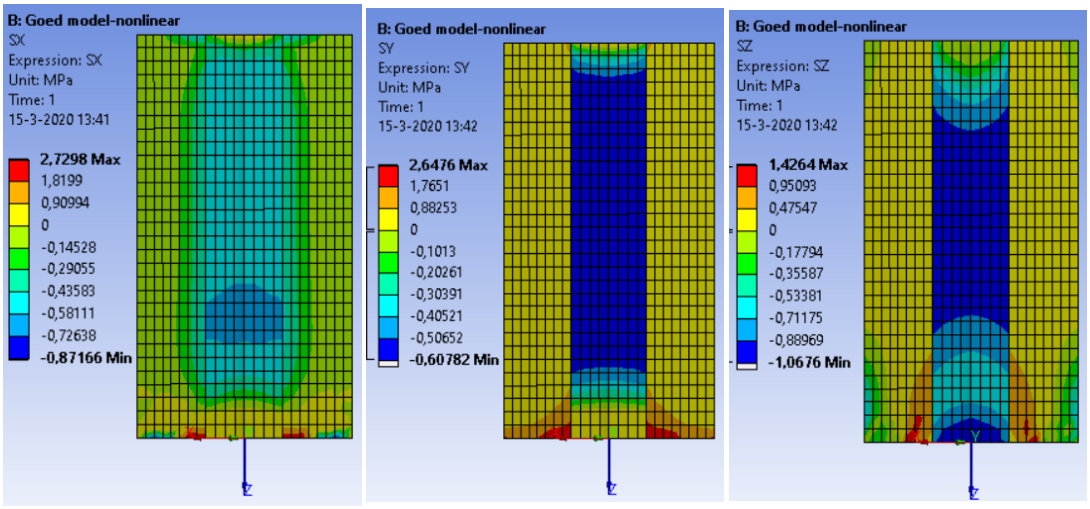

(a) σ_x (b) σ_y (c) σ_z

Figure 10.10: The stresses in the printed element that are caused by the difference in shrinkage. These stresses occur before the vertical load is applied.The shrinkage applied is equivalent to the shrinkage at the experiment

Force-displacement diagram

Result

The output of the FEM model is shown in a force displacement diagram: figure 10.11. The diagram ends at the location where the model did not converge anymore. The diagram is linear.

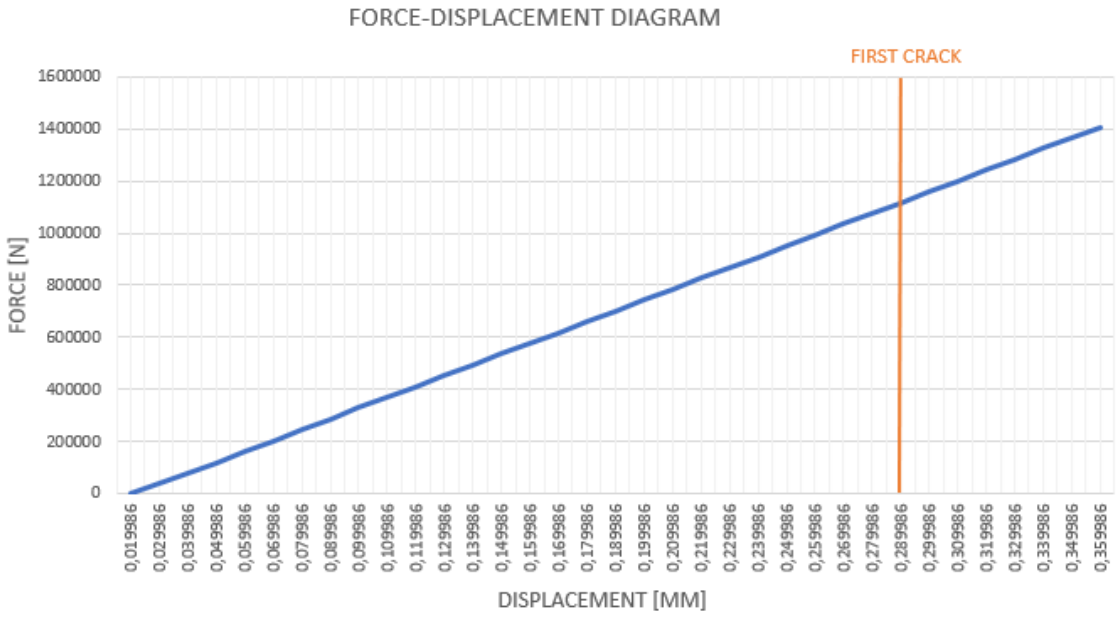

Figure 10.11: The force displacement diagram of the nonlinear model

Analysis

Concrete has a brittle behaviour when it is loaded by a compressive force. It fails without any sign beforehand. This can be seen in the force-displacement diagram: it has linear distribution without any jumps or changes in the slope of the curve just before failure. The difference between a brittle and ductile (this material will give signs before failure) material can be seen in figure 10.12.

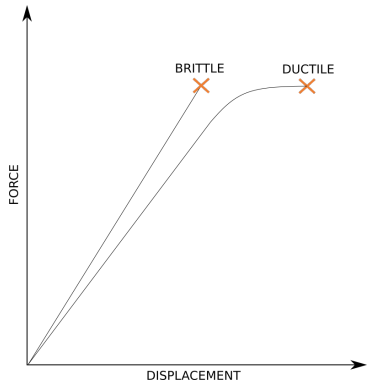

Figure 10.12: Brittle and ductile force-displacement diagram

If the nonlinear model does not converge anymore, there can be assumed that failure has occurred. If the nonlinear model cannot converge, it means that it can't find an equilibrium between the deformations and the loading. If the element fails, it has extremely high, to infinity large deformations. This makes it impossible for the model to converge.

Just after the first crack

Result

The first relevant crack occurs at a prescribed displacement of 0.289986 mm (figure 10.14, on the next page). Figure 10.11 shows no indication the first crack.

The cracks occur at one fourth from the bottom. They are located at the interface between the traditional and printed concrete. The cracks are shown as red circles in figure 10.14a and red lines in figure 10.14b on the next page. The red circles and lines indicate tensile cracks in longitudinal direction.

At the location of the cracks, the maximum principal stresses (figure 10.15b, on the next page) reduces. There are larger tensile stresses around the location of the crack. The minimum principal stresses after the crack (figure 10.15a, on the next page) do not show the any change in the stresses around the crack.

Analysis

The fact that the cracks cannot be seen in the graph indicate that the cracks at this location do not enlarge the vertical displacement.

The cracks occur in the contact area between the traditional and printed concrete. The cracks occurred because the concrete strength at that location is exceeded. The strength is exceeded by relative high tensile stresses in combination with compressive stresses.

The tensile radial and hoop stresses due to the vertical loading occur due to the shear forces caused by the boundary condition. The shear forces have to form an equilibrium in the element, due to which tensile stresses occur (see figure 10.13). The tensile stresses in hoop direction will increase significantly due to the shrinkage in the printed element. (see figure 10.10b).

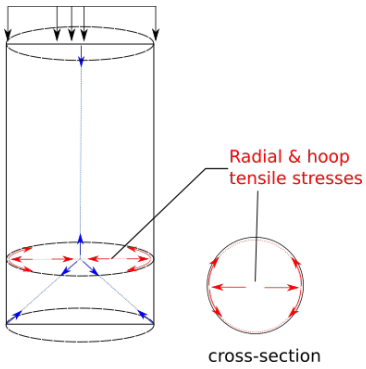

Figure 10.13: The stress equilibrium in a monolith concrete circular element due to a vertical loading applied on top

The minimum stresses are more homogeneous. The largest minimum stresses occur in the printed concrete, the traditional concrete contain smaller stresses.

At the location of the cracks, the maximum principal stresses reduce: please see figure 10.15b, on the next page. Due to the crack, the stresses cannot transfer stresses at that specific location. This reduces the stresses. They will now transfer around the crack. This can be seen in the higher maximum principal stresses around the crack location.

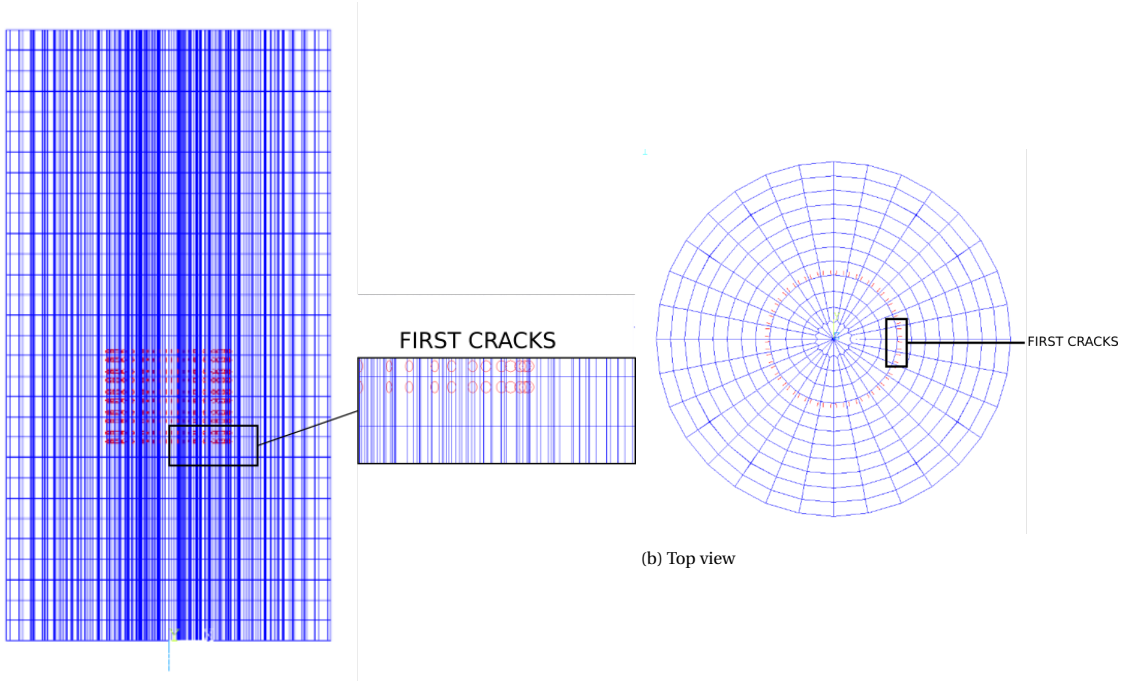

(a) Side view

(b) Top view

Figure 10.14: The location of the first relevant cracks in the concrete printed element

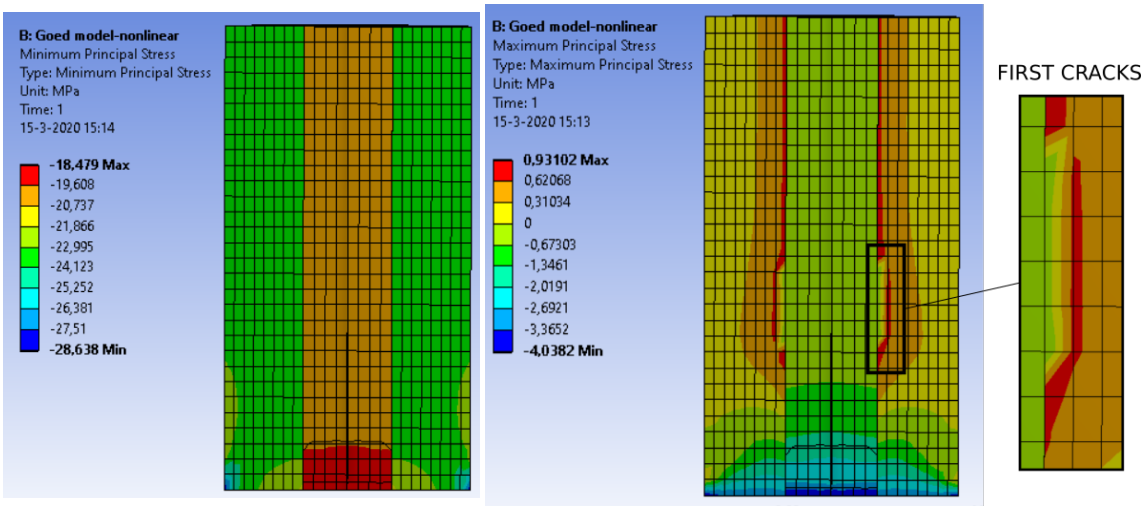

(a) Minimum principal stress

(b) Maximum principal stress

Figure 10.15: The principal stresses of the concrete printed element, just after the first crack has occurred.

Just before failure

Result

When the element has a prescribed displacement at the top of the element of 0.359986 mm, the element is not failed yet. At a vertical displacement of 0.359986 mm the force displacement diagram (figure 10.11) is still linear.

The cracks can be seen in figure 10.16. The first relevant cracks, discussed before, are developed over a larger area. The cracks are still mainly located at the contact area between the printed and traditional concrete at one third of the height (measured from the bottom). They are vertical tensile cracks.

The influence of the cracks is visible in the maximum principal stress distribution (figure 10.17b, on the next page). At the location where the cracks occur, the stress reduces. Around the crack, higher tensile hoop stresses occur. The largest maximum principal stresses are still located at the contact area. The minimum principal stresses are similar to the minimum principal stresses with a lesser prescribed displacement.

Analysis of the results

The force displacement graph (figure 10.11) stays linear. This indicates that the cracks do not enlarge the vertical displacements.

The cracks propagated along the contact area. Which is logical as the largest principal stresses are along the contact area. The cracks at the 1/4 of the bottom propagated to the outside of the printed concrete. (figure 10.17b, on the next page)

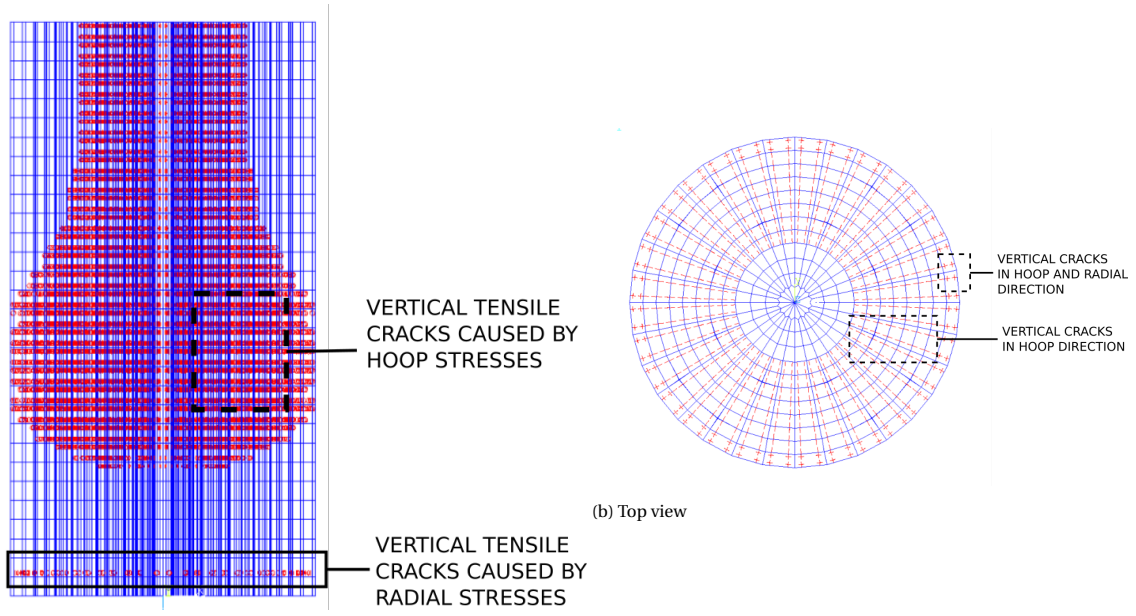

(a) Side view

(b) Top view

Figure 10.16: The cracks in the concrete printed element that occur just before failure

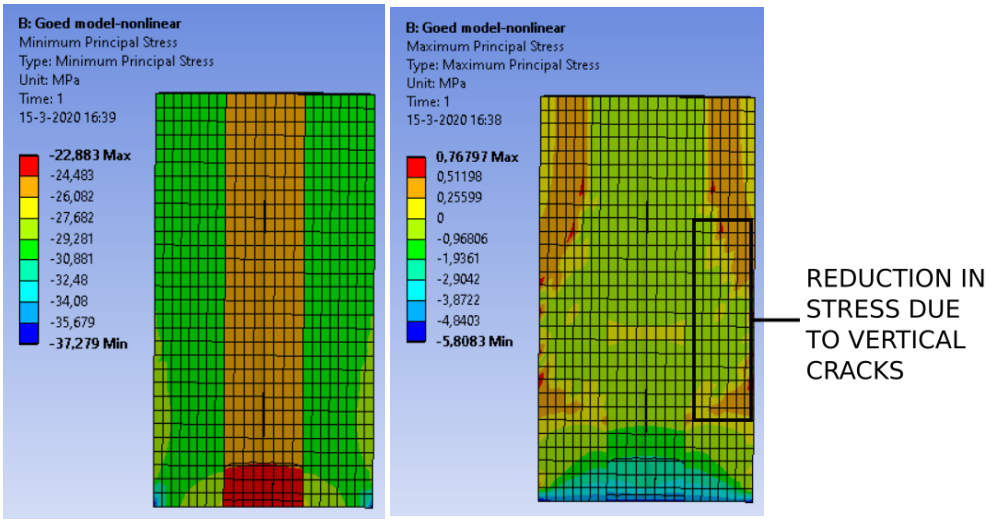

(a) Minimum principal stress (b) Maximum principal stress

Figure 10.17: The principal stresses in the concrete printed element, just before failure

Failure

Result

From a prescribed displacement of 0.379986 mm and higher, the model does not converge anymore. This might mean that the displacements due to the forces became too high, and no equilibrium can be formed. This can be seen in the force-displacement diagram as a sudden end of the graph. This means that a brittle failure has has taken place. Most likely the printed concrete breaks off the traditional concrete at the top of the element. At the bottom of the element the printed concrete will fail in a cone shape. No result of the model is available to prove this statement.

The comparison

The results of the nonlinear model: Section 10.3.3 are compared to the results of the experiment: Section 9.4. This comparison can indicate if the theoretical FEM model behaves similar to the experiment. It can validate the theoretical model. This comparison cannot immediately conclude if the model can be used in practice, as only one experiment is performed.

First of all, the experiment and the theoretical model both have a brittle failure. In the experiment this can be seen by the sudden failure. In the model this can be seen in the fact that the force-displacement diagram does not show any signs that is close to failure.

Secondly, the maximum principal stress distribution in the model shows the highest stresses at the contact area between the traditional and printed concrete (see figure 10.17b). The experiment shows a crack, at the top of the element, between the printed and traditional concrete (figure 9.4a).

Thirdly, the experiment shows that the top of the element has a different crack pattern than the bottom of the element. At the top of the element the printed concrete split into two halves, while the bottom of the element is uncracked (see figure 9.3 and figure 9.4). Figures 10.17a and 10.17b show that the top of the element has different stresses than the bottom of the element. This occurred due to the different boundary condition at the top and the bottom of the element. Chapter 7 explains that a boundary condition, which restricts horizontal displacement, causes a cone crack pattern. The different boundary conditions will probably cause a asymmetric crack pattern.

During the experiment two vertical cracks on either side of the element occur. These cracks occur before failure. These cracks cannot be seen in the Ansys model. They might occur due to geometrical inconsistencies that will always happen during concrete printing.

There can be concluded that the principle of the failure is similar: the brittle failure. The cracks located around the contact area are visible in both the theoretical model and the experiment. Even though the two variants have similarities, too little information form the experiment (no form-displacement diagram) and too little information from the model (no failure crack pattern) is available to properly conclude that they act the exact same way.

10.3.4. Comparison to a monolith column

The results of the nonlinear printed concrete element will be compared to the results of a nonlinear model of a monolith element. This can conclude in the influence of the printed formwork on a monolith element. This will be done with different amounts of shrinkage than used in the comparison to the experiment.

Set-up printed element

The only thing that changes from the initial set-up discussed in Section 10.3.2 is the shrinkage. The shrinkage is the same as the shrinkage applied to the monolith element. The shrinkage causes an initial vertical displacement of 0.015369 mm.(figure 10.18)

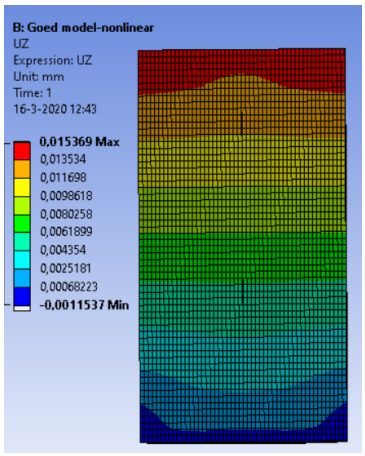

Figure 10.18: The vertical displacement in the printed element due to the difference in shrinkage. This vertical displacement occurs before the vertical loading is applied.

The difference in shrinkage between the two materials causes stresses in the element. These are considered as initial stresses. The initial stresses caused by the difference in shrinkage can be seen in figure 10.19.

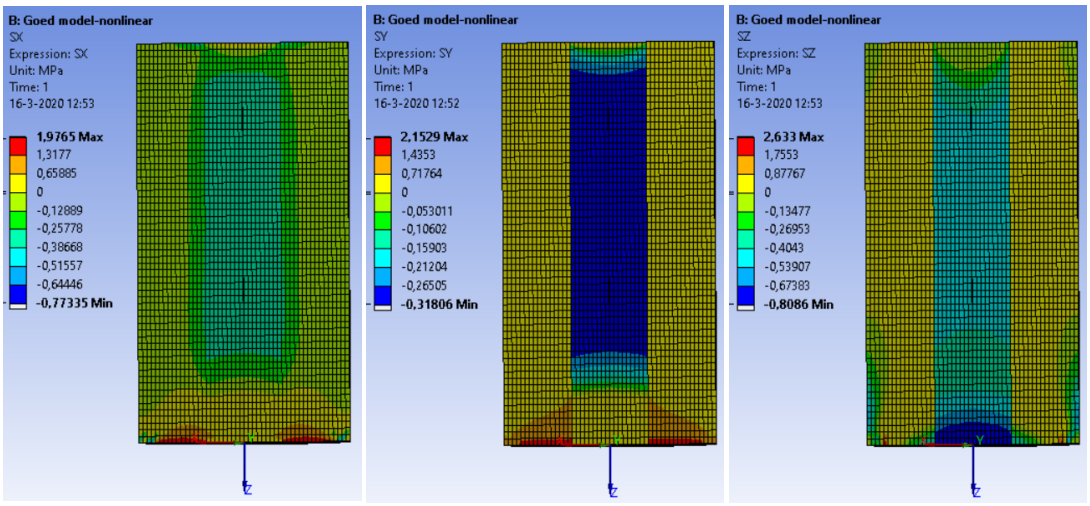

(a) σ_x (b) σ_y (c) σ_z

Figure 10.19: The stresses in the printed element that are caused by the difference in shrinkage. These stresses occur before the vertical load is applied.

Set-up monolith model

The nonlinear monolith element has a similar set-up as the printed nonlinear model (see section 10.3.2). The differences are summed up below:

- **Geometry**

  The traditional concrete has been merged with the printed concrete. The geometry of the model is still divided in the pie parts. The geometry can be seen in figure 10.20.

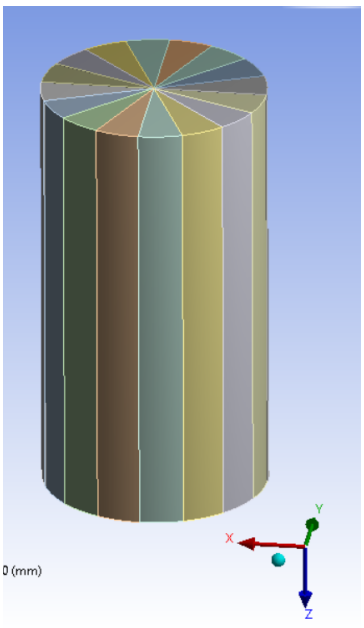

Figure 10.20: The geometry input of the monolith concrete element for a nonlinear model

  Because the largest volume of the element exist of printed concrete, this material is chosen for this monolith element. The APDL input is equal to the one of the nonlinear printed element: figure 10.7a

- **Model**

  Mesh:

  The mesh has been enlarged to increase the run speed of the model:

  $n_{print} + n_{trad} = 10$ and the vertical edge is divided into 30 parts. The mesh can be seen in figure 10.21.

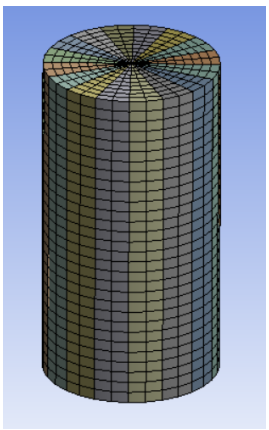

Figure 10.21: The mesh of the monolith concrete element

Shrinkage:

The monolith element only contains of the printed concrete material. The same shrinkage as being used in the printed element for the printed concrete will be used for this model.

Results monolith element

The shrinkage in the monolith element will cause a vertical displacement, this vertical displacement is the starting point of the prescribed displacement. This displacement is equal to: 0.016333mm. This can be seen in figure 10.22. The initial stresses due to the restricted can be seen in figure 10.23

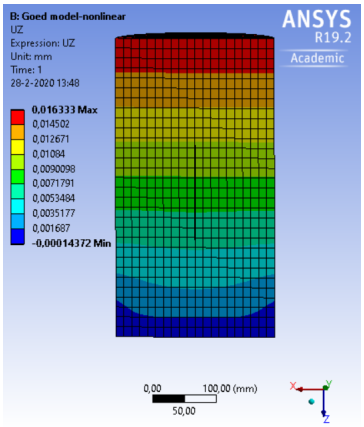

Figure 10.22: The vertical displacement due to shrinkage of the monolith element. This vertical displacement has occurred before the vertical loading is applied.

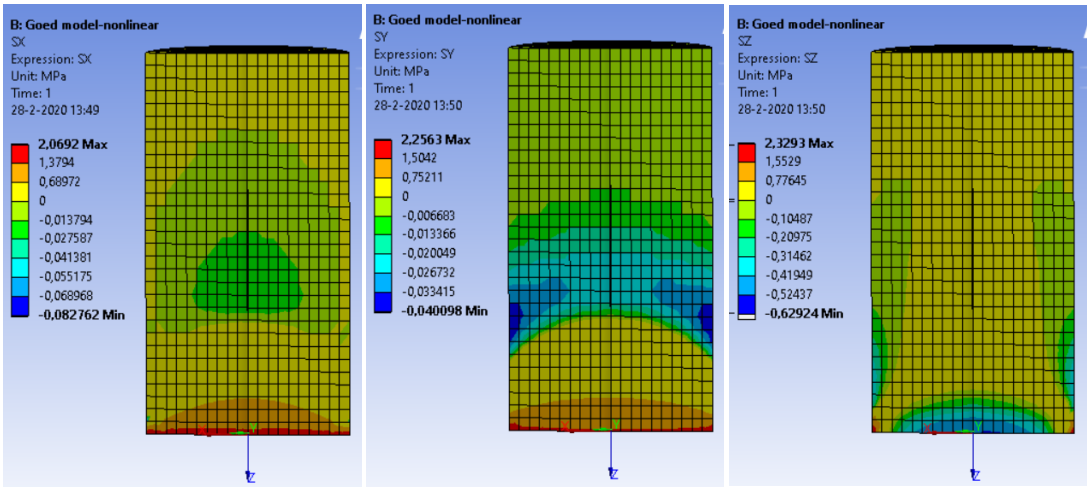

(a) σ_x (b) σ_y (c) σ_z

Figure 10.23: The stresses in the concrete monolith element due to shrinkage. This stresses occur before any vertical loading is applied.

To compare the elements, they will have a prescribed displacement of 0.345 mm. This means that the input value for the printed element will be equal to: 0.345+0.015369=0.360369mm and for the monolith element: 0.345+0.016333=0.361333 mm. The stresses in hoop, radial and longitudinal direction are shown in the following figures 10.24 and 10.25 on the next page:

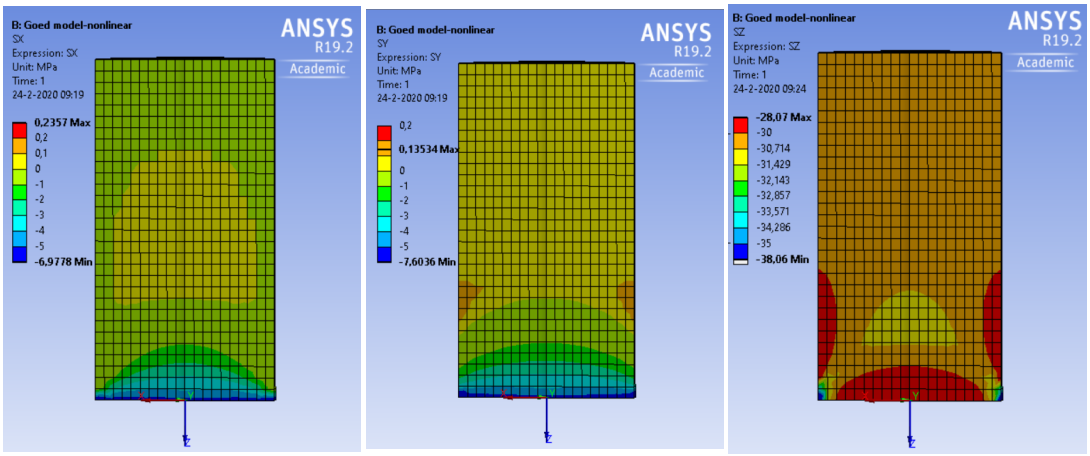

(a) σ_x (b) σ_y (c) σ_z

Figure 10.24: Stresses in the monolith element due to the initial shrinkage (figure 10.23) and a prescribed displacement of 0.345mm.

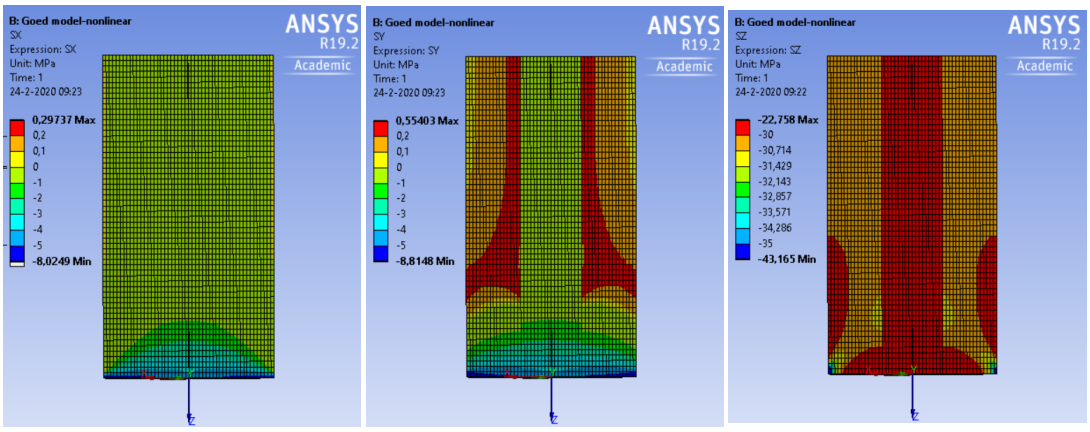

(a) σ_x (b) σ_y (c) σ_z

Figure 10.25: Stresses in the printed element due to the initial shrinkage (figure 10.19) and a prescribed displacement of 0.345mm.

The legends have the same distribution for the monolith, and the printed element. The following things stand out if the stress distributions are compared:

- **Tensile radial stresses occur in the middle of the monolith element. The printed element only contains compressive radial stresses.**

  The stresses close to the boundary condition, located at the bottom surface, are similar for the monolith and the printed element. These stresses are for the comparison not interesting.

  The prescribed deformation in vertical direction will cause compressive longitudinal stresses. Due to lateral expansion, the element wants to expand in the horizontal plane. The boundary condition at the bottom surface restricts these deformations. This causes shear stresses in the vertical plane. As this is a static element, all the nodes must be in equilibrium. This causes the stress distribution which can be seen in figure 10.13. In this figure the radial tensile stresses that occur due to equilibrium can be seen. These tensile stresses will occur in the monolith and printed element. These tensile stresses cannot be seen in the stress distribution for the printed element (figure 10.25a). This is the case due to the influence of shrinkage.

  The following principle occurs: The printed concrete shrinks more than the traditional concrete. The shrinkage of the printed concrete is restricted by the traditional concrete. This causes compressive radial stresses in the traditional and printed concrete. The compressive stresses are the largest in the traditional concrete.The compressive stresses in the printed concrete are smaller and are influenced by the restricted deformation at the contact area (figure10.10a).

The difference in shrinkage between the printed and traditional concrete is the reason for the different stress distribution in both elements.

- **The printed concrete gives tensile hoop stresses in the printed concrete and compressive hoop stresses in the traditional concrete. The monolith element only has small, tensile hoop stresses in the element.**

  The hoop stresses in the element are caused by the prescribed displacement and the stress equilibrium which can be seen in figure 10.13. These tensile stresses influence the stress distribution in the monolith element. The hoop stresses in the printed element are mainly influenced by the difference in shrinkage of the printed and traditional concrete.

  The printed concrete shrinks more than the traditional concrete. This deformation of the printed concrete is restricted by the traditional concrete. This causes tensile hoop stresses in the printed concrete and compressive hoop stresses in the traditional concrete. These hoop stresses can be seen in figure 10.25b.

  The difference in the stress distribution between the two elements is caused by shrinkage. The printed element has larger tensile stresses in the element than the monolith element.

- **The height of the longitudinal compressive stresses are similar of the monolith element and the printed element.**

  The longitudinal stresses are similar, the only exception is the lower compressive stresses in the traditional concrete. This is caused by the smaller Young's modulus of this material.

  Conclusion

  From the analysis it can be seen that the difference in shrinkage between the printed and traditional concrete causes the largest differences in between the stresses in the monolith and printed element.

  From here there can be concluded that the printed element and the monolith element behave different due to the difference in shrinkage between the printed and traditional concrete. There are more factors that influence the strength of the printed element, which have to be taken into account to determine the failure mechanism.

10.4. Conclusions

The nonlinear model is used to compare the results to the experiment and to a monolith element.

The nonlinear model is compared to the experiment to see if the theoretical model matches practice. There can be concluded that element used during the experiment and the element in the Ansys model both have a brittle failure. Cracks occur at the contact area between the printed and traditional concrete in both analysis. To determine if they are exactly alike, too little information is known about the experiment or the failure crack pattern of the Ansys model.

The comparison to monolith element is made to check what the influence of the printed concrete formwork on the compressive load bearing resistance of the element is. From this comparison there can be concluded that the stresses in the monolith element are mainly influenced by the prescribed displacement in vertical direction and to a lesser extend by the shrinkage of the material. The printed element is influenced by the prescribed displacement, difference in shrinkage, Young's modulus of the traditional concrete. Depending on these factors, the failure crack pattern might differ.

11

Sensitivity analysis

11.1. Introduction

The Ansys model is made to model the experiment as close as possible. There are a few parameters (for example the width of the printed concrete) that can be changed in every project. It will most probably influence the stress distribution. This chapter researches to what extend the parameters influences the output of the model.

First the set-up of the sensitivity analysis will be discussed. This will explain which parameters are chosen to calculate the influence for, and how the influence is calculated. Afterwards the results are described, which will be followed by the analysis of the results. The analysis of the results will contain an analysis of the results which will follow in a conclusion.

11.2. Set-up

The sensitivity of a parameter indicates the influence the parameter has on a the output. The influence will be determined within this section by two methods:

- The variant study: Create a list with possible variants (different amounts of shrinkage, different boundary conditions and so on) and compare the outcome of the variants.
- The local sensitivity by Ansys: Ansys changes one input parameter with +10 % and -10%. The output values will be compared to the original to find the local influence of the parameter.

The set-up, results and the analysis of the results will be discussed separately in this chapter. The variant study will always be discussed first, and afterwards the local analysis. The structure can also been seen in figure 11.1 on the next page.

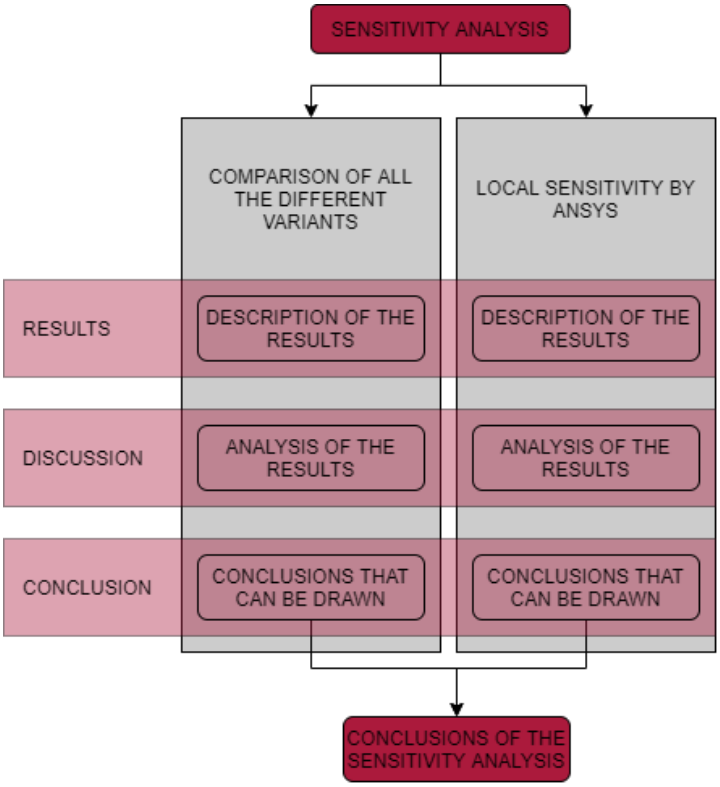

Figure 11.1: The structure of the sensitivity analysis

11.2.1. The variant study

The first method compares the result of multiple variants defined by changing some of the input values from Section 10.2.1 to a parametric value. These parameters are summed up below:

1. **The type of traditional concrete**

   The type of traditional concrete which will used to fill the printed concrete formwork with, can easily vary. During the experiment the type of concrete: C30/37 is used. It is also very interesting to see what influence the following types of concrete have:

   - Concrete with a similar strength as the printed concrete (C50/60)
   - Concrete with a similar Young's modulus as the printed concrete (C70/85)

   The sensitivity analysis is performed on the linear model, this means that only the E-modulus of all material properties, has a direct influence on the result. This parameter has "Young's modulus trad" as name in the Ansys local sensitivity analysis.

2. **The volume ratio printed concrete and traditional concrete**

   The concrete printed formwork had a width of 80mm during the experiment. The total diameter of the element is equal to 250 mm, this means that the traditional concrete had a diameter of 90mm. In this case, a large volume of printed concrete in comparing to traditional concrete is used. To find the influence of the traditional concrete / printed concrete volume ratio on the strength of the column an extra option will be run: $D_{trad} = 180mm, t_{print} = 35mm$

   This parameter is called "Diameter trad" in the sensitivity analysis.

3. **Shrinkage**

   The difference between the shrinkage of the printed concrete and the traditional concrete has influence on the stresses that occur in the cross-section. The influence can be determined to compare different shrinkage options:

- **Shrinkage variant 1:** A small amount of shrinkage in both materials ($T_{print} = 19.6°C, T_{trad} = 20,6°C$).
- **Shrinkage variant 2:** No shrinkage in both materials ($T_{print} = 22°C, T_{trad} = 22°C$).
- **Shrinkage variant 3:** The maximum amount of total shrinkage that can occur. This means that the formwork is printed, and at the same time the traditional concrete is cast. The element will be loaded when all shrinkage has taken place. ($T_{print} = -49.4°C, T_{trad} = -9.71°C$).
- **Shrinkage variant 4:** The shrinkage that occurs when the printed concrete has shrunk completely before the traditional concrete is cast. The element will be loaded when all shrinkage has taken place. This means that the maximum total shrinkage of traditional concrete is used, and no shrinkage in the printed concrete. ($T_{print} = 22°C, T_{trad} = -9.71°C$).

This parameter has "Shrinkage print" and "Shrinkage trad" as name for the input values in the sensitivity analysis.

4. **Contact area**

   There are different types of contact areas (see table 10.1). To define the influence of the contact area, the results of the two most opposite variants are chosen to be compared. These are the frictionless and the bonded.

   This input value is not numerical, this means it is not possible to set this value as parametric in Ansys. This means that the sensitivity analysis has to be divided into 2 parts.

5. **Boundary conditions**

   The boundary condition of the element differs per situation. At the experiment it depends on the friction between the machine plate and the top or/and bottom surface of the element: If the friction between these two elements is really high, it is not possible to deform in x and y direction. If the friction between these two elements is really low, the element can deform freely in x and y direction (see Chapter 7). To find the influence of the different boundary conditions, it is chosen to compare boundary condition version A and version B (see figure 10.4).

   To define the boundary conditions of this element, it must be possible to switch the displacement in x- and y- direction for 0 to "free" and the other way around. "Free" is not considered as a numerical input value, therefore it is not possible to put this parameter in Ansys as variable. This means that the sensitivity analysis has to be divided into 4 parts (2 from the contact area, and 2 from the boundary conditions).

This means that there will be 96 different variants that will be run in model to find the influence on the height of the stresses of the column and the influence on each other.

The maximum and the minimum values of a stress in X- Y- and Z-direction will be the output. These stresses are calculated in the cylindrical coordinate system (figure 11.2, on the next page). To avoid peak stresses in the analysis, the stresses at two cross sections of the element are analysed. The nodes at the location of the cross-section will be selected to calculate the stresses at that specific location. Most peak stresses occur close to the boundary condition, therefore it is important to pick the nodes not that close to the boundary conditions. For this analysis it is chosen to calculate the output of the nodes 39.167mm from the top and the nodes in the middle of the element (figure 11.2, on the next page).

These results will be calculated by Ansys. In the workbench interface, all numerical input and output values can set as "parametric". The "parameter set" that is created, can be used to fill in all the different variants. By clicking on "Update all design points", the output values that are set to "parametric" will be calculated for every variant.

The maximum and minimum output values of the hoop, radial and longitudinal stresses at the nodes are plotted in bar charts, to easily compare all the variants.

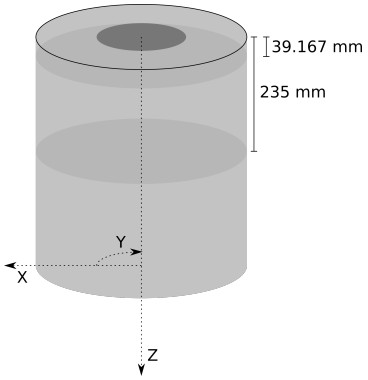

Figure 11.2: The locations where the maximum and minimum values of the stresses are defined in the sensitivity analysis.

11.2.2. The local sensitivity by Ansys

The second way to determine the influence of the different parameters is to calculate their local sensitivity by Ansys.

The parameters, which are used in the variants study, will also be parametric in this local sensitivity analysis. To calculate the local sensitivity, first the Design of Experiments should calculate the stresses. The Design of Experiments computes the output for the change of +10% and -10% of the input values of variant 1. The input values can be seen in table 11.1. This concludes in 12 variations. The local sensitivity will be calculated by ansys in the Response Surface part.

Parameter	-10%	Original	+10%
Diameter traditional concrete [mm]	81	90	99
Shrinkage traditional concrete [°C]	18.57	20.643	22.7
Shrinkage printed concrete [°C]	17.63	19.593	21.5
Displacement in z-direction at the top [mm]	0.45	0.5	0.55
Young's Modulus traditional concrete [MPa]	293463	32496	35647

Table 11.1: The input values local sensitivity analysis

The local sensitivity is shown in a bar chart. The horizontal axis contains the output of the variants (minimum hoop stress, maximum hoop stress, minimum radial stress and so on). The different colours of the bars indicate the different parameter. The height of the bars (the vertical axis) is the local sensitivity in percentage. This local sensitivity is determined in the following way: the maximum output (the maximum stress that occurs when the input parameter is changed with +10% or -10%) minus the minimum output divided by the average output (formula 11.1)

$$\text{Local sensitivity bar chart} = \frac{Output_{max} - Output_{min}}{Output_{average}} \tag{11.1}$$

11.3. Results

11.3.1. The variant study

The hoop, radial and longitudinal stresses of the middle and top of the element have been calculated for all variants. To check the influence and impact of all the parameters the results have been plotted in several graphs. They can be found in Appendix G.

The graphs can be read in a specific way: this can be seen in figure 11.3 on the next page. In this way it is easier to see what factors have a larger or smaller influence on the stress.

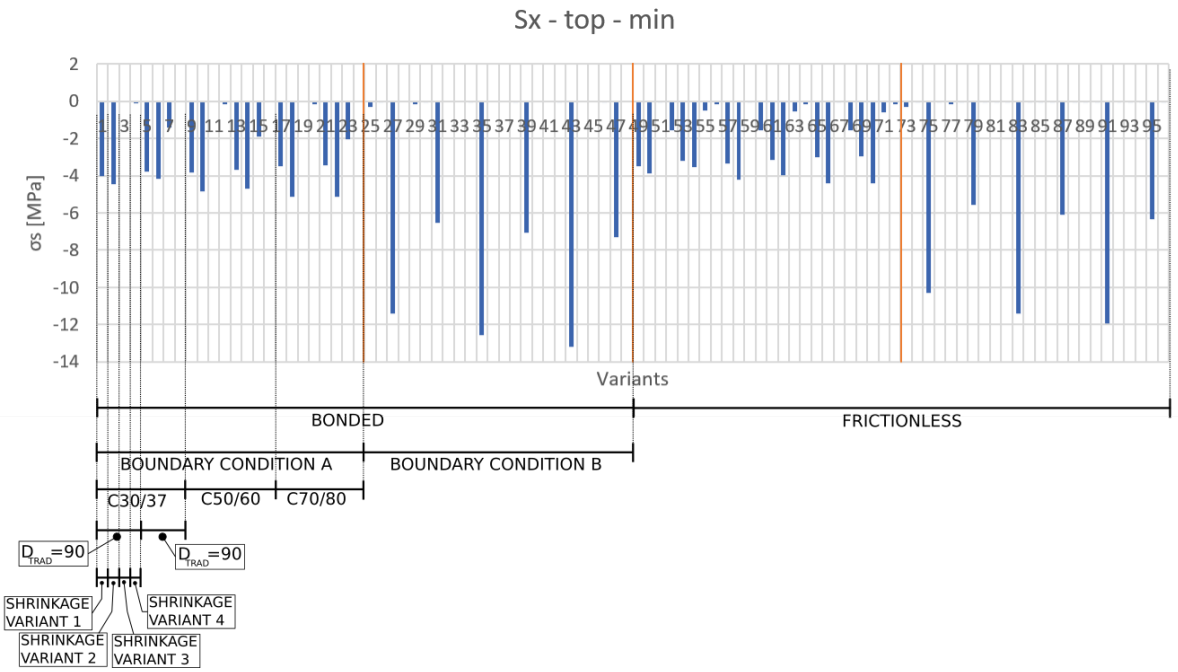

Figure 11.3: An example of the bar chart that shows minimum radial stresses for all the different variants. The figure explains how this, and similar bar charts (Appendix G) can be read.

These results will be mainly used to define the influence of the contact area and the boundary conditions on the stresses in the top and middle part of the element.

The bar charts are divided by orange lines to mark the different parts.

- Part 1: Bonded & boundary condition A
- Part 2: Bonded & boundary condition B
- Part 3: Frictionless & boundary condition A
- Part 4: Frictionless & boundary condition B

To define the influence of the boundary condition and the contact area, the pattern (created by the bars) of a part can be compared to another part. For example: a comparison between part 1 and part 2 to define the influence of the boundary condition in case the contact area is bonded. If the pattern is similar, the parameter has little influence. When the pattern differs, the parameter has a significant influence. The results are discussed per graph.

Sx top min

In this graph the parts containing the same boundary condition look similar (part 1 & part 3 and part 2 & part 4).

- **Part 1 & part 3**

  When shrinkage variant 1 or 2 has been used as input, compressive radial minimum stress at the top of the element occur.

  The input value shrinkage variant 3 has a compressive minimum radial stress in the top of the element, in case the diameter of the traditional concrete is equal to 180 mm. If the diameter is equal to 90mm, the radial stresses is around zero.

  The input value shrinkage variant 4 has a negative minimum stress in case the diameter of the traditional concrete is equal to 90mm. This compressive stress is larger in part 1 than part 3. A diameter of 180mm has stresses close to zero as output.

- **Part 2 & part 4**

  The input value shrinkage variant 3 concludes in a minimum compressive radial stress at the top of the element. This minimum compressive stress is larger when the diameter of the traditional concrete is small (90 mm) instead of the large (180mm). In all the other shrinkage variants, the minimum radial stresses is close to zero.

Sx top max
This graph contains 3 different patterns:

- **Part 1 & part 3**

  These parts have the same boundary condition but different contact area as input. The input values: shrinkage variant 1 and variant 2, give maximum radial stresses close to zero. The shrinkage variant 3 and variant 4 do give (positive) maximum radial stresses. When the diameter of the traditional concrete is small (90 mm) the output of shrinkage variant 3 is larger than shrinkage variant 4. When the diameter of the traditional concrete is large (180mm) the output of shrinkage variant 4 is larger than the shrinkage variant 3.

- **Part 2**

  Almost all maximum radial stresses are close to zero, a positive radial stress occur when the input value: shrinkage part 4 is used.

- **Part 4**

  All maximum radial stresses are close to zero.

Sy top min
Three different patterns can be seen in this graph:

- **Part 1 & part 3**

  When the shrinkage variants 1, 2 and 4 are used as input value, a negative minimum hoop stress occurs. Shrinkage variant 4 gives the largest minimum stresses, and shrinkage variant 1 the smallest. Shrinkage variant 3 as input value gives positive minimum hoop stresses.

  The output is smaller for the frictionless variant than for the bonded variant.

- **Part 2**

  When shrinkage variant 3 and variant 4 are used as input, negative minimum hoop stresses occur. Shrinkage variants 1 and 2 has hoop stresses close to zero as result.

- **Part 4**

  Only shrinkage variant 3 as input gives (negative) minimum hoop stresses. The other shrinkage variants give minimum hoop stresses close to zero.

Sy top max
There are three different patterns to be found in this graph:

- **Part 1 & part 2**

  Shrinkage variant 1 and variant 2 give maximum stresses close to zero. The other variants give positive maximum hoop stresses. Shrinkage variant 3 has larger maximum stresses as result than shrinkage variant 4. Boundary condition A gives larger maximum stresses than boundary condition B.

- **Part 3**

  This pattern look similar to the pattern of part 1 and part 2 but, when the diameter of the traditional concrete is small (90 mm), shrinkage variant 3 gives a maximum stress close to zero.

- **Part 4**

  Shrinkage variant 3 only gives a significant positive maximum hoop stress in this part. These stresses are higher when the diameter of the traditional concrete is 90mm than when the diameter is 180mm.

Sz top min
All the parts have the same pattern. All the variants contain negative minimum stresses in longitudinal direction. When the input value: shrinkage variant 3 is used, the minimum stresses are significant lower than in the other variants. In this variant a small difference between the different Young's Modulus can be seen.

Sz top max
All the parts of this plot have a very similar pattern. The shrinkage variants 1 and 2 give negative maximum stresses.

The input value shrinkage variant 3 gives a maximum stress close to zero for boundary condition B. Boundary condition A gives a small maximum positive stress . The input value shrinkage variant 4 gives a negative maximum stress as output.

Sx mid min
This graph has the same pattern over all the parts. When shrinkage variant 3 is used, a negative radial minimum stress occurs. In case of all the other shrinkage variants, no significant stress as output. The radial stress is larger if the traditional concrete has a diameter of 90mm instead of 180 mm.

Sx mid max
There are two different patterns that can be recognised in this graph:

- **Part 1 & part 2**

  The contact area is bonded for both the parts. Positive radial maximum stresses occur in case the shrinkage variant 4 is used as input value. If the traditional concrete has a diameter of 90mm, the maximum stresses are larger than when a diameter of 180mm is used.

- **Part 3 & part 4**

  The maximum radial stresses that occur for part 3 and part 4 are all close to zero.

Sy mid min
There are two different types of patterns that can be seen in the graph:

- **Part 1 & part 2**

  These parts both have bonded as input value for the contact area. Negative minimum hoop stresses occur when shrinkage variant 3 or 4 is used. For the other variant the stresses are close to zero. When the diameter is small (90mm), shrinkage variant 3 gives larger minimum stresses than shrinkage variant 4. When the diameter is large (180 mm), shrinkage variant 4 gives larger minimum stresses than shrinkage variant 3.

- **Part 3 & part 4**

  Only when shrinkage variant 3 is used as input, it gives significant (negative) minimum stresses as output. A diameter of 90 mm gives larger minimum hoop stresses than a diameter of 180 mm.

Sy mid max
There are two clear patterns in this graph:

- **Part 1 & part 2**

  The input values shrinkage variant 3 and shrinkage variant give significant positive maximum hoop stresses. The output gives higher maximum stresses if shrinkage variant 3 is used instead of shrinkage variant 4. Shrinkage variant 1 and 2 have maximum stresses close to zero as output

- **Part 3 & part 4**

  In these parts only the shrinkage variant 3 as input value gives (positive) maximum hoop stresses. The other shrinkage variants give maximum stresses close to zero.

Sz mid min
This bar chart is very similar to Sz top min.

Sz mid max
All the parts of this plot also have the same pattern. The shrinkage variants 1 and 2 give negative maximum stresses. The input value shrinkage variant 3 gives a maximum stress close to zero.In case boundary condition A is used, this stress is mostly positive, in case boundary condition B is used, this maximum stress is mostly negative. The input value shrinkage variant 4 gives a negative maximum stress as output. This stress is smaller than when shrinkage variants 1 or 2 are used.

11.3.2. Local Sensitivity Analysis by Ansys

Appendix G shows the results from the local sensitivity analysis from ansys. The results are discussed per bar chart (per part).

Part 1 (figure G.1, Appendix G)
This sensitivity analysis bar chart can be divided in 3 types of patterns:

- **The hoop and radial stresses in the top of the element**

  The radial stresses are primarily influenced by the traditional shrinkage (negative sensibility). To less extend it is also influenced by the displacement in z-direction at the top of the column and the Young's Modulus of the traditional concrete (both negative sensibility). The shrinkage in the printed concrete has a small positively sensibility for the radial stresses.

  The minimum hoop stresses are influenced by the shrinkage in the printed and traditional concrete, the displacement in z-direction and the Young's modulus of the traditional concrete. They all have a negative sensibility. The shrinkage in the printed concrete has the largest influence.

  The shrinkage in the traditional concrete has a positive sensibility for the hoop stresses at the top of the element. The shrinkage in the printed concrete, displacement in z-direction at the top of the element and the Young's modulus of the traditional concrete have a negative sensibility. The shrinkage in the printed concrete has the highest influence on the hoop stresses.

- **The hoop and radial stresses in the middle of the element**

  Shrinkage has the the highest sensibility for the hoop and radial stresses in the element. The shrinkage in the printed concrete has a positive sensibility and the shrinkage in the traditional concrete has a negative sensibility for the radial stresses. This is the same for the minimum hoop stresses, the maximum hoop stresses are opposite: The shrinkage in the traditional concrete has a positive sensibility and the shrinkage in the printed concrete a negative sensibility.

- The longitudinal stresses in the top and middle of the element.

  The sensibilities for the stresses in longitudinal direction are similar for the top and the middle of the element. For the minimum longitudinal stresses this means that the shrinkage in printed concrete and the displacement in z-direction at the top of the element have the largest influence on the stress. They have a negative sensibility.

  The maximum longitudinal stresses have a negative sensibility for the following parameters: the shrinkage in the traditional concrete, the displacement in z-direction and the Young's modulus in the traditional concrete. The shrinkage in the printed concrete has a positive sensibility to a lesser extend. The shrinkage and the displacement in z-direction have the largest influence.

Part 2 (figure G.2, Appendix G)
The sensibilities are similar for the top and the middle of the element.

- **The radial and hoop stresses**

  The radial stresses are mainly influenced by shrinkage. The shrinkage in the traditional concrete have a negative sensibility for the hoop stresses, the shrinkage in the printed concrete have a positive sensibility.

  The hoop stresses are also mainly influenced by shrinkage. For the minimum hoop stress, the shrinkage in the traditional concrete has a negative sensibility and the shrinkage in the printed concrete a positive sensibility. This is opposite for the maximum hoop stress.

- **The longitudinal stresses**

  The minimum longitudinal stresses have a negative sensibility in the following parameters: The shrinkage in the printed concrete and the displacement in z-direction at the top of the element. The displacement in z-direction has the largest influence on the stress.

  For the maximum longitudinal stress a negative sensibility is apparent for the parameters: shrinkage in traditional concrete, displacement in z-direction at the top and the Young's modulus for the traditional concrete. The shrinkage in the printed concrete has a small positive sensibility. The shrinkage and the displacement in z-direction have the largest influence.

Part 3 (figure G.3, Appendix G)
The local sensitivity analysis of part 3 has the most similarities to part 1. This means that this graph will also be split in 3 parts

- **Hoop and radial stresses at the top of the element**

  The maximum and minimum radial stresses at the top of the element are pretty similar to each other. The shrinkage in the traditional concrete has the largest influence (negative sensibility). The displacement in z-direction at the top and the Young's modulus also have a negative sensibility. The shrinkage in the printed concrete has a positive sensibility.

  A negative sensibility for the shrinkage in the printed concrete (largest) and a negative sensibility for the displacement in z-direction can be seen at the hoop stresses. The shrinkage in the traditional concrete and the Young's modulus have a positive sensibility for the hoop stresses. The diameter of the traditional concrete has a small positive sensibility for the hoop stresses.

- **Hoop and radial stress at the middle of the element**

  The radial stresses have a negative sensibility for the shrinkage in traditional concrete and a positive sensibility for the shrinkage in the printed concrete. The maximum radial stress is also a little influenced by the diameter in the traditional concrete (negative influence).

  The hoop stresses are mainly influenced by shrinkage. The minimum hoop stress has a negative sensibility for the traditional concrete and a positive sensibility for the printed concrete. The sensibilities of the maximum hoop stresses are the other way around.

- **Longitudinal stresses at the middle and the top of the element**

  The stresses in the middle and the top of the element are similar. The displacement in z-direction has the most influence on the minimum stresses (negative sensibility). The shrinkage in the printed concrete has a smaller influence on the stresses (negative sensibility).

  The maximum longitudinal stresses are mostly influenced by the displacement in z-direction at the top of the element andthe Young's modulus in the traditional concrete (both negative sensibility). The shrinkage in the traditional concrete has a lower, but also negative sensibility.

Part 4 (figure G.4, Appendix G)
The sensibilities of the middle and the top of the element are similar. This part is divided into 2.

- **Hoop and radial stresses in the top and middle of the element**

  The shrinkage in the printed and traditional concrete have most influence on the hoop and radial stresses. The shrinkage in the traditional concrete has a negative sensibility for the radial stresses. The shrinkage in the printed concrete has a positive sensibility. One remarkable thing at the radial stresses is the relatively high influence of the diameter of the traditional concrete on the maximum radial stresses at the middle of the element.

  The minimum hoop stresses have a negative sensibility for the shrinkage in the traditional concrete and a positive sensibility for the shrinkage in the printed concrete. This is the opposite for the maximum hoop stresses.

- **Longitudinal stresses in the top and middle of the element**

  The minimum longitudinal stresses are mainly influenced by the displacement in z-direction at the top. To less extend by the shrinkage in the printed concrete (both negative sensivitiy).

  The maximum longitudinal stresses have the largest negative sensibility for the displacement in z-direction and the Young's modulus in the traditional concrete. The shrinkage in the traditional concrete has a smaller negative sensibility. The shrinkage in the printed concrete only has a small positive sensibility.

11.4. Analysis of the results

In the analysis of the results, the results will be analysed and explained. The goal of this section is to understand the results discussed in Section 11.3. The analysis of the results will be split in the variants study and the local sensitivity determined by Ansys.

11.4.1. The variants study

With this part the influence of the boundary condition and the contact area be determined. This will be done by explaining the following statements that can be formed from the results.

- **The contact area has influence on the hoop and radial stresses at the middle and top of the element**

  This statement can be made due to the fact that the parts 1 & 2 don't have the same pattern as the parts 3 & 4, for the hoop and radial stresses in the bar charts. The effect of the influence will be discussed separately for the two parameters that causes hoop and radial stresses.

- **Hoop and radial stresses occur due to the restricted shrinkage in the printed and traditional concrete.**

  The difference between the bonded and frictionless parts are mostly caused by the shrinkage variant 4. Shrinkage variant 4 implies that the printed concrete has shrunk completely before the traditional concrete is cast. When the contact area is bonded, the printed concrete restricts the traditional concrete to shrink. This causes hoop and radial stresses. When the contact area between the materials is frictionless, the traditional concrete can shrink without being restricted by the printed concrete. This means that no hoop or radial stresses will occur due to restricted shrinkage.

  In the variants 1 and 3, the printed concrete shrinks more than the traditional concrete. This means that the printed concrete applies a pressure on the traditional concrete, this is independent of the contact area. Variant 2 has no shrinkage in both the materials. This makes the hoop and radial stresses independent of the contact area.

- **The prescribed displacement in vertical direction causes hoop and radial stresses in some cases.**

  The displacement in vertical direction applied at the top of the element will not cause hoop or radial stresses for boundary condition B. For boundary condition A it will. To see if they influence the result, the bar charts that contain the hoop and radial stresses at the top of the element are of interest. If the patterns of part 1 and part 3 of the bar chart are alike, the contact area does not influence the stresses

significantly. If they differ, the contact area has influence. In the graphs it can be seen that the radial stresses reduce a bit in part 3 in comparing to the stresses in part 1. The patterns looks, in general similar. Some shrinkage variants have a larger change in result than other.

There can be concluded that the shrinkage affects the amount the contact area influences the hoop and radial stresses.

- **The boundary condition has only influence on the hoop and radial stresses at the top of the element**

  There are two different types of boundary conditions: a restriction in horizontal and vertical direction at the top and the bottom of the element, and one with only a restriction in vertical direction. The top of the element is more close to the boundary condition than the middle of the element. This concludes that the boundary condition has more influence in the top of the element than in the middle of the element.

  A significant difference in the pattern of the bar chart for the parts with boundary condition A in comparing to the parts with boundary condition B is present. The hoop and radial stresses are influenced by the boundary condition. Any movement in the hoop or radial direction is restricted by boundary condition A. This restricted deformation causes stresses, as the element wants to deform in the horizontal plane due to shrinkage and lateral expansion. In case of boundary condition B, the deformation in the horizontal plane are not restricted and the deformations can occur.

11.4.2. The local sensitivity analysis

The local sensitivity in Ansys is determined for the following parameters: diameter in the traditional concrete, shrinkage in the traditional concrete, shrinkage in the printed concrete, displacement in z-direction at the top and the Young's modulus. The results are given in a bar chart, with the output on the horizontal axis and the local sensitivity in percentage on the vertical axis. This local sensitivity can be positive or negative.

A positive sensitivity means the following: if the value of the parameter increases, the value of the stress increases. A negative sensitivity means that if the value of the parameter increases, the value of the stress decreases. The figure 11.4 on the next page explains it in a graph. This means the following

- Positive sensibility: If the value of the parameter(input) increases the stress (output) increases
- Negative sensibility: If the value of the parameter(input) increases the stress (output) decreases

The shrinkage is a extraordinary case. If the value of the parameter "shrinkage" increases, the temperature input increases. The basis input value for shrinkage will be below the surrounding temperature. If the input value increases, the input value will be more close to the surrounding temperature of 22 degrees. This means that the concrete will shrink less if the parameter increases, and will shrink even more when the parameter decreases. The following statements can be made:

- Positive sensibility: If the value of the parameter shrinkage increases the shrinkage decreases and the stress increases
- Negative sensibility: If the value of the parameter shrinkage increases the shrinkage decreases and the stress decreases

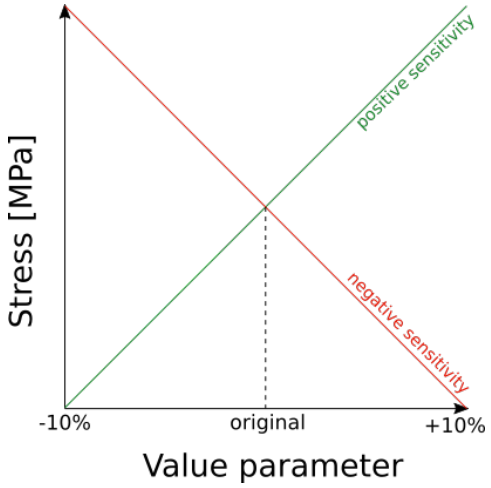

Figure 11.4: The positive and negative local sensitivity curve

Part 1 (figure G.1, Appendix G)

- **The diameter of the traditional concrete has in all cases little influence on the stresses**

  If the diameter of the traditional concrete changes with +10% or -10%, there won't be that much difference in the result for variant 1.

- **The shrinkage of traditional concrete has significant influence in the hoop and radial stresses.**

  If the input value of the shrinkage is reduced with 10% the printed concrete shrinks more than the traditional concrete. This means that the shrinkage of the printed concrete is restricted by the traditional concrete. The restricted deformation causes compressive radial stresses in both materials (figure 10.19a), compressive hoop stresses in the traditional concrete and tensile hoop stresses in the printed concrete.

  If the traditional concrete shrinks too, it reduces size, this gives the printed concrete more space to shrink. This means that the difference in shrinkage between the two materials changes the stresses in the element. The shrinkage of the traditional concrete reduces the stresses that occur due to the shrinkage in the printed concrete.

  If the input value of the shrinkage is increased with 10% it will be larger than the surrounding temperature of 22 °C. This means that the traditional concrete will expand instead of shrink. This will increase the stresses that occur in the element due to the shrinkage of the printed concrete. Only 17% ($\frac{22.7-22}{22.7-18.57} * 100\% = 17\%$) of the range between the two input values are caused by an expansion in the traditional concrete. This is a small influence on the result

  The shrinkage in the traditional concrete has a negative sensibility for the minimum and maximum radial stresses and the minimum hoop stresses in the element. This means that radial and minimum hoop stresses increase when the shrinkage increases.

  The radial stresses and the hoop stresses in the traditional concrete are negative (compressive). The shrinkage of the traditional concrete reduces difference in shrinkage between the two materials ant therefore the compressive stresses. This concludes in a negative sensibility.A positive sensibility is the case at the maximum hoop stresses at the top and middle of the element.This means that if the shrinkage increases, the stresses decrease. Tensile hoop stresses occur due to the shrinkage of the printed concrete. The tensile stresses reduce when the shrinkage of the traditional concrete increases. Which concludes with a positive sensibility.

- **The shrinkage of the traditional concrete has influence on the maximum longitudinal stresses**

  The longitudinal stresses are created by the vertical displacement in z-direction in the top and, in case the element is bonded, by the difference in shrinkage of both materials.

  The difference in shrinkage causes longitudinal stresses if the two materials are bonded. Bonded means that the two materials can not deform independently. If the two materials have a frictionless contact area, there won't be any stresses due to the restricted deformation of the difference in shrinkage. If the difference in shrinkage influences the longitudinal stresses significantly, the local sensitivity of the bonded variant must be larger than the sensitivity of the frictionless variant.

  The local sensitivity of the shrinkage of the traditional concrete is similar for the bonded and the frictionless variant. This means that the difference in shrinkage does not have a large influence on the sensitivity. Variant 1, on which this local sensitivity is based, has a small difference in shrinkage between the two materials. This also explains the small influence on the longitudinal stresses.

  The displacement in vertical direction introduces longitudinal compressive stresses in the element. The higher the Young's modulus of the concrete, the larger the compressive stresses will be. As the traditional concrete has a smaller Young's Modulus than the printed concrete, the maximum longitudinal stresses are located in the traditional concrete. If the traditional concrete shrinks, less prescribed displacement is needed to reach uz=0.5mm. This means that the longitudinal stress reduces when the traditional concrete increases. The traditional concrete has a positive influence on the result. This coincides with a negative sensitivity.

- **The shrinkage of the printed concrete has significant influence in the radial and hoop stresses of the model.**

  The printed concrete shrinks more than the traditional concrete for the main part of the sensitivity analysis. The traditional concrete restricts the deformation that takes place due to shrinkage. This causes stresses.

  The input value +10% causes less shrinkage in the printed concrete than in the traditional concrete. This causes a different stress distribution, and therefore a change in the local sensitivity analysis. 23% ($\frac{21.5-20.643}{21.5-17.63} * 100\% = 23\%$) of the input values to determine the local sensitivity of the printed concrete has a shrinkage smaller than the shrinkage in the traditional concrete.

  In some cases the shrinkage of the printed concrete has a positive influence, in other cases a negative influence:

  The shrinkage of the printed concrete causes compressive radial stresses. The printed concrete shrinks more than the traditional concrete. The traditional restricts the printed concrete to deform. This causes compressive radial stresses. The largest compressive stresses are located at the middle of the element (Sx min) and the smallest compressive stresses are at the outer part of the printed concrete (see figure 10.19a). If the shrinkage of the printed concrete increases, higher compressive stresses occur in the cross section. This is a negative influence and caused by a negative sensitivity.

  If the element has boundary condition A as input, it cannot move in vertical and horizontal direction at the top of the element. The shrinkage and the lateral expansion will be restricted. This causes compressive stresses in the traditional and printed concrete at the top of the element.

  Boundary condition B gives tensile hoop stresses in the printed concrete and compressive hoop stresses in the traditional concrete. The increase of shrinkage will give an increase in the tensile hoop stresses in the printed concrete and an increase in the compressive stresses in the traditional concrete. This can be seen in a positive sensibility in the minimum hoop stresses and a negative sensibility in the maximum hoop stresses.

  The middle of the element is not influenced by the boundary condition. This means that the sensibility is similar to the ones with principal.

- **The shrinkage of the printed concrete has influence on the minimum longitudinal stresses.**

  This explanation will be similar to the shrinkage in the traditional concrete in longitudinal direction.

  The difference in shrinkage between the two materials nearly influence the stresses in longitudinal direction. The shrinkage in the printed concrete does reduce the longitudinal stresses in the element

due to the prescribed displacement of 0.5mm at the top of the element. The larger the shrinkage the lesser stresses occur in the longitudinal direction. This is a negative sensibility and a positive influence.

- **The displacement in z-direction has only influence in the hoop and radial stresses at the top of the element in case boundary condition A is used.**

  The printed and the traditional concrete have a Poisson ratio of 0.2. This means that the concrete element wants to deform in the horizontal plane in case of a deformation in the vertical plane. Boundary condition A restricts the element to move in x- and y-direction at the top and bottom of the column. This means that the lateral contractions are restricted in the top and bottom part of the element in case boundary condition A is used. The restricted deformation causes compressive stresses in the hoop and radial direction. If the deformation in vertical direction increases, the compressive stresses in the hoop and radial stresses increases. The displacement in vertical direction at the top has a negative sensibility and a negative influence on the result.

- **The displacement in z-direction has significant influence in the longitudinal stresses**

  A displacement in vertical direction is restricted at the bottom of the element. When a displacement in z-direction is applied at the top of the element, the element is pushed together. This causes compressive stresses in the element. If the prescribed displacement at the top of the element increases, the compressive stresses increase. The vertical displacement in z-direction at the top has a negative sensibility and a negative influence on the stresses.

- **The Young's modulus in the traditional concrete has a large influence on the maximum longitudinal stresses**

  The has a prescribed displacement at the top of the element. The stresses that occur in the element due to this displacement depend on the E-modulus of the material. If the material has a high E-modulus, it is stiff and a relatively high pressure needs to be applied to reach the prescribed displacement. When the material has a low E-modulus, it is not stiff at all and a relatively low pressure is needed to apply the same displacement. The pressure needed to apply this deformation causes compressive stresses in the element. If the Young's modulus of the traditional concrete increases, larger compressive stresses will occur. The Young's modulus has a negative sensiblity and a negative influence on the compressive longitudinal stresses.

11.5. Ideal choice of input values

The sensitivity analysis gives information about the influence of the parameters. This section will give insight in what the influence brings to result in the load bearing strength of the element.

The concrete will have triaxial stress behaviour. It will be most strong if all the stresses from the three principal directions are compressive. Triaxial compressive stresses increase the strength of the concrete material. This will create an ideal situation for the concrete printed element. Hoop and/or radial tensile stresses will occur in all variants. If a triaxial behaviour exists of compressive and tensile stresses, the strenght of the element can be determined with a biaxial behaviour [15] (see figure 11.5). This means that the material will be most strong when the tensile stresses are the smallest. There can be concluded that the tensile stresses should be reduced as much as possible.

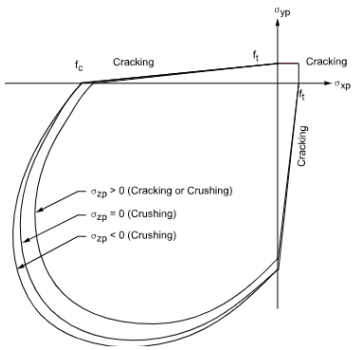

Figure 11.5: Biaxial failure surface [2]

In this section, the prescribed displacement is assumed to cause enough compressive longitudinal stresses in the element that all longitudinal stresses are compressive.

The prescribed displacement causes tensile stresses in the hoop and radial direction. The stresses that occur when a displacement of 0.3mm is applied can be seen in figure 11.6 on the next page

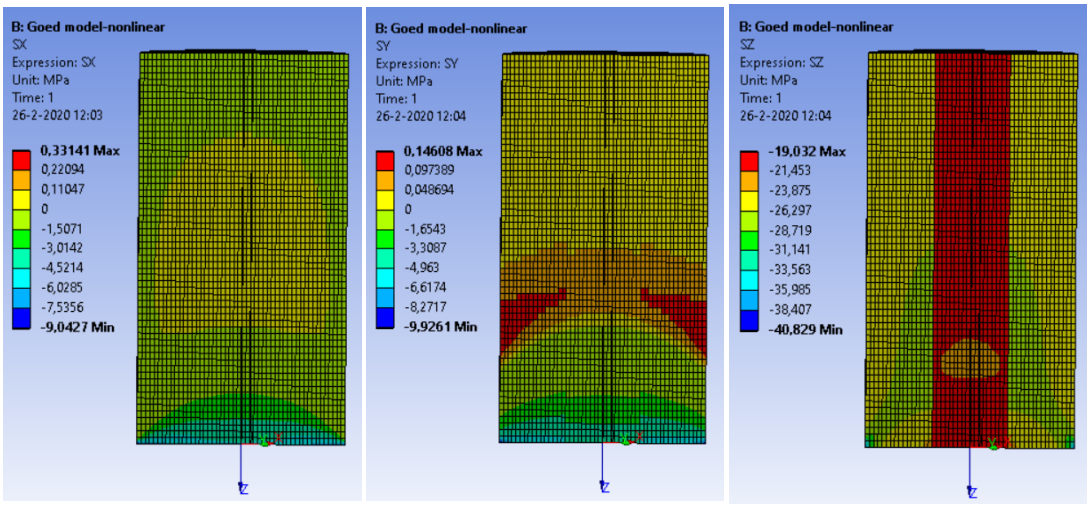

(a) σ_x (b) σ_y (c) σ_z

Figure 11.6: Stresses in the concrete printed element due to a vertical displacement of 0.3mm

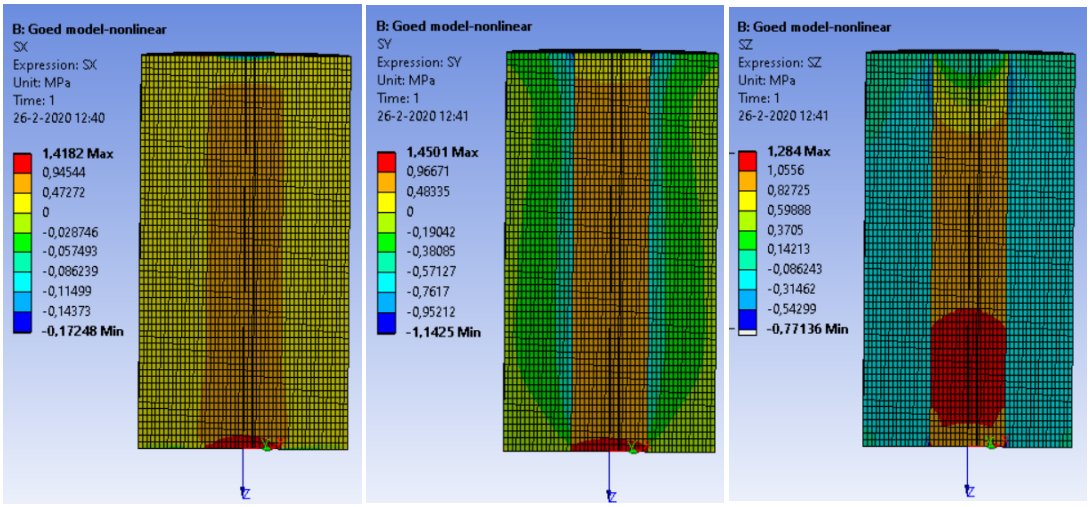

(a) σ_x (b) σ_y (c) σ_z

Figure 11.7: Stresses in the concrete printed element due to a shrinkage of 0.028 ‰in the traditional concrete

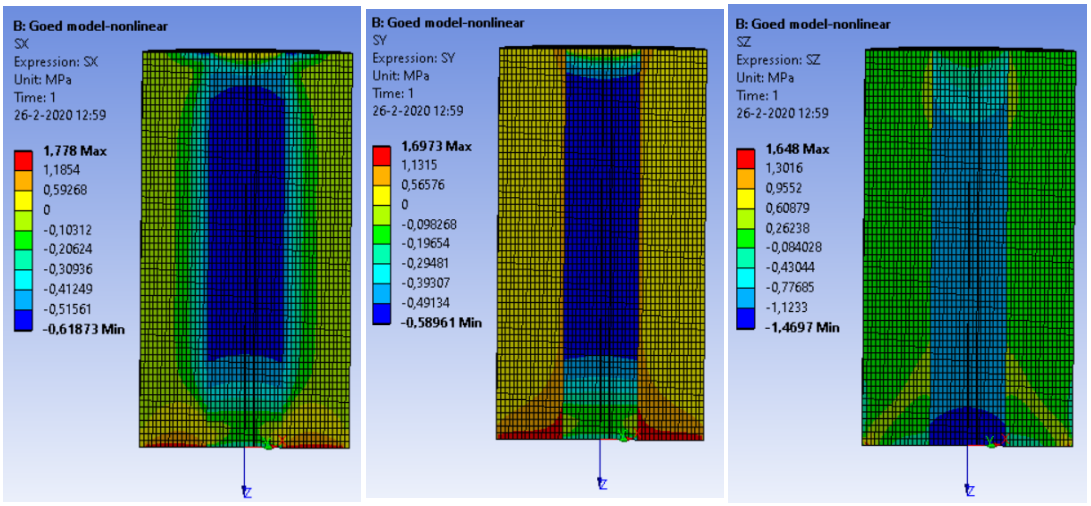

(a) σ_x (b) σ_y (c) σ_z

Figure 11.8: Stresses in the printed element due to a shrinkage of 0.028 ‰in the printed concrete

Because there will be only compressive stresses in the longitudinal direction, the parameters from the sensitivity analysis that influence the stresses in hoop or radial direction are discussed:

Contact area: The contact area will only influence the stresses if the shrinkage in the traditional concrete will be smaller than the shrinkage in the printed concrete. This will separate the two elements structurally. This means that there won't be any stresses due to the shrinkage of the element. The only radial and hoop stresses that occur are the ones due to the prescribed vertical displacement.

Boundary condition: The prescribed displacement causes compressive stresses in longitudinal direction. Shrinkage will cause tensile stresses in radial and hoop direction close to the boundary condition. This should be avoided, by making sure that the stresses due to the prescribed displacement are larger than the stresses due to shrinkage. As can be seen in the figures 11.6, 11.7 and 11.8

Shrinkage: The stresses in hoop and radial direction are (especially in the middle of the element) mainly influenced by the shrinkage in the printed and traditional concrete. Concluded form the variant study, it is important to know whether the traditional or the printed concrete has a larger shrinkage. This causes a different stress distribution in case the boundary condition is bonded.

The different stress distributions can be seen in the figures 11.8 and the figures 11.7. From these pictures it can be seen that the shrinkage has a large influence on the stresses in hoop and radial direction. To get the element with the largest load bearing resistance the tensile stresses are the ones to be reduced.

There can be concluded that, the highest tensile stresses will occur if the printed concrete shrinks more than the traditional concrete. These high tensile stresses occur close to the contact area between the printed and traditional concrete in hoop direction (figure 11.8b).

The difference in height of the tensile stresses between the figure 11.8 and figure 11.7 is not that much. This means that one of the two types of shrinkage is not considered as better. It is better to choose the time of casting in such a way that the difference in shrinkage is as little as possible. Take into account that the shrinkage curve of different types of concrete can be different. This means that the largest difference in shrinkage might occur earlier than at t = infinity, this can be seen in figure 8.4. The largest stresses will occur in the largest difference in shrinkage between the two materials.

From this it can be concluded that it is not possible without any extra steps as pre-loading to reach triaxial compressive behaviour. This means that the tensile stresses in the element should be as small as possible. The smallest tensile stresses will occur if the difference in shrinkage between the two materials is as small as possible. Another possibility is if the traditional concrete shrinks more than the printed concrete, and the contact area is considered as frictionless.

11.6. Conclusions

A linear model is made to function as a basis for the nonlinear model. The hand calculations have validated the model. A sensitivity analysis, split into two parts: a variant study, and a local sensitivity analysis are used to define the influence of the following parameters:

- **Contact area**

  Contact area has influence on the hoop and radial stresses in case the shrinkage of the printed concrete that has to occur after filling the element is smaller than the shrinkage that still has to occur of the traditional concrete. If, in this case, the input "frictionless" is used, no stresses in the hoop and radial direction occur. If the input "bonded" is used, tensile stresses in the traditional concrete, and compressive stresses in the printed concrete will occur.

  The contact area has little influence on the stresses in all the other variants.

- **Boundary condition**

  The boundary condition only influences the stresses in the top and the bottom of the element.

- **Diameter traditional concrete**

  A change in the diameter of the traditional concrete has relatively little influence on the stresses of the element. If the diameter increases significant, the influence will be noticeable. If the shrinkage of the printed concrete is larger than the shrinkage of the traditional concrete, the stresses in the element reduce if the diameter increases. If the shrinkage of the traditional concrete is larger than the shrinkage of the printed concrete, the stresses increase if the diameter increases.

- **Shrinkage traditional concrete**

  The shrinkage of the printed concrete has a significant positive influence if the printed concrete still have to shrink more after casting the traditional concrete than the traditional concrete. If the shrinkage of the traditional concrete increases, the difference in shrinkage between the two materials decreases and the stresses in all directions decrease.

  If the traditional concrete still have to shrink more than the printed concrete, the difference in shrinkage between the two materials increase, which concludes in an increase of stresses in all the directions.

- **Shrinkage printed concrete**

  The shrinkage in the printed concrete has a negative influence on the stresses if the shrinkage in the printed concrete that still has to occur after casting is larger than the shrinkage in the traditional concrete.

  The shrinkage in the printed concrete has a positive influence on the stresses if the shrinkage that still has to occur after casting is larger for the traditional concrete than for the printed concrete.

- **Displacement in z-direction at the top of the element**

  The displacement in vertical direction always has a large negative inlfuence on the longitudinal stresses of the element.

  In case boundary condition A is used as input the lateral expansion due to the displacement in vertical direction will cause compressive stresses in the hoop and radial direction.

- **Young's modulus of the traditional concrete**

  The stresses needed to create the prescribed vertical displacement are increased when the Young's modulus increases. This means that the longitudinal stresses increase.

To create an element with the largest load bearing resistance, the tensile stresses due to the prescribed displacement and stresses in the element should be reduced as much as possible. Therefore it is best to create an element that has almost no difference in shrinkage between the two materials or create a material where the contact area is frictionless and the traditional concrete shrinks more than the printed concrete. In both variants this concludes in little influence of stresses that occur due to the difference of shrinkage.

IV

Final Remarks

The final remarks will consist of a conclusion, discussion and the recommendations. The conclusion will contain the answer to the research question. The discussion will discuss the conclusions, this means that it will show the flaws of the research. The recommendations will contain a list of further research subjects to create a better result. The relation form this part to the other parts can be seen in figure 11.9.

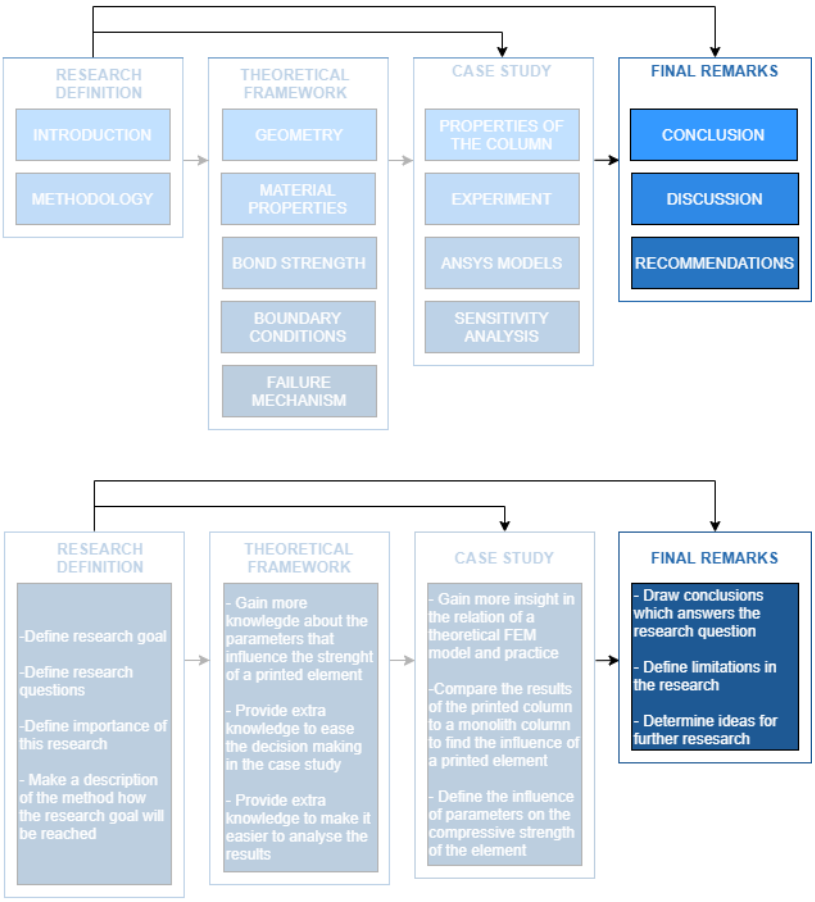

Figure 11.9: Methodology final remarks

12

Discussion

This chapter will discuss the flaws of the research. It will question the trustworthiness of the results and conclusions.

- **The development of the stiffness when the concrete ages**

  The autogenous shrinkage of concrete increases as the concrete gets older, at the same time the Young's modulus will also increase. The time dependent influence of the Young's modulus on the stresses on the element is not taken into account. As result, the of stresses due to restricted shrinkage will reduce. This phenom is not taken into account, this causes smaller initial stresses due to the difference in shrinkage.

  Besides the Young's modulus, the tensile and compressive strength also develop, and increase when the concrete hardens.

- **Relaxation in the concrete element**

  Relaxation is the phenomenon that the stresses in a concrete element reduce if the loading is applied for a long time. Creep is related to relaxation and implies that the deformations in a concrete element increase if a load is applied for a long time [**?**]. Both creep and relaxation are not implemented in this research. This means that if the element is older than at the time of the experiment and therefore loaded for a longer time, the deformations due to the loading will increase and the stresses due to the loading will decrease. This might give a different conclusion.

- **The geometry**

  This research is based on a concrete printed element. This concrete printed element is straight, relatively short and circular. If any of these properties are changed the conclusion might not hold anymore. Any change in the geometry can cause a different stress distribution and therefore a different failure mode.

- **Stresses that occur due to the restricted shrinkage**

  Within this research it is assumed that no shrinkage occurs during loading of the element. The difference in shrinkage is considered as an initial stress distribution. The stress distribution that occurs due to the restricted shrinkage and loading is unknown, and cannot be assumed to be equal to a summation of the two stress distributions. This means that this conclusions might not hold for long term loading.

- **Nonlinear model & the experiment**

  The failure of the nonlinear model is compared to the experiment. As there is only one experiment tested, it is not sure if most printed element will fail and crack the same way. The nonlinear model does not show the failure of the model, it shows all the cracks just before failure. It is an assumption how the model will actually fail. This means that the comparison of the nonlinear model and the experiment is mainly based on educated assumptions.

- **The variant study & local sensitivity**

  Within the variant study and the local sensitivity, the maximum and minimum stresses at the top of the element are compared. This means that the whole stress distribution of the element is not considered. This has as result that it is still unknown what the influence the parameters have on the stress distribution of the element. It only considers the height of the stresses

  The sensitivity analysis and the variant study are based on the linear model. This has as result that the influence the parameters have on failure is not taken into account. A change in the parameter might cause a different type of failure.

- **The local sensitivity analysis**

  The local sensitivity analysis is only based on the first variant of the four different parts (variant 1, 25, 49 and 73). This means that the basis of the sensitivity analysis follows from those variants. Only one parameter from those variants is changed to calculate the influence of that parameter. This means that it is, for example, unknown what the sensitivity is of the diameter of the traditional concrete if the shrinkage variant 4 is used.

13

Conclusion

In the introduction, the following research question has been defined: *What is the influence of printed lost formwork on the load bearing capacity of a circular element?* In this chapter the answer to this question is given.

A (non)linear finite element model is developed to show the stress distribution of a printed element. The printed formwork represents a hollow concrete printed cylinder with an outer diameter of 250mm, an inner diameter of 90mm and a height of 470mm. This printed hollow formwork is filled with traditional concrete of the class C30/37. The nonlinear model is constructed to analyse the failure mechanism. This mechanism is then compared to a regular monolith concrete element. The linear model is constructed to analyse the sensitivity of several parameters. When combining these results, a comprehensive conclusion can be drawn.

From the nonlinear model, the following is concluded:

- The first cracks is located at the contact area between the printed and traditional concrete. The cracks run in vertical direction.
- The stresses in hoop direction cause the first cracks in the element.
- The element fails brittle

The nonlinear model of the printed element is compared to a model of a monolith element. It is concluded that the load bearing resistance of the printed element cannot be calculated the same way as a monolith concrete element, because large differences can be seen in the stress distribution between the printed and monolith element. This is primarily caused by the difference in shrinkage between the printed and traditional concrete.

The linear model is used for the sensitivity analysis which confirms the conclusion from the aforementioned comparison; The difference in shrinkage between the printed and traditional concrete has the highest influence on the hoop and radial stresses. The longitudinal stresses are mostly influenced by the vertical loading and the Young's modulus of the traditional concrete.

The combination of the vertical loading and the difference in shrinkage causes tensile stresses in at least one direction. The load bearing capacity of the element therefore is determined by the maximum tensile stress in the element. Due to the vertical loading of the element, tensile stresses in the longitudinal direction are unlikely. Therefore, radial and hoop stresses are more of interest.

It is concluded that the influence of the printed formwork on the load bearing resistance of a cast element mostly depends on the difference in shrinkage between the two materials.

14

Recommendations

The recommendations will first discuss the things that have to be taken into account to create the largest load bearing resistance of a short printed concrete column. Thereafter, ideals for further research are summed up.

In order to increase the load bearing capacity of the printed element, it is recommended to decrease the difference in shrinkage behaviour between the two materials. An option to achieve this, is to delay the casting of the traditional concrete to create a similar shrinkage behaviour for both materials. Take into account that the shrinkage graphs of two different materials can differ. The largest stresses will occur at the largest difference between the shrinkage of both materials, this doesn't have to be at the moment the maximum shrinkage occurred.

The influence of the difference in shrinkage on the load bearing capacity can be reduced by having a frictionless contact area between the printed and traditional concrete and a shrinkage which is larger in the traditional than in the printed concrete.

Before this research was performed little was known about the stress distribution and the failure mechanism of a printed column. This research is limited, as it was performed on a short circular printed element. More research is necessary to actually construct a concrete printed column of more realistic dimensions.

- Scaling the circular short element will be the first step to become a bit closer to a realistic column. The increased length of the element will cause a different stress distribution. Different parameters, in addition to the ones influencing the short circular element, will influence the strength of the column. One factor that will become relevant in the case of a full size column is the effect of buckling. No indication how a full size concrete printed column will perform in case it is loaded by a compressive force is available.

- The possibility to create columns in almost every shape is a large advantage of concrete printing. This research has discussed a circular printed element, which is actually a short circular column. This circular column hardly uses the available freedom of form. There might be shapes that increase the influence of the printed formwork on the load bearing resistance of the element.

- The load bearing resistance of a short circular printed element has been researched for the most common load case: a compressive force. It is interesting to research what would happen if the element if is loaded eccentrically or horizontally. This will cause bending moments and shear stresses in the column. It will cause a whole different stress distribution and failure mechanism.

- In this research, reinforcement has not been used. Traditional reinforcement can be put in the concrete printed formwork, before the traditional concrete is cast. Reinforcement implemented in the printed concrete is something which is researched a lot currently. There are possibilities to use fibres in the printed concrete, or to put a steel cable in the printed concrete. It would be very interesting to test these methods in the printed column. It might increase the load bearing resistance.

V

Appendix

A

Experiment on the hollow printed element

To test the influence of cable reinforcement in a printed element, a compression test is performed on several printed elements by BAM and TU Eindhoven. This section will discuss the observations and results of the experimented hollow concrete element

During this experiment 4 relevant columns are tested:

- Three hollow printed columns without reinforcement: S0V0-A, S0V0-B and S0V0-C
- One hollow printed column without reinforcement filled with traditional concrete: S0V1

As can be see in the summation, all columns have a name according to their characteristics. S0 indicates as an unreinforced column, V0 as not filled and V1 as filled. Within this part of the research only the unreinforced hollow columns are relevant. The filled concrete column is discussed in Chapter 9. This means the columns S0V0-A, S0V0-B, S0V0-C are discussed in this appendix.

[mm]	D_{top}	W_{top}	D_{bottom}	W_{bottom}	h
S0V0-A	250	85/90	265	105	470
S0V0-B	250	90	260	95	470
S0V0-C	245	80/85	250	85	475

Table A.1: Dimensions of the hollow elements which are used in the experiment (figure A.1)

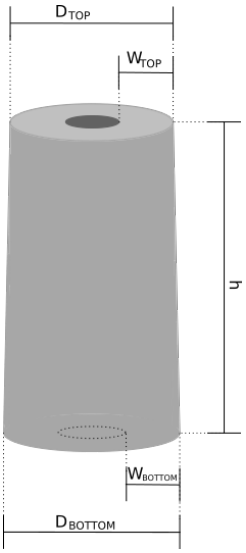

Figure A.1: The definition of the dimensions of the hollow element

The printed formwork is made of the concrete: Weber 3D 160-1. During the experiment the concrete compressive strength of the printed concrete has been determined. A strip has been printed, three test specimen are cut out of this strip. All the specimen have the following size: 40x40x100 mm^3. During a compressive strength test, the average compressive strength of the specimen is determined to be equal to 45,3 MPa.

To analyse the result the dimensions are measured before the experiment took place. The results can be found in table A.1.The dimensions of the column were irregular, so differences of half a centimetre might occur. This table shows that the elements are not completely symmetric, this might influence the crack patterns that occur during the experiment.

S0V0 columns			
	S0V0-A	S0V0-B	S0V0-C
Failure load [kN]	-2014.57	-2307.7392	-1992.2178
Failure stress [MPa]	-45,1	-51,1	-47,3
Average deformation at failure [mm]	-0.4422	-0.28385	-0.5286

Table A.2: The loading and failure at the time of failure for the concrete printed hollow elements

A.1. The experiment

Due to the process of concrete printing, the top surface of the concrete element wasn't completely flat. To make the experiment as trustworthy as possible, the element is sawn 3mm from the top surface. To make sure small inconsistencies will not affect the final result, carboard is place betweem the machine and the top / bottom surface. The experiment is performed with a standard displacement controlled test machine. The results of the experiment can be seen in table A.2.

A.2. Observations

Halfway the experiment two cracks occur: vertical, from the top of the column to 1/4 of the height of the column, see figure A.5. The two cracks are at opposite location. This happens when the column is loaded by a force in between -800 kN and 1250 kN. The cracks can be seen in the force-displacement diagrams of the experiment, which are shown in the figures A.2, A.3 and A.4 on the following pages. When the column fails the two cracks became larger and a big part of the column falls off. This can be seen in figure A.6. A horizontal crack is located perpendicular to the part which fell off.

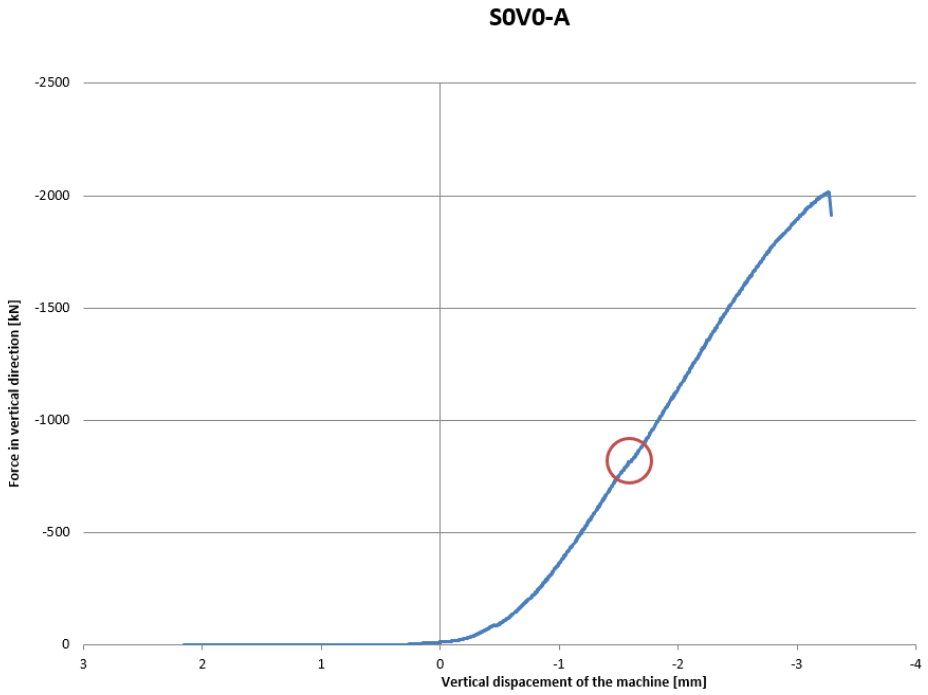

Figure A.2: Force displacement diagram of concrete printed hollow element: S0V0A, during the experiment

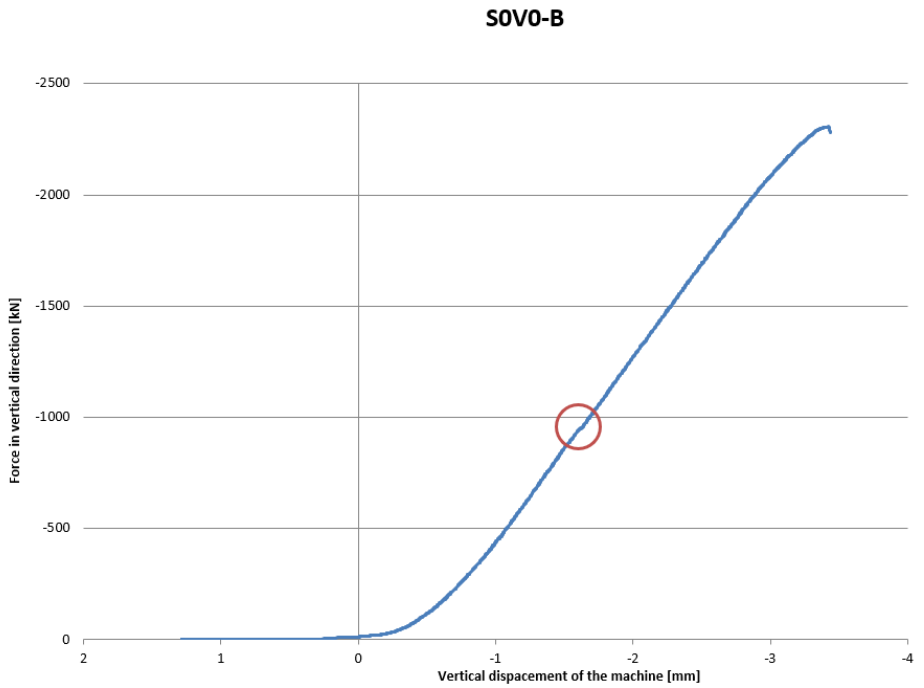

Figure A.3: Force displacement diagram of concrete printed hollow element: S0V0B, during the experiment

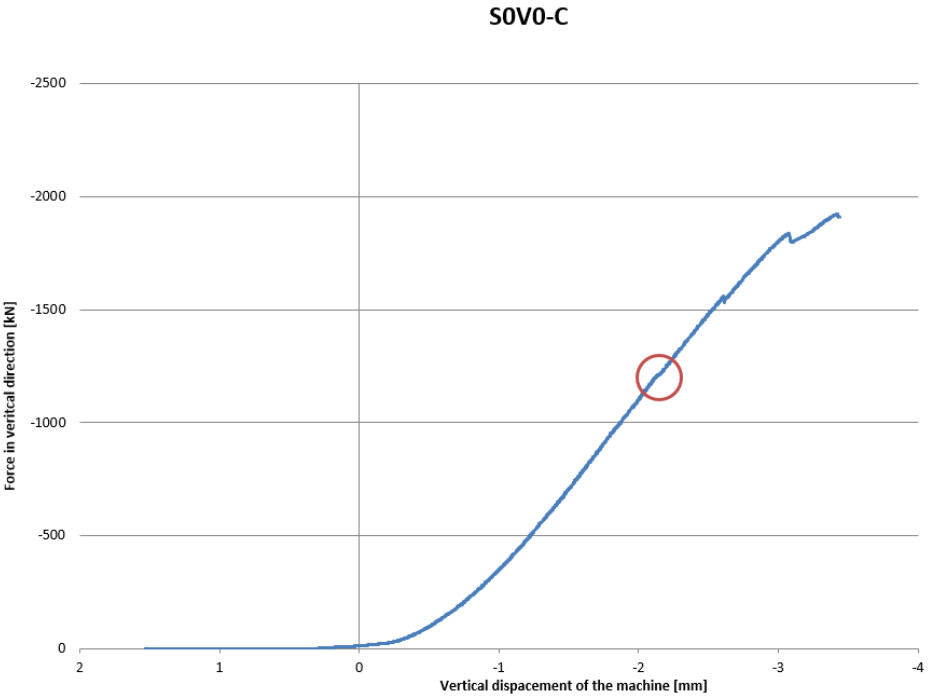

Figure A.4: Force displacement diagram of concrete printed hollow element: S0V0C, during the experiment

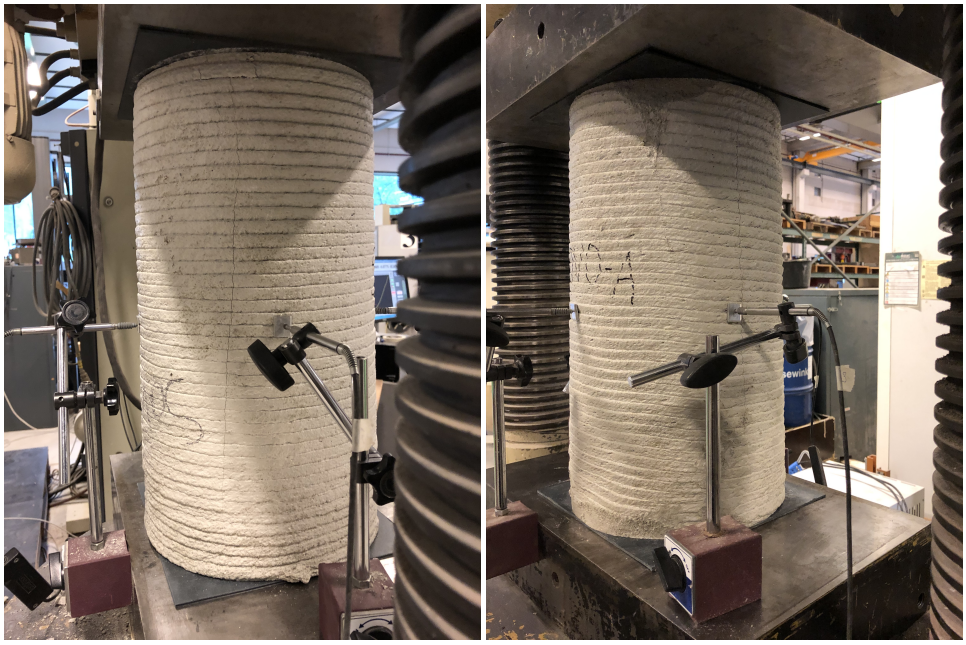

(a) Left side (b) Right side

Figure A.5: The first crack in the concrete printed hollow element: S0V0-A

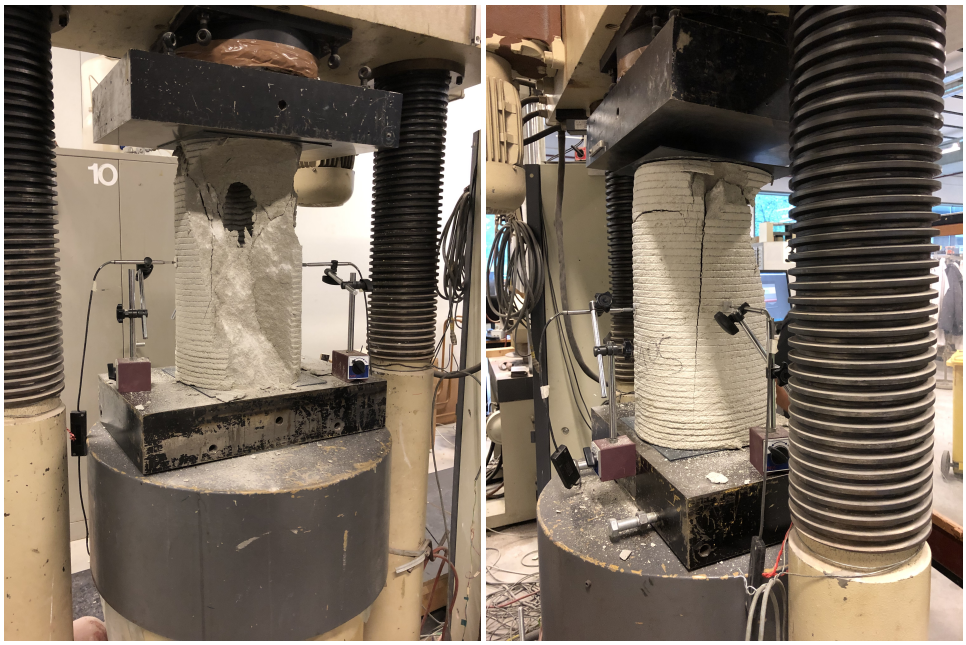

(a) Front (b) Left side

Figure A.6: The crack patterns at failure of concrete printed hollow element: S0V0-A

Figure A.7: The top of the element at failure of printed concrete element: S0V0-A

B

Hand-calculations

B.1. Introduction

More insight in the strength and the behaviour of the element is needed to check whether results are right or wrong. Multiple hand-calculations have been performed for this reason: strength of the element, stresses due to deformation, stresses due to shrinkage, and bond strength.

B.2. Strength of the element

The maximum strength of the concrete filled printed element will lay in between two limits: one in which the concrete printed formwork does not add extra strength and one in which the concrete printed formwork and the traditional concrete will act as one monolith element. The two limits can be seen in figure B.1. To calculate the load bearing resistance of a round concrete element, a GTB-table can be used. In this case, the concrete element does not have longitudinal reinforcement is used and is only loaded with a compressive force. This means the GTB-value is equal to 1.0. (figure B.4)

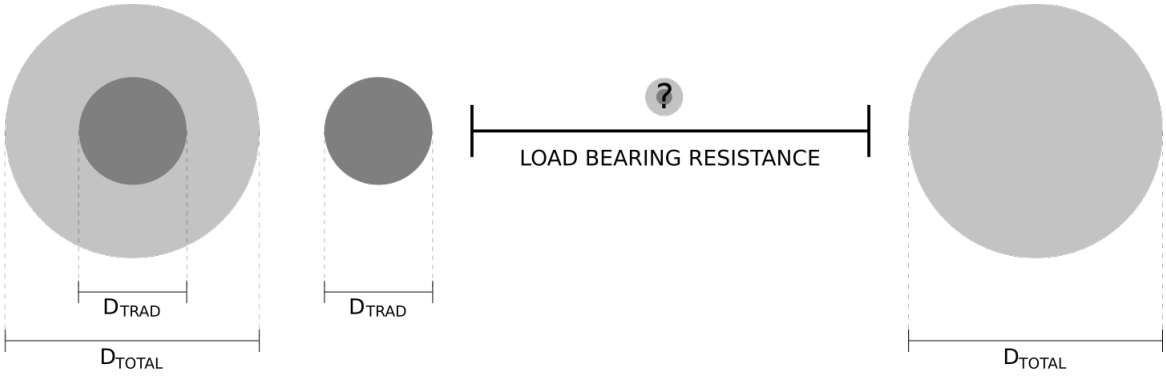

Figure B.1: Maximum and minimum load bearing resistance due to a compressive force of the printed element.

Maximum compressive normal force for a monolith column ($D = 250mm$):

$$N_{max,mono} = A_{column} * f_{ck} * value_{GTB}$$
$$N_{max,mono} = -1/4 * PI * 250^2 * 45.3 * 1.0 * 10^{-3} = -2223.66kN \tag{B.1}$$

Maximum compressive normal force on the hollow column ($D = 250mm, d = 90mm$):

$$N_{max,250} = A_{column} * f_{ck} * value_{GTB}$$
$$N_{max,250} = -((1/4 * PI * 250^2) - (1/4 * PI * 90^2)) * (45.3) * 1.0 * 10^{-3} = -1935.47kN \tag{B.2}$$

Maximum compressive normal force on the inner part of the column ($d = 90mm$):

$$\begin{aligned} N_{max,90} &= A_{column} * f_{ck} * value_{GTB} \\ N_{max,90} &= -1/4 * PI * 90^2 * (36.1) * 1.0 * 10^{-3} = -229.66kN \end{aligned} \tag{B.3}$$

Maximum compressive normal force when the two parts are summed up:

$$\begin{aligned} N_{max} &= N_{max,90} + N_{max,250} \\ N_{max} &= -229.66 + -1935.47 = -2165.13kN \end{aligned} \tag{B.4}$$

Stresses in the concrete element

The calculated stresses in the concrete element will be used to validate the linear Ansys model. They can be calculated with the law of Hooke (formula B.5). This calculation assumes a linear material and isotropic material behaviour. The material properties from Chapter 8, table 8.2 are used. The element in this calculation is considered to be monolith. The monolith element is considered to be made of printed concrete, as this material has the largest volume in case study design.

$$\begin{vmatrix} \sigma_x \\ \sigma_y \\ \sigma_z \end{vmatrix} = \frac{E}{(1+\nu)*(1-2*\nu)} * \begin{vmatrix} 1-\nu & \nu & \nu \\ \nu & 1-\nu & \nu \\ \nu & \nu & 1-\nu \end{vmatrix} \begin{vmatrix} \dot{\epsilon_x} \\ \epsilon_y \\ \epsilon_z \end{vmatrix} \tag{B.5}$$

$$\epsilon_z = \frac{-\delta_z}{l} = \frac{-0,5}{470} = -0.0010638 \tag{B.6}$$

$$\begin{aligned} \epsilon_x &= \nu * \epsilon_z = -0.2 * -0.0010638 = 0.0002128 \\ \epsilon_y &= \nu * \epsilon_z = -0.2 * -0.0010638 = 0.0002128 \end{aligned} \tag{B.7}$$

$$\begin{aligned} u_x &= \epsilon_z * D = -0.0002128 * 250 = 0.0532mm \\ u_y &= \epsilon_z * D = -0.0002128 * 250 = 0.0532mm \end{aligned} \tag{B.8}$$

With these values formula B.5 can be solved:

$$\begin{vmatrix} \sigma_x \\ \sigma_y \\ \sigma_z \end{vmatrix} = \frac{40891}{(1+0.2)*(1-2*0.2)} * \begin{vmatrix} 1-0.2 & 0.2 & 0.2 \\ 0.2 & 1-0.2 & 0.2 \\ 0.2 & 0.2 & 1-0.2 \end{vmatrix} \begin{vmatrix} \dot{0.0002128} \\ 0.0002128 \\ -0.0010638 \end{vmatrix} = \begin{vmatrix} 0 \\ 0 \\ -43.5010638 \end{vmatrix}$$

There won't be any stresses in x- and y- direction because the deformation in these directions is not restricted.

B.3. Stresses in the element due to restricted shrinkage

Stresses due to shrinkage only occur if the deformation is restricted. In figure B.2, on the next page it can be seen that the printed concrete deforms more than the traditional concrete. In this case it is assumed that the bond between the printed and traditional concrete is infinite strong. This makes deformation of the printed concrete at the bond is equal to the deformation of the traditional concrete. A triangle deformation form is used as simplification for this calculation (see figure B.2, on the next page).

The shrinkage calculated in Chapter 8, table 8.2 is used for this calculation.

$$\begin{aligned} u &= l_{tot} * shrinkage \\ u_{trad} &= l_{tot} * shrinkage_{trad} \\ u_{trad} &= 470 * -0.000019 = -0.008930mm \\ u_{print} &= l_{tot} * shrinkage_{print} \\ u_{print} &= 470 * -0.00003376 = -0.01586720mm \end{aligned} \tag{B.9}$$

$$u_{print} - u_{trad} = -0.01586720 + 0.008930 = -0.00693720 \tag{B.10}$$

$$u_1 = -(\frac{T_{print} * (u_{print} - u_{trad})}{0.5 * D_tot})$$
$$u_1 = -(\frac{80 * (0.00693720)}{0.5 * 250}) = 0.0022199mm \tag{B.11}$$

$$u_2 = (u_{print} - u_{trad}) - \frac{T_{print} * (u_{print} - u_{trad})}{0.5 * D_tot}$$
$$u_2 = -0.00693720 - \frac{80 * (-0.00693720)}{0.5 * 250} = -0.00124870mm \tag{B.12}$$

$$\sigma = \epsilon * E$$
$$\sigma_{trad} = \frac{u_2}{L_tot} * E_{trad}$$
$$\sigma_{trad} = \frac{-0.00124870}{470} * 32496 = -0.08633MPa$$
$$\sigma_{print} = \frac{u_1}{L_tot} * E_{print}$$
$$\sigma_{print} = \frac{0.0022199}{470} * 40891 = 0.19313MPa \tag{B.13}$$

A compressive stress of -0.08633 MPa in the traditonal concrete and a tensile stress of 0.19313 MPa can occur in the concrete element due to restricted shrinkage. The amount of shrinkage is similar to the amount of shrinkage used in the theoretical model, to easily compare these two.

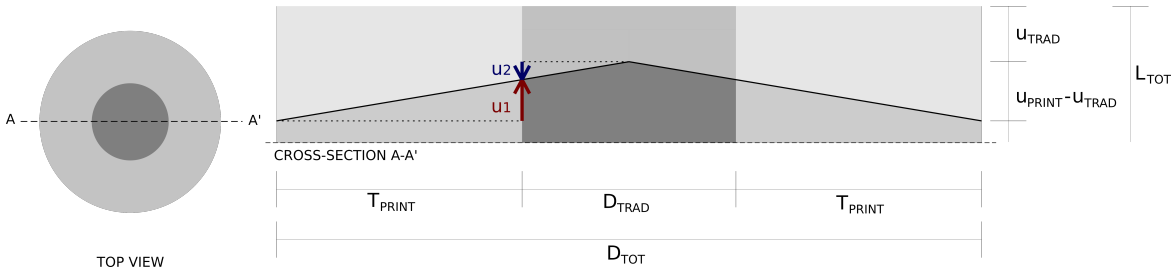

Figure B.2: The deformations at the top of the element due to shrinkage of the materials. This a simplified schematization to calculate the stresses that occur due to the restricted difference in vertical shrinkage.

Shrinkage in the horizontal plane Shrinkage will also give stresses in the cross-section. Figure B.3 on the next page, shows the way shrinkage causes stresses in the cross-section of the element.

The shrinkage at D=90 for printed concrete:

$$Shrinkage_{print,hoop} = c_{in} * Shrinkage = 90 * \pi * 0.00003376 = 0.0095454mm \tag{B.14}$$

The shrinkage at D=90 for traditional concrete:

$$Shrinkage_{trad,hoop} = c_{in} * Shrinkage = 90 * \pi * 0.000019 = 0.0053721mm \tag{B.15}$$

The difference in shrinkage will cause stresses in the cross-section:

$$\sigma_{shrinkage,hoop} = \frac{shrinkage_{print,hoop} - shrinkage_{trad,hoop}}{c_{in}} * E_{trad}$$
$$\sigma_{shrinkage,hoop} = \frac{0.0095454 - 0.0053721}{90 * \pi} * 32496 = 0.479642MPa \tag{B.16}$$

Total horizontal shrinkage:

$$Shrinkage_{total,horiz} = D_{trad} * shrinkage_{trad} + 2 * T_{print} * shrinkage_{print}$$
$$Shrinkage_{total,horiz} = 90 * 0.000019 + 2 * 80 * 0.00003376 = 0.0071116mm \tag{B.17}$$

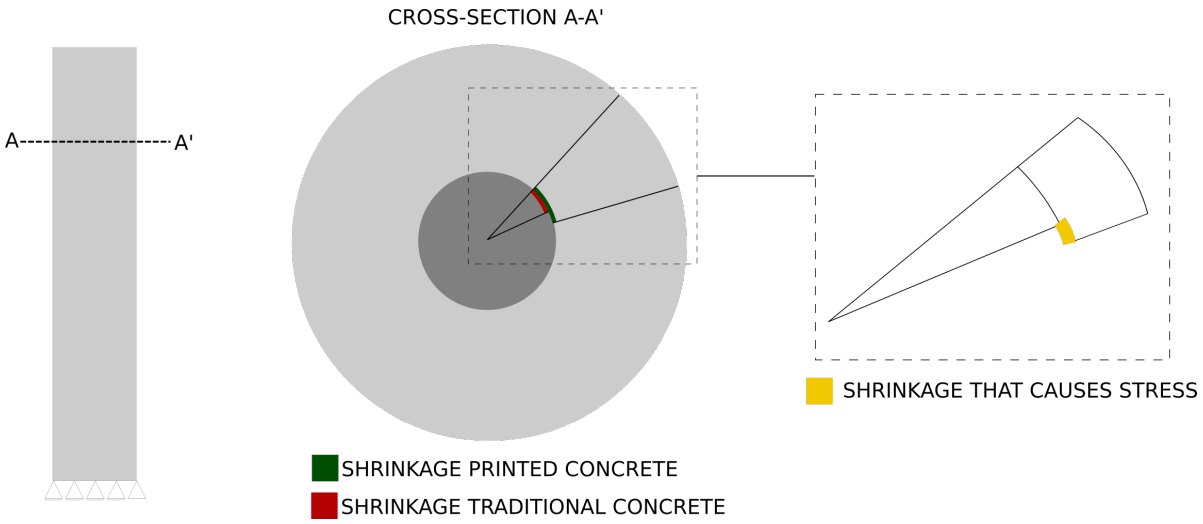

Figure B.3: The deformations in the cross-section of the element due to shrinkage of the materials. This a schematization to calculate the stresses that occur due to the restricted difference in hoop direction

B.4. Conclusion

The conclusions contain the results of the different hand calculations:

Strength of the column:

From these hand calculations a few expectations for the model and the experiment can be made. First of all will the strength of the concrete element lay in between -178.76 kN and -1772.05 kN.

Stresses in the column:

The stresses that occur when the concrete element is loaded by a vertical displacement of $u_z = 0.5mm$ is calculated. This has been done for a monolith column, completely made from printed concrete. The stress that occur in vertical direction is equal to: -43.5 MPa. Because the element can move freely in horizontal direction, there won't be any stresses in x- or y- direction. The column will, due to Poisson, deform in x- and y direction with 0.0532mm.

Restricted shrinkage:

The large difference in shrinkage between the two material can cause stresses in the element. The shrinkage in vertical direction can cause a compressive stress of -0.08633 MPa in the traditional concrete and a tensile stress of 0.19313 MPa in the printed concrete.

The shrinkage in hoop direction will cause a stress of 0.480 MPa in the traditonal concrete.

]

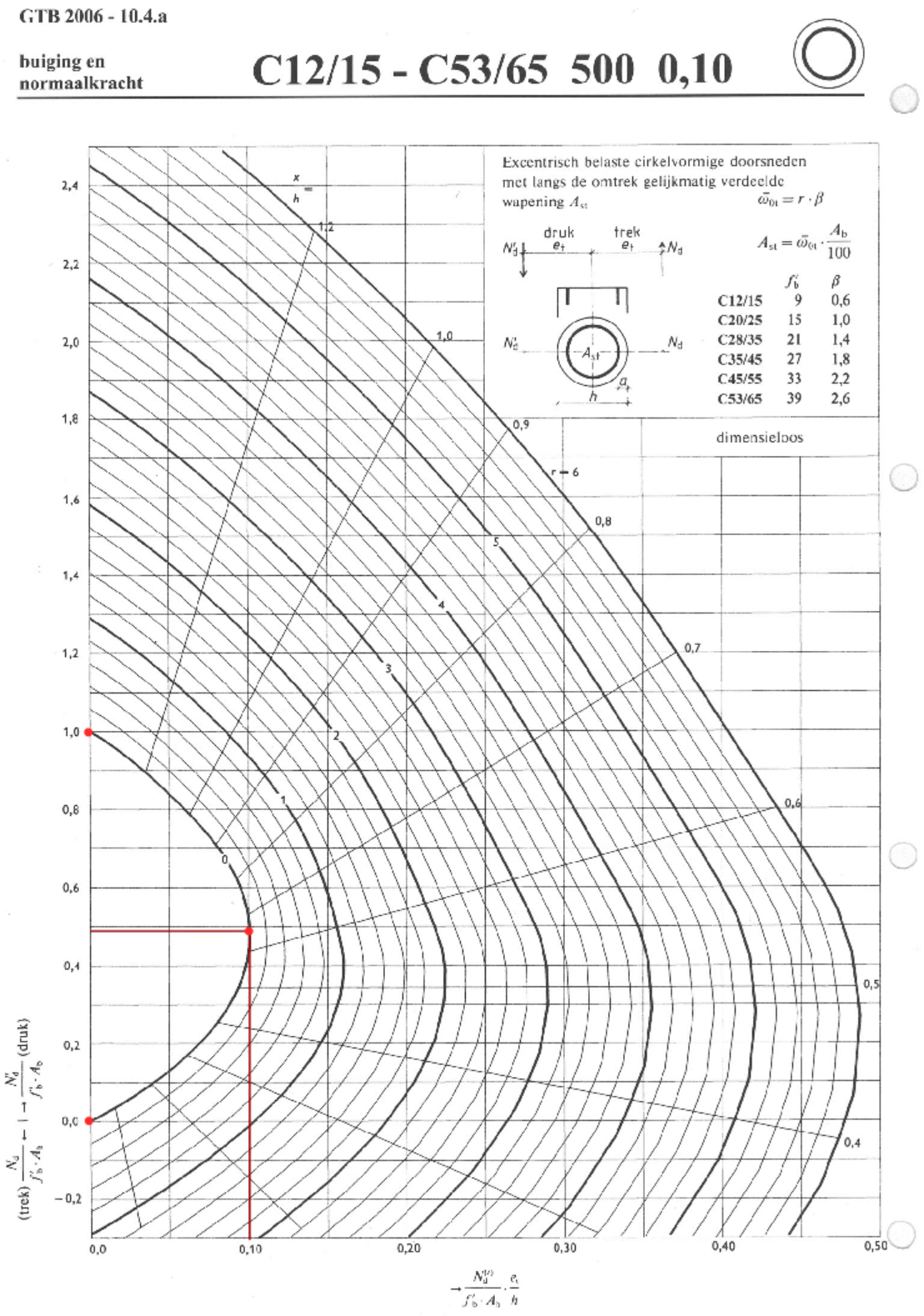

Figure B.4: GTB graph for a round concrete column. This graph can be used to define the load bearing strength of a circular concrete element [25]

C

Validation of the linear model

The model can be validated by some of the hand calculations performed in Chapter B.

Stresses in the column:

"The stresses that occur at a loading of $u_z = 0.5mm$ at the top of the element are determined. This has been done for a monolith column, completely made from printed concrete. The stresses that occur are only in vertical direction: -43.5 MPa. The column will, due to Poisson also deform in x- and y direction with 0.0532mm." - Chapter B.

As can be seen in figure C.1, the compressive stresses in the printed concrete are in between -42.0567 and -44 MPa, which is similar to the result of the hand calculation. Due to the different Youngs modulus of the printed and traditional concrete, the stresses differ per material.

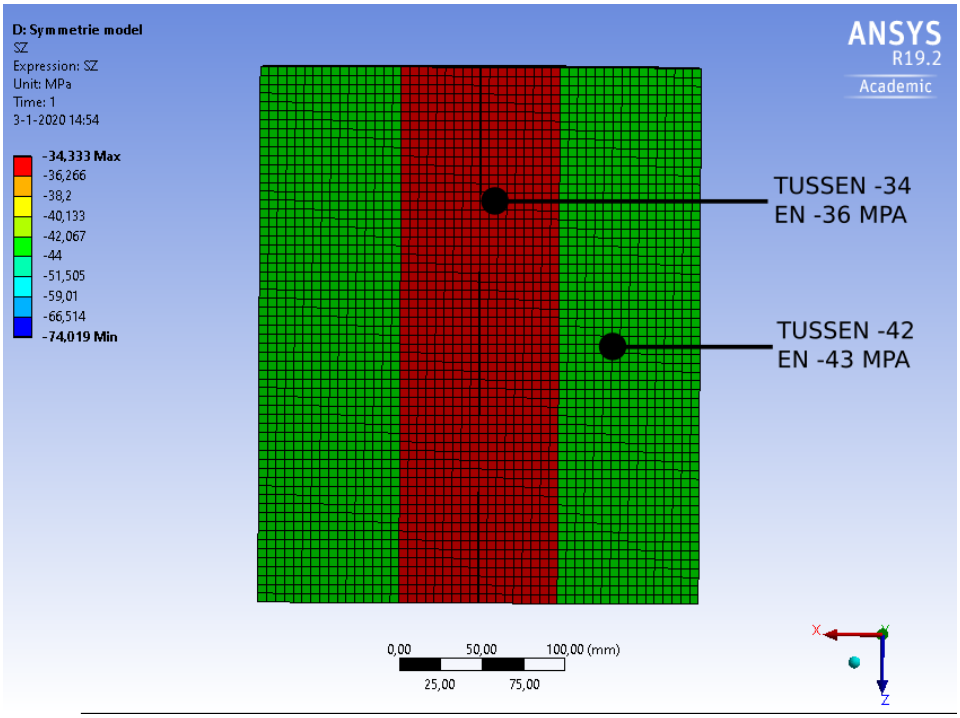

Figure C.1: Stresses in vertical direction in the concrete printed element due to a prescribed displacement of: $u_z = 0.5$

Restricted shrinkage:

"The large difference in shrinkage between the two material can cause stresses in the element. The shrinkage in vertical direction can cause a compressive stress of -0.08633 MPa in the traditional concrete and a tensile stress of 0.19313 MPa in the printed concrete." - Chapter B.

Figure C.2 shows the deformation in vertical direction for shrinkage. It can be seen that the outer part of the printed concrete deforms with -0.015415 mm in vertical direction. This is similar to the vertical deformation calculated at Chapter B. The deformation of the printed concrete lays in between -0.015mm and -0.014mm. This is larger than the expected value at the hand calculations. During the hand calculations the deformation of the column has been estimated by a triangle (see Chapter B). In reality it will probably look a bit more like figure C.2. The different deformation pattern, shows that the traditional concrete is pulled.

The stresses in vertical direction of the restricted shrinkage can be seen in figure C.3 on the next page. The printed concrete, which also had a similar deformation as the hand calculation, shows a similar stress: between 0 and 0.2 MPa. The printed concrete shows higher compressive stresses than expected. This can be explained by the fact that the printed concrete pulled the traditional concrete down more than expected.

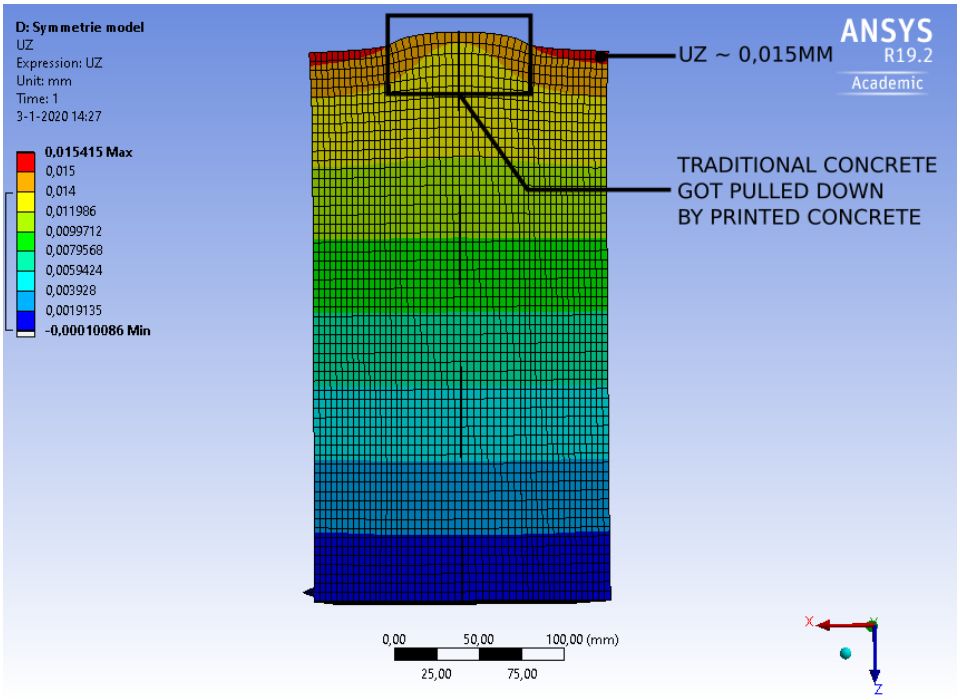

Figure C.2: Deformations in vertical direction in the concrete printed element due to the restricted shrinkage. (Deformation scaling factor: 5)

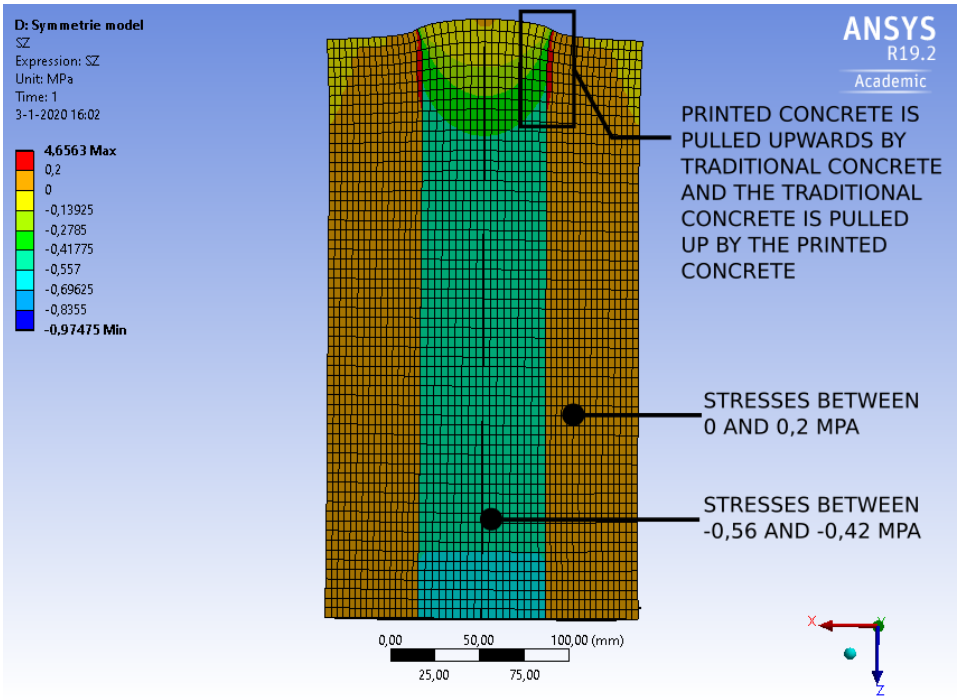

Figure C.3: The vertical stresses in the concrete printed element due to the restricted shrinkage. (Deformation scaling factor: 5)

"The shrinkage in radial direction will cause a stress of 0.480 MPa in the traditonal concrete." - Chapter B.

The deformation in horizontal direction is calculated as: 0.0071116 mm in total. This is equal to 0.0035558 per side. This is a little bit smaller than the deformation of calculated with Ansys (see figure C.4).

A stress of 0.480 MPa in the traditional concrete is calculated by hand. According to the Ansys model, these stresses will be a bit lower. The stresses in the printed concrete will reduce over the cross section.

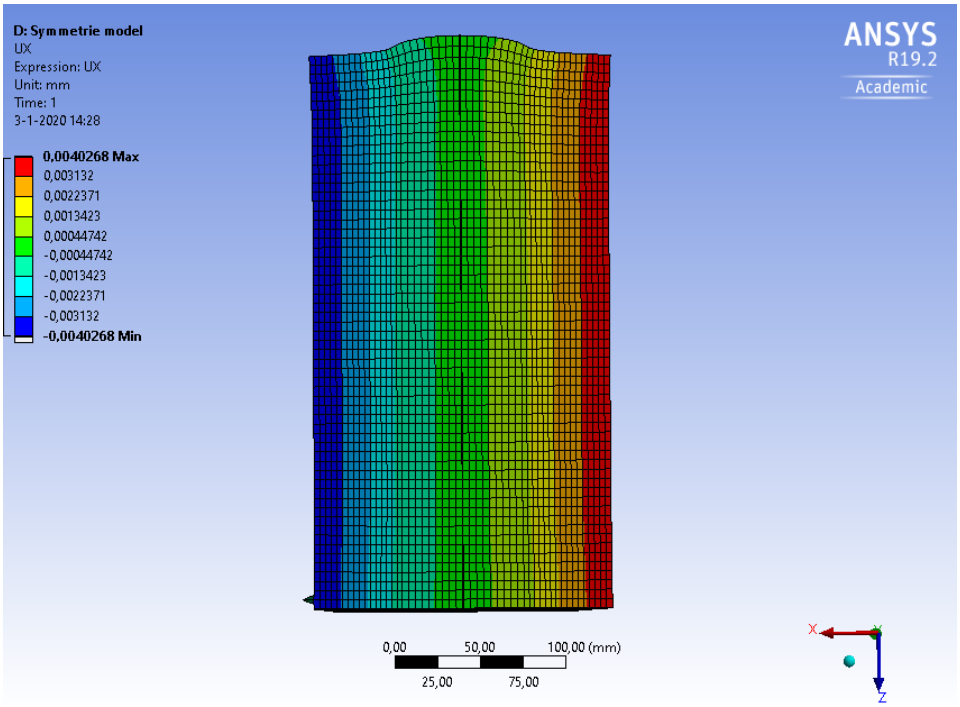

Figure C.4: The deformation in radial direction in the printed element due to the restricted shrinkage. (Deformation scaling factor: 5)

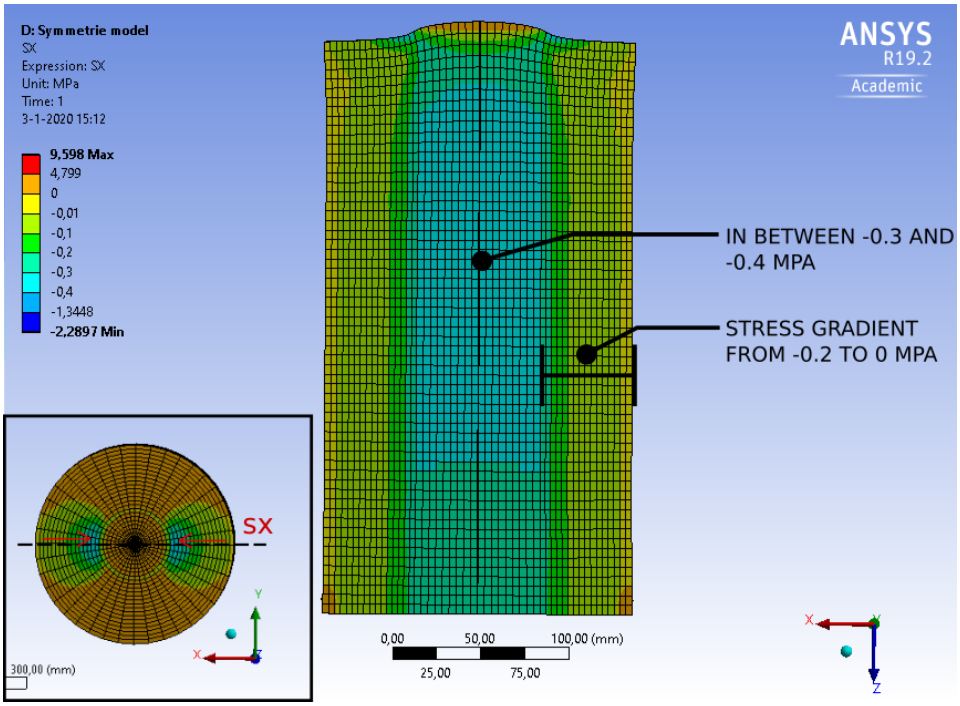

Figure C.5: The stresses that occur in x-direction due to restricted shrinkage (Deformation scaling factor:5)

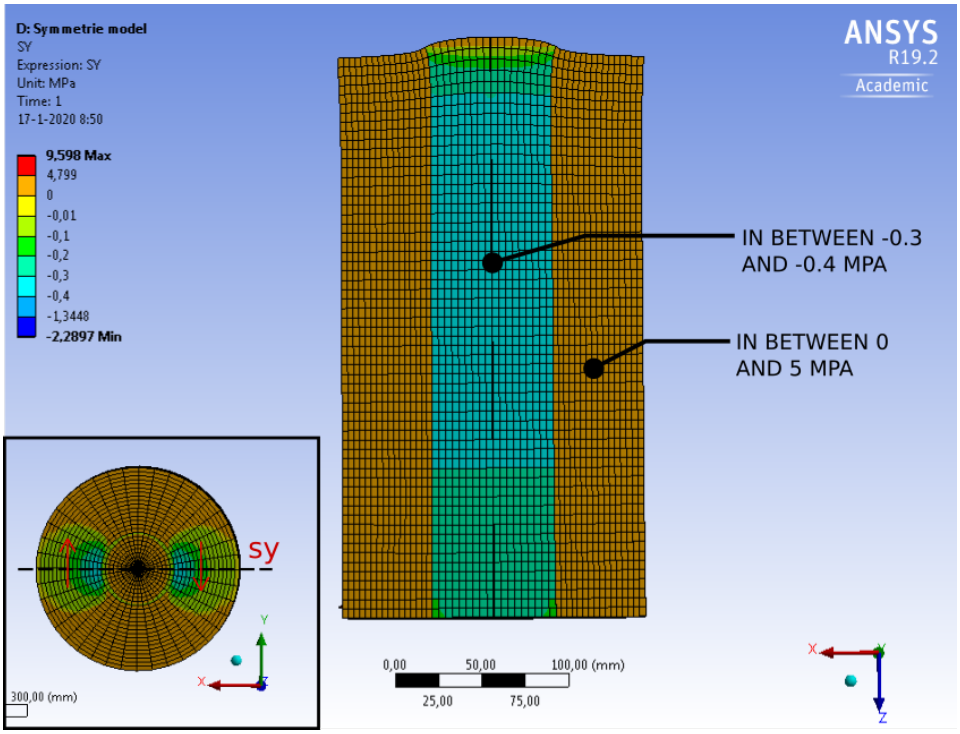

Figure C.6: The stresses that occur in y-direction due to restricted shrinkage (Deformation scaling factor:5)

The hand calculations and the Ansys calculations are not exactly the same, but are really similar. In combination with the hand calculation and common sense there can be concluded that the Ansys model is right.

D

Theoretical background information nonlinear Ansys model

A solid65 element can be used for (reinforced) concrete, which is able to crack and crush. It can also handle with plastic deformations and creep. The element exist of eight nodes, which all have three degrees of freedom. [3]

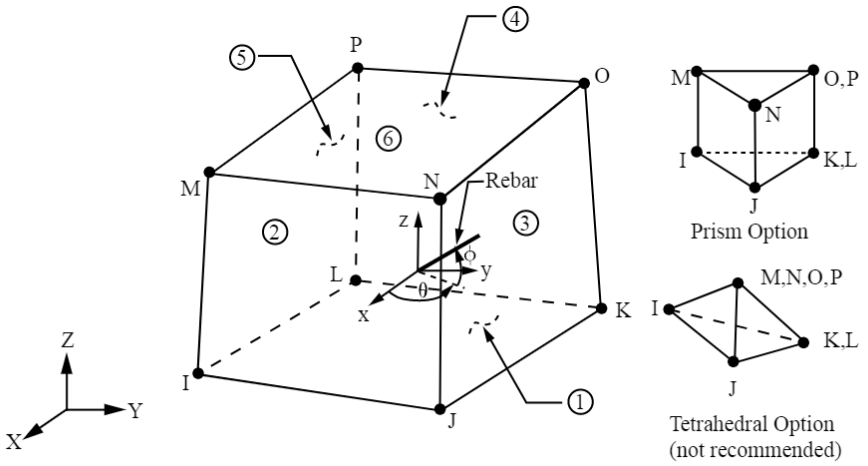

Figure D.1: Solid65 element [3]

The material is defined with a concrete material model, which predicts the failure of brittle materials. This material model can be used by: TB,CONCR,STLOC,C1,C2,C3,C4,C5,C6,C7,C8. Different parameters can be filled in to define the concrete material [3]:

- C3 = Ulitmate uniaxial tensile strength
- C4 = Ulitmate uniaxial compressive strength
- C5 = Ultimate biaxial compressive strength
- C6 = Ambient hydrostatic stress state
- C7 = Ultimate compressive strength for a state of biaxial compression superimposed on hydrostatic stress state σ_h^a
- C8 = Ulitmate compressive strength for a state of uniaxial compression superimposed on hydrostatic stress state σ_h^a

This element is capable to crack and crush. The stresses in the element occur in three directions, this causes a multiaxial stress state. Willam Warnke criterion is used to define when the cracking or crushing occurs. This is done with the following formula [2]:

$$\frac{F}{f_c} - S \geq 0 \tag{D.1}$$

with:
F = function, depending if the principal stresses are positive or negative, which is dependent on the principal stress state ($\sigma_{xp}, \sigma_{yp}, \sigma_{zp}$)
S = Failure surface dependent on the input parameters ($f_t, f_c, f_{cb}, f_1, f_2$)
f_c = uniaxial crushing strength

Cracking or crushing occurs when formula D.1 is satisfied.
The formula F depends on the domain of the principal stresses. There are four domains:

1. $$0 \geq \sigma_1 \geq \sigma_2 \geq \sigma_3$$
2. $$\sigma_1 \geq 0 \geq \sigma_2 \geq \sigma_3$$
3. $$\sigma_1 \geq \sigma_2 \geq 0 \geq \sigma_3$$
4. $$\sigma_1 \geq \sigma_2 \geq \sigma_3 \geq 0$$

The four domains are also visible in the figure that shows the Willam Warnke failure surface (figure D.2).

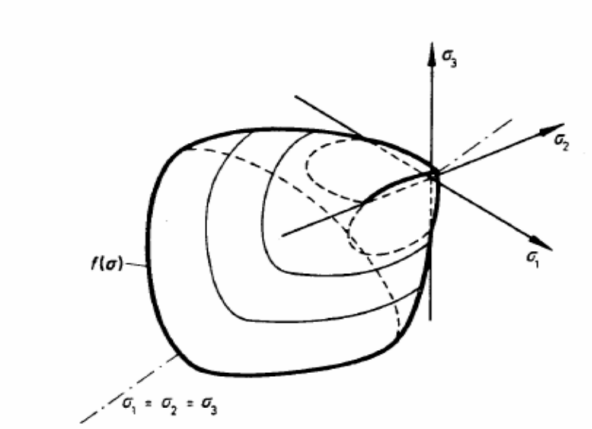

Figure D.2: A drawing of the Willam Warnke failure surface [31]

The element will crack if the tensile principal stresses are outside the failure surface. The Young's modulus, parallel to the principal tensile stress direction, of the concrete element will immediately be equal to zero. If the principal stresses are compressive and located out of the failure surface, the material will crush. The stiffness of the material at that specific location will immediately be close to zero MPa. [14] [3]. This can be seen in figure D.3

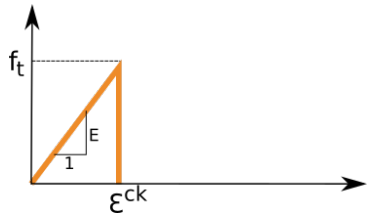

Figure D.3: The graph that shows the instant reduction in Young's modulus to zero if the tensile strength of the material is reached. f_t = uniaxial tensile strength, ϵ_{ck} = strain perpendicular to the crack face, E= Young's modulus of the material. This is the default input of a Solid 65 element in Ansys.

E

Validation nonlinear model

The validation of the nonlinear model will be done to compare it to the linear model. Before the nonlinear model has cracked, the results should be similar. Because a different element is used, there might occur small differences.

To make sure no cracking has occured yet, there will be a vertical deformation of 0.1 mm applied on both models. The shrinkage in the nonlinear model will be equal to the shrinkage in the linear model.

The figures E.1, E.2 and E.3 show a comparison between the stresses in x, y and z-direction for the model. The same distribution of the legend is used for both the variants, so the stresses can be easily compared.

The stresses in x and y direction look very similar. The maximum and minimum height of the stress differs only a little bit. The stresses in z direction differ a bit more. The height of the stresses are for both variants similar, only small differences occur. A small difference can be seen in figure E.3a. A small yellow dot can be seen in the middle of the traditional concrete, this is cannot be seen in the nonlinear model (figure E.3b). It appeared to be a stress which is very close to the boundary of the legend. This means that the stresses are not that far apart, only a small difference in stress causes the yellow colour.

Only small differences can be seen in the stresses of the two models. This means that there can be assumed that they are similar

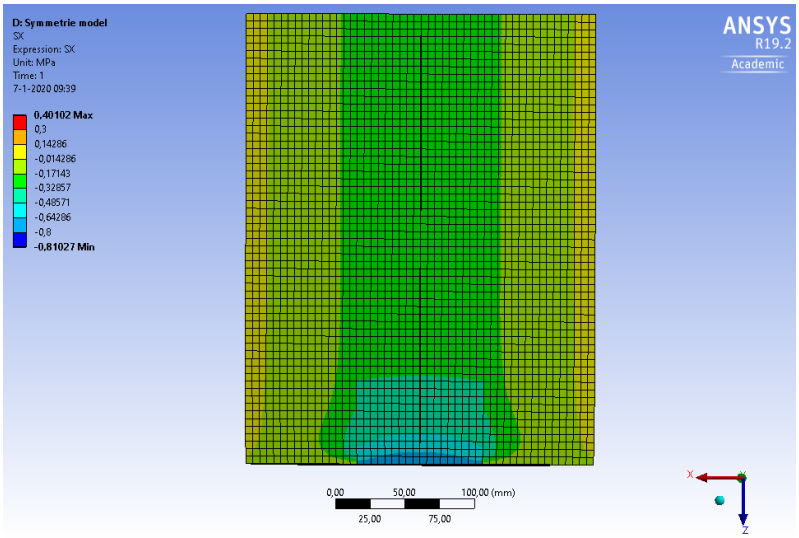

(a) σ_x linear model

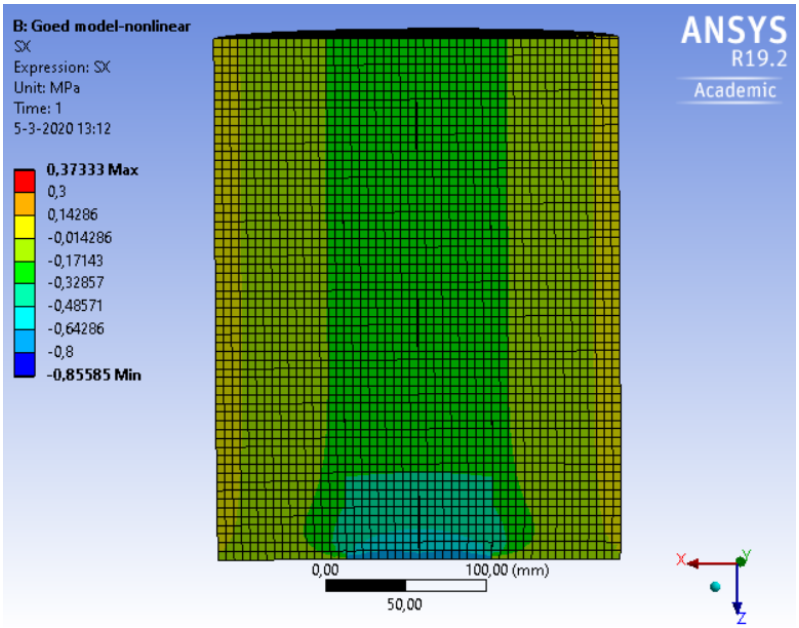

(b) σ_x non-linear model

Figure E.1: Comparison of σ_x for the linear and non-linear model. Both elements have an equal loading: the different in shrinkage and a vertical prescribed displacement

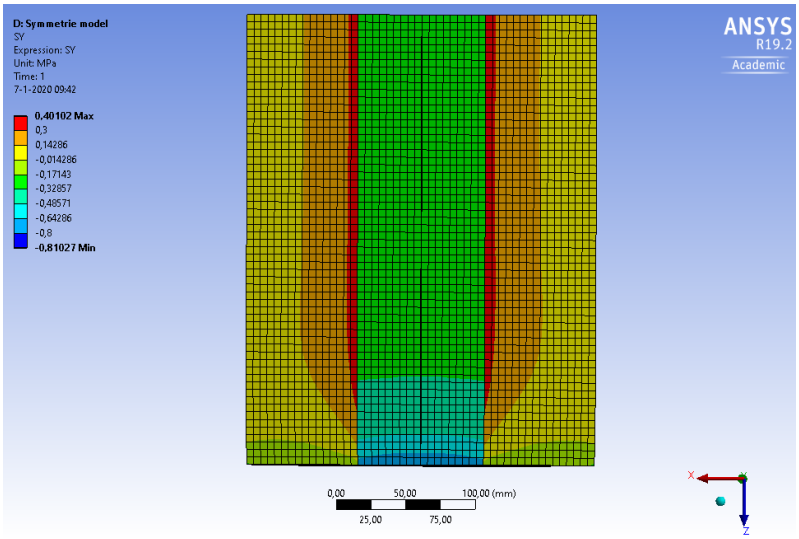

(a) σ_y linear model

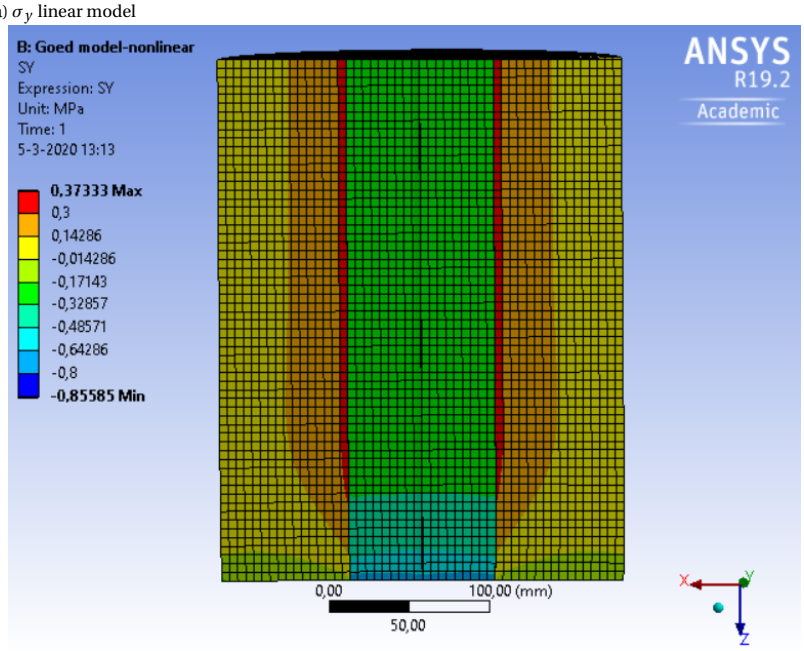

(b) σ_y non-linear model

Figure E.2: Comparison of σ_y for the linear and non-linear model. Both elements have an equal loading: the different in shrinkage and a vertical prescribed displacement

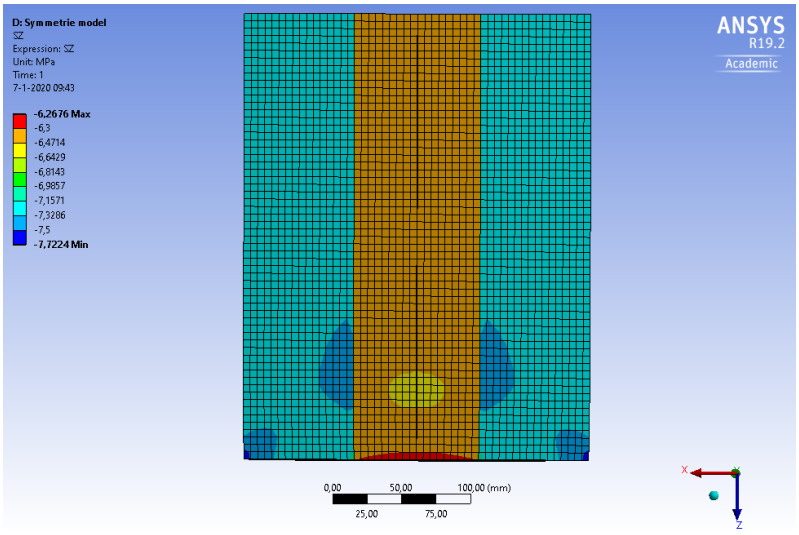

(a) σ_z linear model

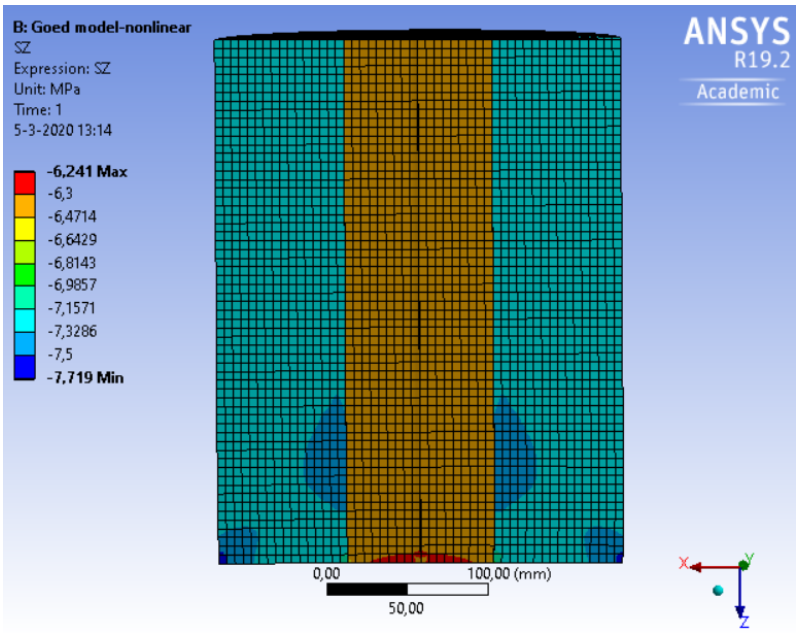

(b) σ_z non-linear model

Figure E.3: Comparison of σ_z for the linear and non-linear model. Both elements have an equal loading: the different in shrinkage and a vertical prescribed displacement

F

The different variants used for the sensitivity analysis

Variant	Contact area	Boundary Condition	E-Modulus [MPa]	D_{trad} [mm]	u_z [mm]	Shrinkage variant
1	bonded	A	C30/37	90	0.5	1
2	bonded	A	C30/37	90	0.5	2
3	bonded	A	C30/37	90	0.5	3
4	bonded	A	C30/37	90	0.5	4
5	bonded	A	C30/37	180	0.5	1
6	bonded	A	C30/37	180	0.5	2
7	bonded	A	C30/37	180	0.5	3
8	bonded	A	C30/37	180	0.5	4
9	bonded	A	C50/60	90	0.5	1
10	bonded	A	C50/60	90	0.5	2
11	bonded	A	C50/60	90	0.5	3
12	bonded	A	C50/60	90	0.5	4
13	bonded	A	C50/60	180	0.5	1
14	bonded	A	C50/60	180	0.5	2
15	bonded	A	C50/60	180	0.5	3
16	bonded	A	C50/60	180	0.5	4
17	bonded	A	C70/80	90	0.5	1
18	bonded	A	C70/80	90	0.5	2
19	bonded	A	C70/80	90	0.5	3
20	bonded	A	C70/80	90	0.5	4
21	bonded	A	C70/80	180	0.5	1
22	bonded	A	C70/80	180	0.5	2
23	bonded	A	C70/80	180	0.5	3
24	bonded	A	C70/80	180	0.5	4

Table F.1: The different variants, used in the variant study of part 1: boundary condition A & bonded contact area.

Variant	Contact area	Boundary Condition	E-Modulus [MPa]	D_{trad} [mm]	u_z [mm]	Shrinkage variant
1	bonded	B	C30/37	90	0.5	1
2	bonded	B	C30/37	90	0.5	2
3	bonded	B	C30/37	90	0.5	3
4	bonded	B	C30/37	90	0.5	4
5	bonded	B	C30/37	180	0.5	1
6	bonded	B	C30/37	180	0.5	2
7	bonded	B	C30/37	180	0.5	3
8	bonded	B	C30/37	180	0.5	4
9	bonded	B	C50/60	90	0.5	1
10	bonded	B	C50/60	90	0.5	2
11	bonded	B	C50/60	90	0.5	3
12	bonded	B	C50/60	90	0.5	4
13	bonded	B	C50/60	180	0.5	1
14	bonded	B	C50/60	180	0.5	2
15	bonded	B	C50/60	180	0.5	3
16	bonded	B	C50/60	180	0.5	4
17	bonded	B	C70/80	90	0.5	1
18	bonded	B	C70/80	90	0.5	2
19	bonded	B	C70/80	90	0.5	3
20	bonded	B	C70/80	90	0.5	4
21	bonded	B	C70/80	180	0.5	1
22	bonded	B	C70/80	180	0.5	2
23	bonded	B	C70/80	180	0.5	3
24	bonded	B	C70/80	180	0.5	4

Table F.2: The different variants, used in the variant study of part 2: boundary condition B & bonded contact area.

Variant	Contact area	Boundary Condition	E-Modulus [MPa]	D_{trad} [mm]	u_z [mm]	Shrinkage variant
1	frictionless	A	C30/37	90	0.5	1
2	frictionless	A	C30/37	90	0.5	2
3	frictionless	A	C30/37	90	0.5	3
4	frictionless	A	C30/37	90	0.5	4
5	frictionless	A	C30/37	180	0.5	1
6	frictionless	A	C30/37	180	0.5	2
7	frictionless	A	C30/37	180	0.5	3
8	frictionless	A	C30/37	180	0.5	4
9	frictionless	A	C50/60	90	0.5	1
10	frictionless	A	C50/60	90	0.5	2
11	frictionless	A	C50/60	90	0.5	3
12	frictionless	A	C50/60	90	0.5	4
13	frictionless	A	C50/60	180	0.5	1
14	frictionless	A	C50/60	180	0.5	2
15	frictionless	A	C50/60	180	0.5	3
16	frictionless	A	C50/60	180	0.5	4
17	frictionless	A	C70/80	90	0.5	1
18	frictionless	A	C70/80	90	0.5	2
19	frictionless	A	C70/80	90	0.5	3
20	frictionless	A	C70/80	90	0.5	4
21	frictionless	A	C70/80	180	0.5	1
22	frictionless	A	C70/80	180	0.5	2
23	frictionless	A	C70/80	180	0.5	3
24	frictionless	A	C70/80	180	0.5	4

Table F.3: The different variants, used in the variant study of part 3: boundary condition A & frictionless contact area.

Variant	Contact area	Boundary Condition	E-Modulus [MPa]	D_{trad} [mm]	u_z [mm]	Shrinkage variant
1	frictionless	B	C30/37	90	0.5	1
2	frictionless	B	C30/37	90	0.5	2
3	frictionless	B	C30/37	90	0.5	3
4	frictionless	B	C30/37	90	0.5	4
5	frictionless	B	C30/37	180	0.5	1
6	frictionless	B	C30/37	180	0.5	2
7	frictionless	B	C30/37	180	0.5	3
8	frictionless	B	C30/37	180	0.5	4
9	frictionless	B	C50/60	90	0.5	1
10	frictionless	B	C50/60	90	0.5	2
11	frictionless	B	C50/60	90	0.5	3
12	frictionless	B	C50/60	90	0.5	4
13	frictionless	B	C50/60	180	0.5	1
14	frictionless	B	C50/60	180	0.5	2
15	frictionless	B	C50/60	180	0.5	3
16	frictionless	B	C50/60	180	0.5	4
17	frictionless	B	C70/80	90	0.5	1
18	frictionless	B	C70/80	90	0.5	2
19	frictionless	B	C70/80	90	0.5	3
20	frictionless	B	C70/80	90	0.5	4
21	frictionless	B	C70/80	180	0.5	1
22	frictionless	B	C70/80	180	0.5	2
23	frictionless	B	C70/80	180	0.5	3
24	frictionless	B	C70/80	180	0.5	4

Table F.4: The different variants, used in the variant study of part 4: boundary condition B & frictionless contact area.

Variant	Contact area	Boundary Condition	E-Modulus [MPa]	n_{trad}	n_{print}	D_{trad} [mm]	u_z [mm]	Input shrinkage trad [°C]	input shrinkage print [°C]
1	bonded	A	32496	9	16	90	0.5	20.64	19.59
2	bonded	A	32496	9	16	90	0.5	22	22
3	bonded	A	32496	9	16	90	0.5	-9.71	-46.43
4	bonded	A	32496	9	16	90	0.5	-9.71	22
5	bonded	A	32496	8	14	180	0.5	20.64	19.59
6	bonded	A	32496	8	14	180	0.5	22	22
7	bonded	A	32496	8	14	180	0.5	-9.71	-46.43
8	bonded	A	32496	8	14	180	0.5	-9.71	22
9	bonded	A	37000	9	16	90	0.5	20.64	19.59
10	bonded	A	37000	9	16	90	0.5	22	22
11	bonded	A	37000	9	16	90	0.5	-9.71	-46.43
12	bonded	A	37000	9	16	90	0.5	-9.71	22
13	bonded	A	37000	8	14	180	0.5	20.64	19.59
14	bonded	A	37000	8	14	180	0.5	22	22
15	bonded	A	37000	8	14	180	0.5	-9.71	-46.43
16	bonded	A	37000	8	14	180	0.5	-9.71	22
17	bonded	A	41000	9	16	90	0.5	20.64	19.59
18	bonded	A	41000	9	16	90	0.5	22	22
19	bonded	A	41000	9	16	90	0.5	-9.71	-46.43
20	bonded	A	41000	9	16	90	0.5	-9.71	22
21	bonded	A	41000	8	14	180	0.5	20.64	19.59
22	bonded	A	41000	8	14	180	0.5	22	22
23	bonded	A	41000	8	14	180	0.5	-9.71	-46.43
24	bonded	A	41000	8	14	180	0.5	-9.71	22

Table F.5: The input values for the variant study, part 1

Variant	Contact area	Boundary Condition	E-Modulus [MPa]	n_{trad}	n_{print}	D_{trad} [mm]	u_z [mm]	Input shrinkage trad [°C]	input shrinkage print [°C]
25	bonded	B	32496	9	16	90	0.5	20.64	19.59
26	bonded	B	32496	9	16	90	0.5	22	22
27	bonded	B	32496	9	16	90	0.5	-9.71	-46.43
28	bonded	B	32496	9	16	90	0.5	-9.71	22
29	bonded	B	32496	8	14	180	0.5	20.64	19.59
30	bonded	B	32496	8	14	180	0.5	22	22
31	bonded	B	32496	8	14	180	0.5	-9.71	-46.43
32	bonded	B	32496	8	14	180	0.5	-9.71	22
33	bonded	B	37000	9	16	90	0.5	20.64	19.59
34	bonded	B	37000	9	16	90	0.5	22	22
35	bonded	B	37000	9	16	90	0.5	-9.71	-46.43
36	bonded	B	37000	9	16	90	0.5	-9.71	22
37	bonded	B	37000	8	14	180	0.5	20.64	19.59
38	bonded	B	37000	8	14	180	0.5	22	22
39	bonded	B	37000	8	14	180	0.5	-9.71	-46.43
41	bonded	B	41000	9	16	90	0.5	20.64	19.59
42	bonded	B	41000	9	16	90	0.5	22	22
43	bonded	B	41000	9	16	90	0.5	-9.71	-46.43
44	bonded	B	41000	9	16	90	0.5	-9.71	22
45	bonded	B	41000	8	14	180	0.5	20.64	19.59
46	bonded	B	41000	8	14	180	0.5	22	22
47	bonded	B	41000	8	14	180	0.5	-9.71	-46.43
48	bonded	B	41000	8	14	180	0.5	-9.71	22

Table F.6: The input values for the variant study, part 2

Variant	Contact area	Boundary Condition	E-Modulus [MPa]	n_{trad}	n_{print}	D_{trad} [mm]	u_z [mm]	Input shrinkage trad [°C]	input shrinkage print [°C]
49	frictionless	A	32496	9	16	90	0.5	20.64	19.59
50	frictionless	A	32496	9	16	90	0.5	22	22
51	frictionless	A	32496	9	16	90	0.5	-9.71	-46.43
52	frictionless	A	32496	9	16	90	0.5	-9.71	22
53	frictionless	A	32496	8	14	180	0.5	20.64	19.59
54	frictionless	A	32496	8	14	180	0.5	22	22
55	frictionless	A	32496	8	14	180	0.5	-9.71	-46.43
56	frictionless	A	32496	8	14	180	0.5	-9.71	22
57	frictionless	A	37000	9	16	90	0.5	20.64	19.59
58	frictionless	A	37000	9	16	90	0.5	22	22
59	frictionless	A	37000	9	16	90	0.5	-9.71	-46.43
60	frictionless	A	37000	9	16	90	0.5	-9.71	22
61	frictionless	A	37000	8	14	180	0.5	20.64	19.59
62	frictionless	A	37000	8	14	180	0.5	22	22
63	frictionless	A	37000	8	14	180	0.5	-9.71	-46.43
64	frictionless	A	37000	8	14	180	0.5	-9.71	22
65	frictionless	A	41000	9	16	90	0.5	20.64	19.59
66	frictionless	A	41000	9	16	90	0.5	22	22
67	frictionless	A	41000	9	16	90	0.5	-9.71	-46.43
68	frictionless	A	41000	9	16	90	0.5	-9.71	22
69	frictionless	A	41000	8	14	180	0.5	20.64	19.59
70	frictionless	A	41000	8	14	180	0.5	22	22
71	frictionless	A	41000	8	14	180	0.5	-9.71	-46.43
72	frictionless	A	41000	8	14	180	0.5	-9.71	22

Table F.7: The input values for the variant study, part 3

Variant	Contact area	Boundary Condition	E-Modulus [MPa]	n_{trad}	n_{print}	D_{trad} [mm]	u_z [mm]	Input shrinkage trad [°C]	input shrinkage print [°C]
73	frictionless	B	32496	9	16	90	0.5	20.64	19.59
74	frictionless	B	32496	9	16	90	0.5	22	22
75	frictionless	B	32496	9	16	90	0.5	-9.71	-46.43
76	frictionless	B	32496	9	16	90	0.5	-9.71	22
77	frictionless	B	32496	8	14	180	0.5	20.64	19.59
78	frictionless	B	32496	8	14	180	0.5	22	22
79	frictionless	B	32496	8	14	180	0.5	-9.71	-46.43
80	frictionless	B	32496	8	14	180	0.5	-9.71	22
81	frictionless	B	37000	9	16	90	0.5	20.64	19.59
82	frictionless	B	37000	9	16	90	0.5	22	22
83	frictionless	B	37000	9	16	90	0.5	-9.71	-46.43
84	frictionless	B	37000	9	16	90	0.5	-9.71	22
85	frictionless	B	37000	8	14	180	0.5	20.64	19.59
86	frictionless	B	37000	8	14	180	0.5	22	22
87	frictionless	B	37000	8	14	180	0.5	-9.71	-46.43
88	frictionless	B	41000	9	16	90	0.5	20.64	19.59
89	frictionless	B	41000	9	16	90	0.5	22	22
90	frictionless	B	41000	9	16	90	0.5	-9.71	-46.43
91	frictionless	B	41000	9	16	90	0.5	-9.71	22
92	frictionless	B	41000	8	14	180	0.5	20.64	19.59
93	frictionless	B	41000	8	14	180	0.5	22	22
94	frictionless	B	41000	8	14	180	0.5	-9.71	-46.43
95	frictionless	B	41000	8	14	180	0.5	-9.71	22

Table F.8: The input values for the variant study, part 4

G

Sensitivity Analysis

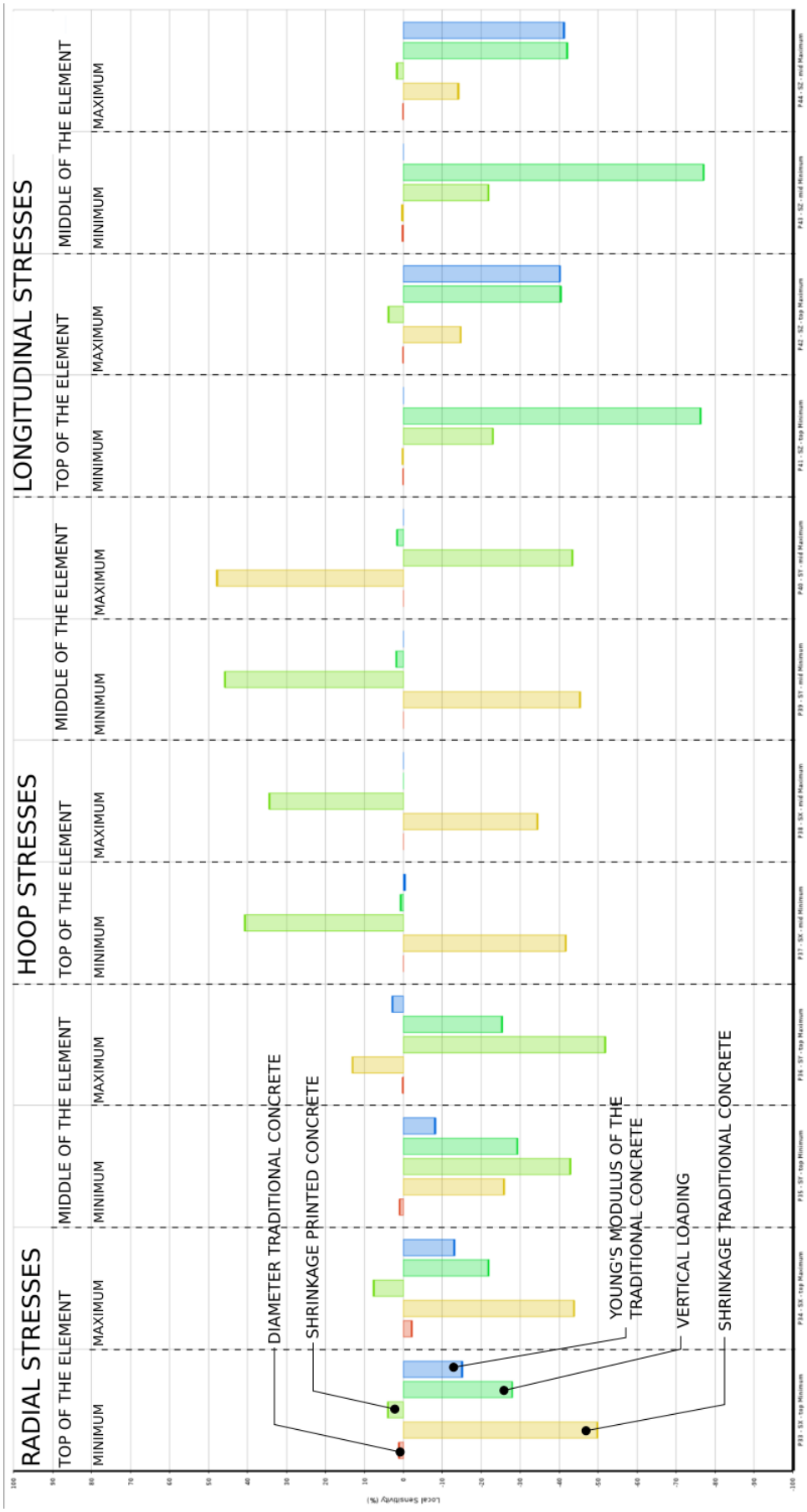

Figure G.1: The results of the local sensitivity Analysis for Part 1: boundary condition A and bonded.

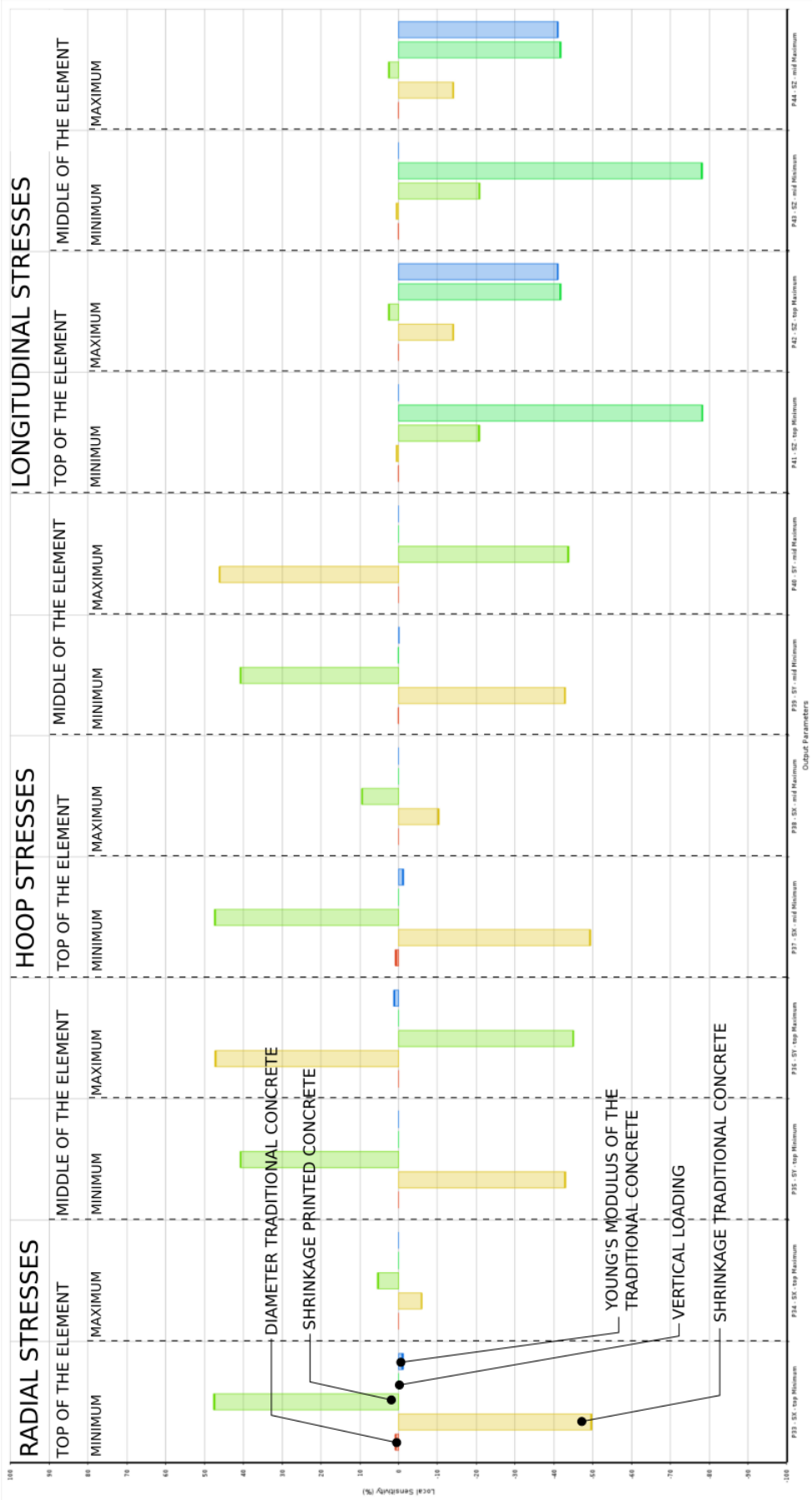

Figure G.2: The results of the local sensitivity Analysis for Part 2: boundary condition B and bonded.

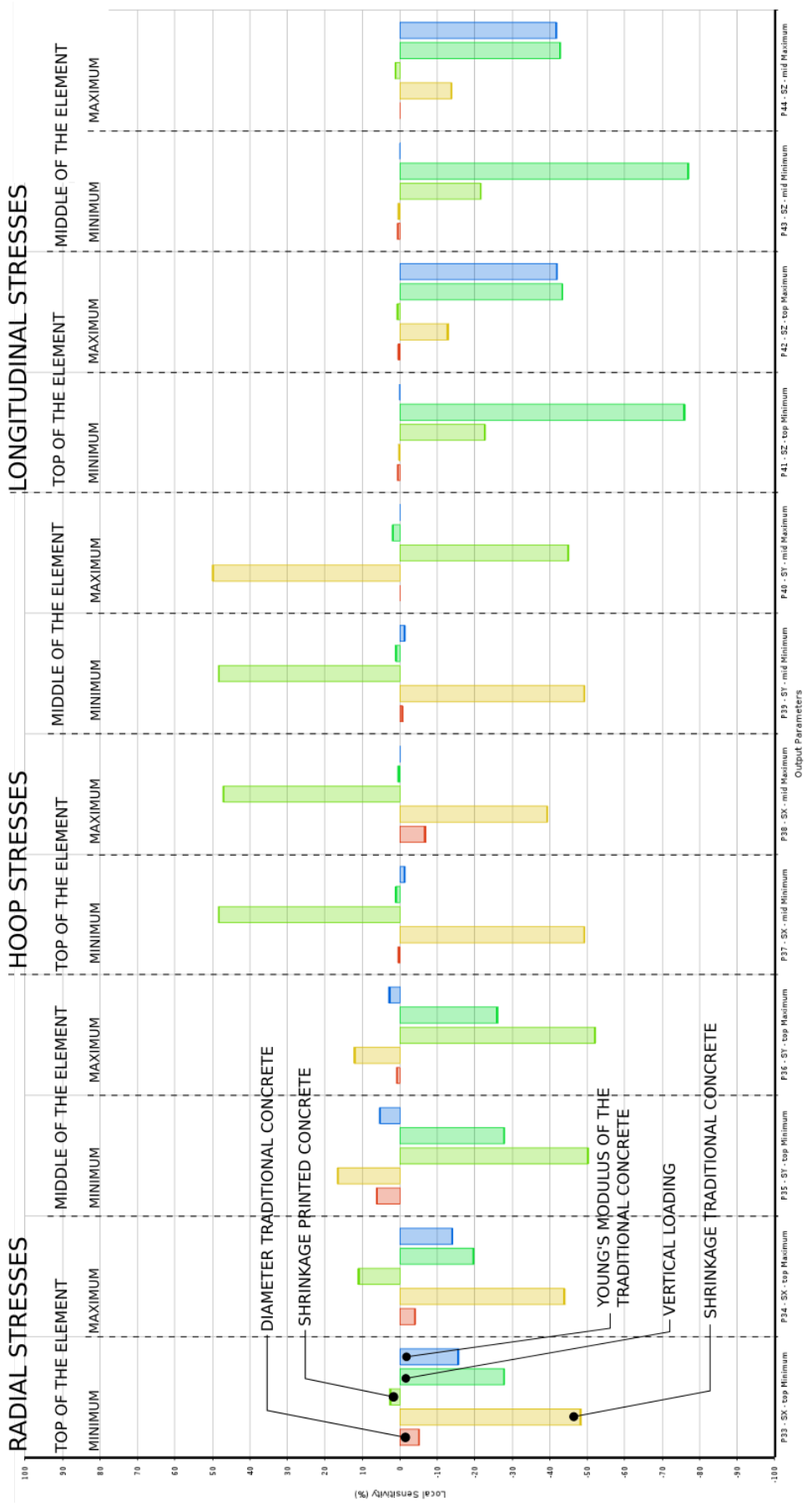

Figure G.3: The results of the local sensitivity Analysis for Part 3: boundary condition A and frictionless.

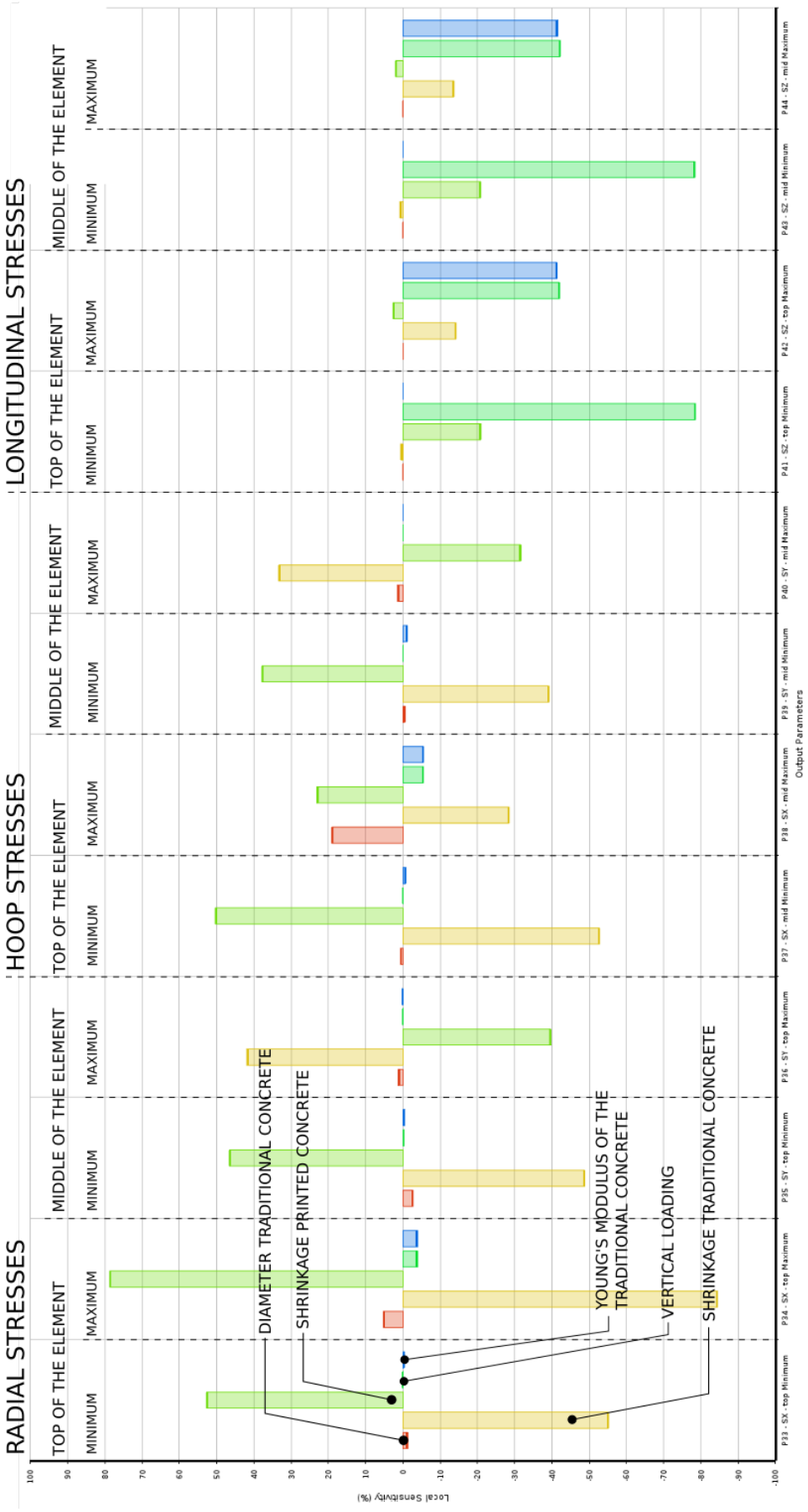

Figure G.4: The results of the local sensitivity Analysis for Part 4: boundary condition B and frictionless.

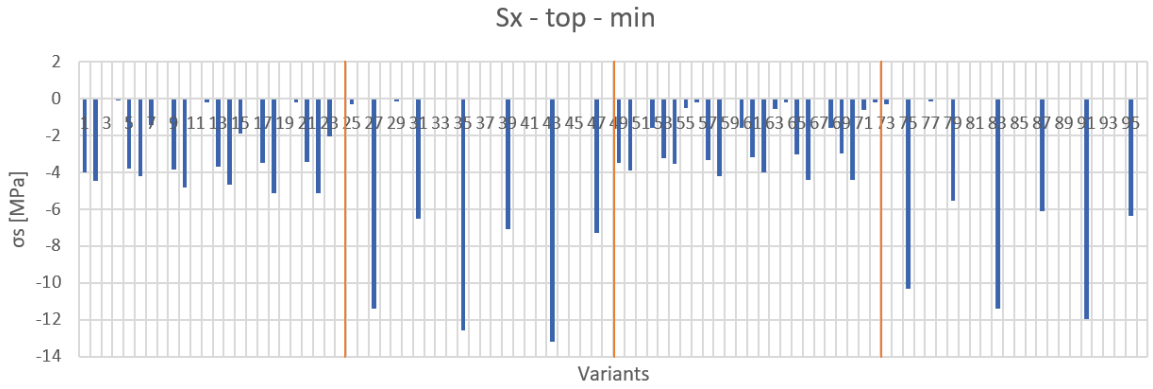

Figure G.5: The result of the variant study: Minimum σ_x at the top of the element

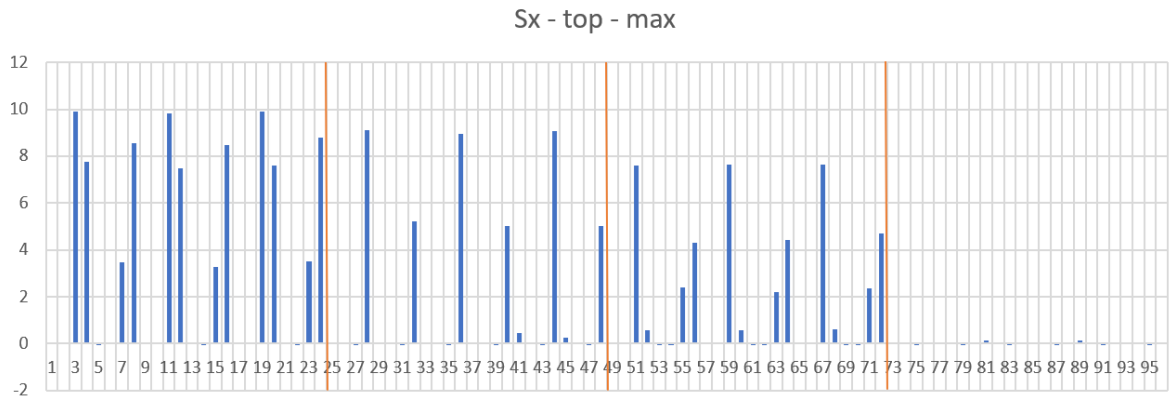

Figure G.6: The result of the variant study: Maximum σ_x at the top of the element

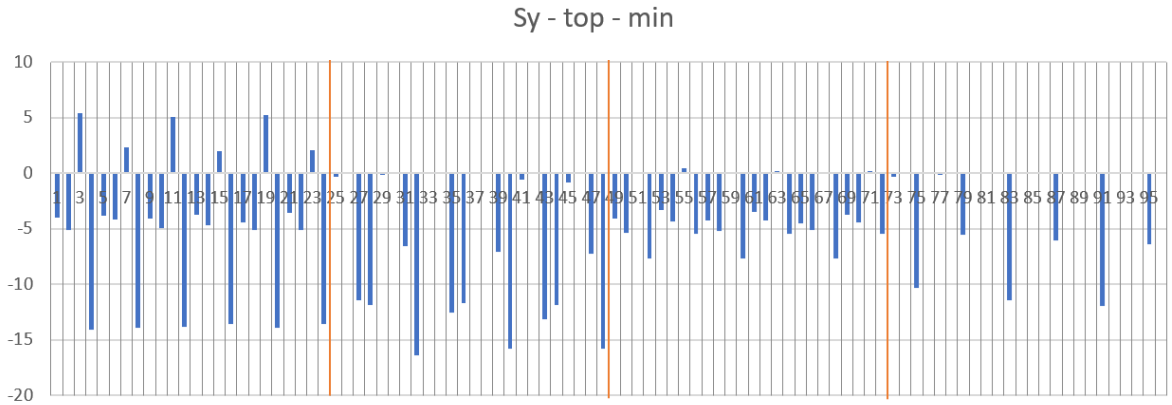

Figure G.7: The result of the variant study: Minimum σ_y at the top of the element

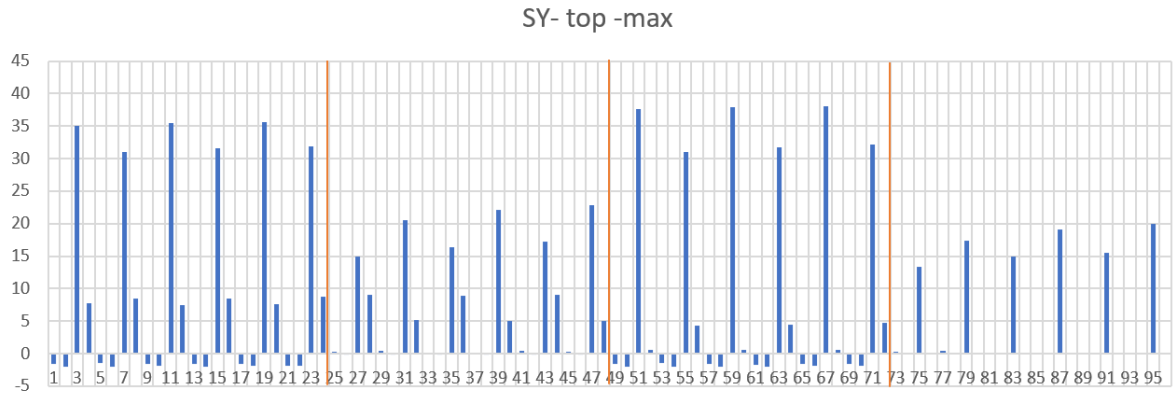

Figure G.8: The result of the variant study: Maximum σ_y at the top of the element

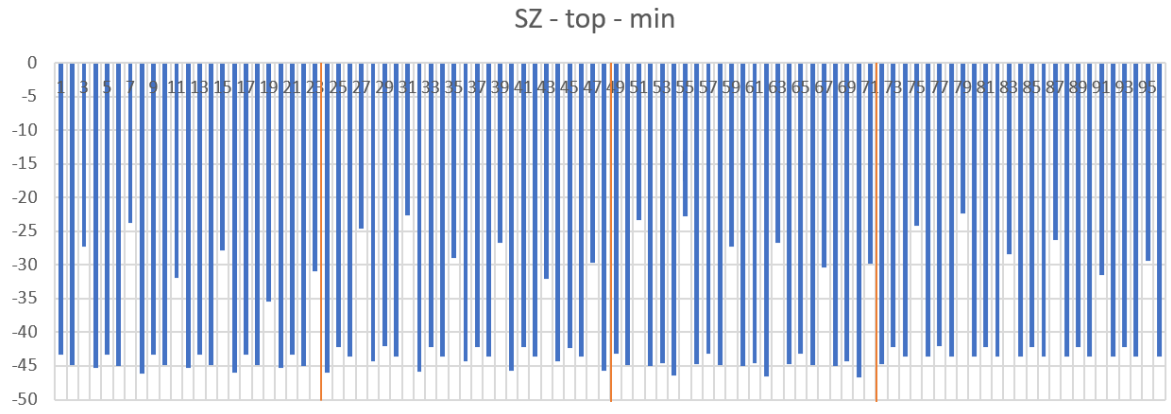

Figure G.9: The result of the variant study: Minimum σ_z at the top of the element

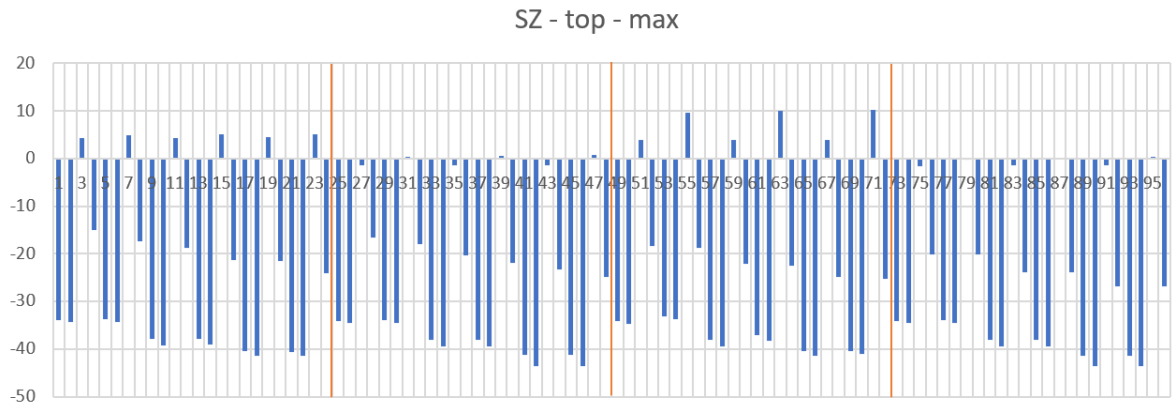

Figure G.10: The result of the variant study: Maximumσ_z at the top of the element

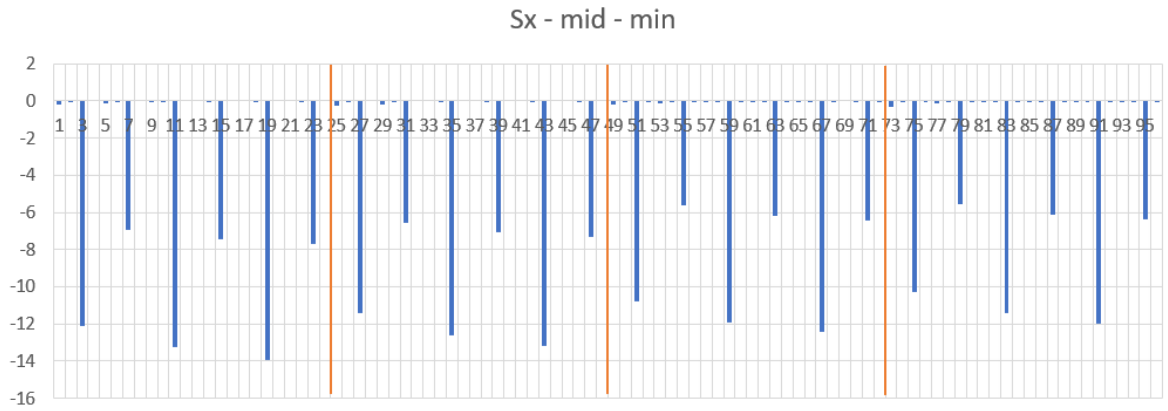

Figure G.11: The result of the variant study: Minimum σ_x at the middle of the element

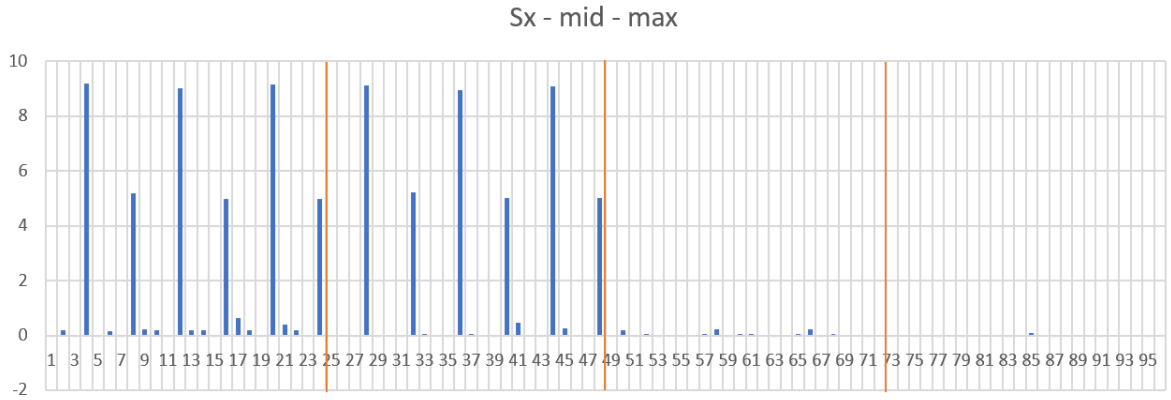

Figure G.12: The result of the variant study: Maximum σ_x at the middle of the element

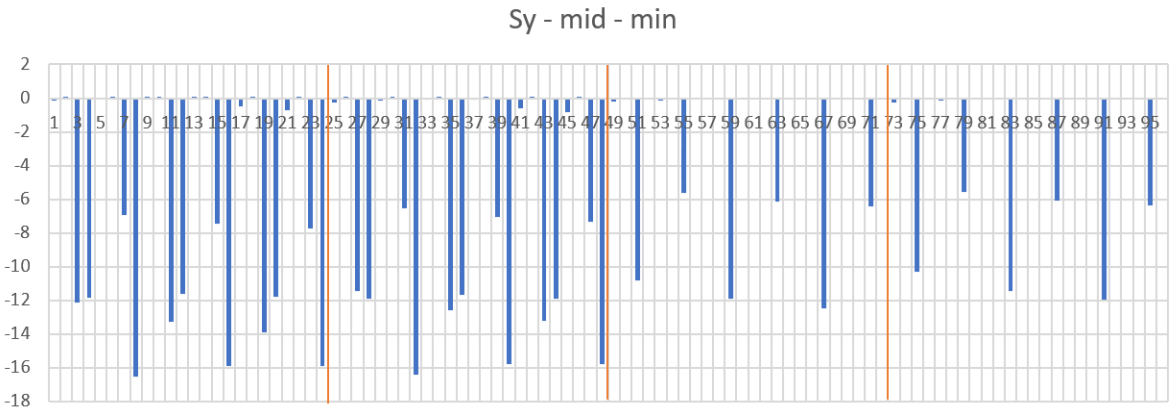

Figure G.13: The result of the variant study: Minimum σ_y at the middle of the element

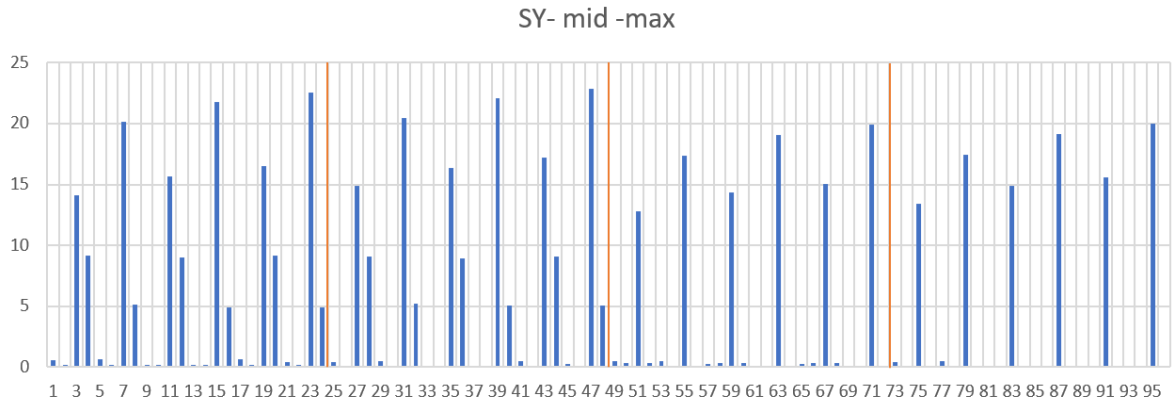

Figure G.14: The result of the variant study: Maximum σ_y at the middle of the element

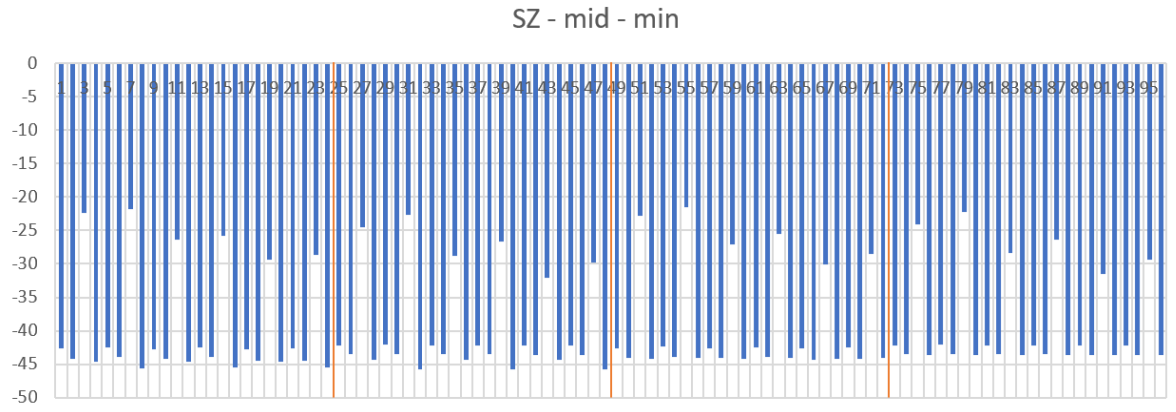

Figure G.15: The result of the variant study: Minimum σ_z at the middle of the element

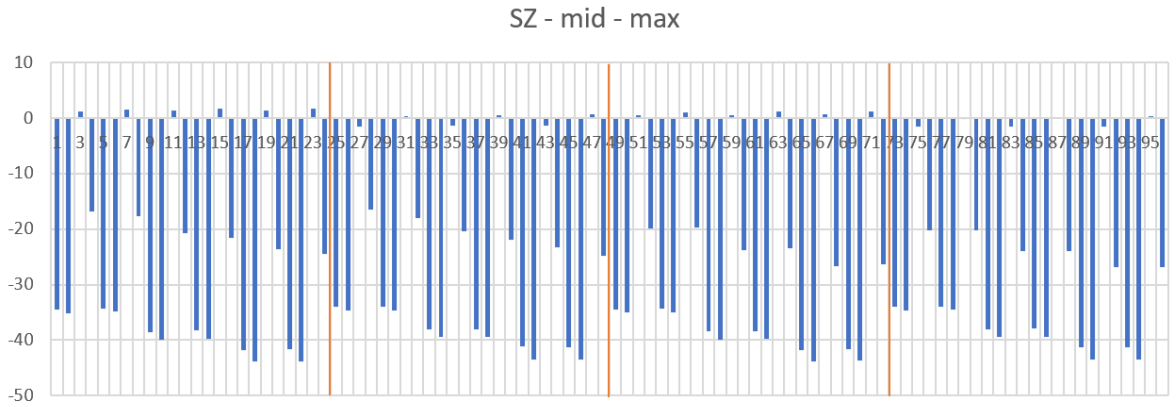

Figure G.16: The result of the variant study: Maximum σ_z at the middle of the element

Bibliography

American Society for Testing and Materials. E965-15. Standard Test Method for Measuring Pavement Macrotexture Depth Using a Volumetric technique. *ASTM International*, i:1–4, 2015. doi: 10.1520/E0965-15.2.

Ansys. 4.10. Concrete, a. URL `http://www.mm.bme.hu/{~}gyebro/files/ans{_}help{_}v182/ans{_}thry/thy{_}mat7.html{#}thyeq3domaincccnov2001`.

Ansys. Solid65 Element Description, b. URL `https://ansyshelp.ansys.com/account/secured?returnurl=/Views/Secured/corp/v192/ans{_}elem/Hlp{_}E{_}SOLID65.html?q=TBDATA`.

ASTM C39. C39/C39M-14: Standard Test Method for Compressive Strength of Cylindrical Concrete Specimens. *American Society for Testing and Materials*, pages 1–7, 2016. doi: 10.1520/C0039.

Simon Austin, Peter Robins, and Youguang Pan. Tensile bond testing of concrete repairs. *Materials and Structures*, 28(5):249–259, 1995. ISSN 00255432. doi: 10.1007/BF02473259.

Simon Austin, Peter Robins, and Youguang Pan. Shear bond testing of concrete repairs. *Cement and concrete research*, 29(7):1067–1076, 1999.

U. T. Bezerra, S. M. S. Alves, N. P. Barbosa, and S. M. Torres. Hourglass-shaped specimen: compressive strength of concrete and mortar (numerical and experimental analyses). *Revista IBRACON de Estruturas e Materiais*, 9(4):510–524, 2016. doi: 10.1590/s1983-41952016000400003.

Justin Blaber and Antonia Antoniou. Ncorr, 2017. URL `http://www.ncorr.com/index.php/downloads`.

Freek P. Bos, Rob J.M. Wolfs, Zeeshan Y. Ahmed, and Theo A.M. Salet. Additive manufacturing of concrete in construction: potentials and challenges of 3D concrete printing. *Virtual and Physical Prototyping*, 11(3): 209–225, 2016. ISSN 17452767. doi: 10.1080/17452759.2016.1209867.

Freek P. Bos, Rob J.M. Wolfs, Zeeshan Y. Ahmed, and Theo A.M. Salet. Large scale testing of digitally fabricated concrete (DFC) elements. In *RILEM International Conference on Concrete and Digital Fabrication*, pages 129–147, 2018.

Luc C it lourard, Tomasz Piotrowski, and Andrzej Garbacz. Near-to-surface properties affecting bond strength in concrete repair. *Cement and Concrete Composites*, 46:73–80, feb 2014. ISSN 09589465. doi: 10.1016/j.cemconcomp.2013.11.005.

T Craipeau, T Lecompte, F Toussaint, and A Perrot. Evolution of Concrete / Formwork Interface in Slipforming process. *Digital Concrete*, 2018.

James Mitchell Crow. The concrete conundrum. *Chemistry world*, (March):62–64, 2008.

L. Dahmani, A. Khennane, and S. Kaci. Crack identification in reinforced concrete beams using ANSYS software. *Strength of Materials*, 42(2):232–240, 2010. ISSN 15739325. doi: 10.1007/s11223-010-9212-6.

David Darwin, Charles W. Dolan, and Arthur H. Nilson. *Design of Concrete Structures*. McGraw-Hill Education, 15 edition, 2016. ISBN 9780073397948.

Yan He, Xiong Zhang, R. Douglas Hooton, and Xiaowei Zhang. Effects of interface roughness and interface adhesion on new-to-old concrete bonding. *Construction and Building Materials*, 151:582–590, 2017.

Heidelberg Cement Group. Beton als bouwmateriaal. In *Betonpocket*, chapter 2, pages 15–34. 2016.

Dooil Hwang and Behrokh Khoshnevis. Concrete Wall Fabrication By Contour Crafting. *ISARC 2004 21st International Symposium on Automation and Robotics in Construction*, 2004.

Maria Kaszyńska, Marcin Hoffmann, Szymon Skibicki, Adam Zieliński, Mateusz Techman, Norbert Olczyk, and Tomasz Wróblewski. Evaluation of suitability for 3D printing of high performance concretes. *MATEC Web of Conferences*, 163, jun 2018. doi: 10.1051/matecconf/201816301002.

Marjolein P.A.M. Marijnissen and Aant Van Der Zee. 3D Concrete Printing in Architecture: a research on the potential benefits of 3D Concrete Printing in Architecture. *eCAADe*, 2:299–308, 2017. URL `http://papers.cumincad.org/data/works/att/ecaade2017{_}087.pdf`.

Nederlands Normalistatie-instituut. *NEN-EN 1992-1-1+C2 Eurocode 2: Ontwerp en berekening van betonconstructies - Deel 1-1: Algemene regels en regels voor gebouwen.* Number november. 2011. ISBN 0000105058.

Nederlands Normalistatie-instituut. Nen-en 13670 Het vervaardigen van betonconstructies, 2019.

Biranchi Panda, Yi. Wei D. Tay, Suvash C. Paul, T.A.N. Ming JEN, Kah Fai LEONG, and I.A.N. GIBSON. Current Challenges and future perspectives of 3D concrete printing. In *Proceeding of 2nd International Conference on Progress in Additive Manufacturing (Pro-AM 2016), Singapore*, 2016.

B Parmentier, V Pollet, and G Zarmati. De verhinderde betonkrimp. *Wtcb*, 3(2):12, 2009.

R Sagel, FPJ van Geest, and WC Dees. *GTB 2006: grafieken en tabellen voor beton; complete uitgave*. Betonvereniging, Gouda, 2006.

Saint-Gobain Weber Beamix B.V. Product datasheet Weber 3D 160-1, 2019.

Pedro M.D. Santos and Eduardo N.B.S. Júlio. A state-of-the-art review on roughness quantification methods for concrete surfaces. *Construction and Building Materials*, 38:912–923, 2013. ISSN 09500618. doi: 10.1016/j.conbuildmat.2012.09.045. URL `http://dx.doi.org/10.1016/j.conbuildmat.2012.09.045`.

J Silfwerbrand and H Beushausen. Bonded concrete overlays–bond strength issues. In *Proceedings ICCRRR 2005 International Conference on Concrete Repair, Rehabilitation and Retrofitting, Cape Town, South Africa, Taylor & Francis Group, London*, pages 19–21, 2006.

Johan Silfwerbrand, Hans Beushausen, and Luc Courard. Bond. In *Bonded Cement-Based Material Overlays for the Repair, the Lining or the Strengthening of Slabs or Pavements*, chapter 4, pages 51–79. Springer, 2011.

Stichting Betonprisma. Krimp. *Betoniek*, 10(22):1–9, 1997.

K.J. Willam and E.P. Warnke. Constitutive model for the traixial behaviour of concrete. In *International Association for Bridge and Structural Engineering*, page 174, Begramo,Italy, 1975.